SSC-338

FATIGUE PREDICTION ANALYSIS VALIDATION FROM SL - 7 HATCH CORNER STRAIN DATA

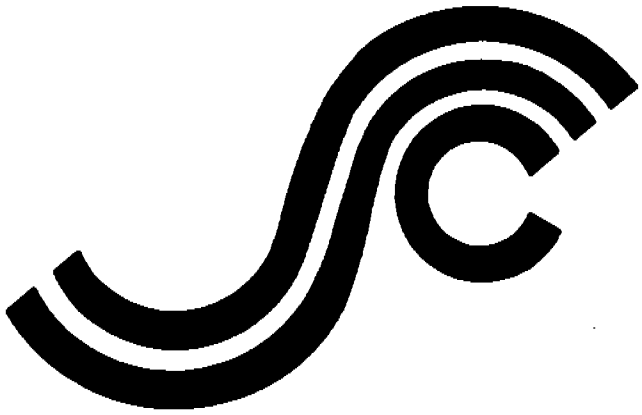

SHIP STRUCTURE COMMITTEE

1990

SHIP STRUCTURE COMMITTEE

The SHIP STRUCTURE COMMITTEE is constituted to prosecute a research program to improve the hull structures of ships and other marine structures by an extension of knowledge pertaining to design, materials, and methods of construction.

RADM J. D. Sipes, USCG, (Chairman)
Chief, Office of Marine Safety, Security and Environmental Protection
U. S. Coast Guard

Mr. Alexander Malakhoff
Director, Structural Integrity Subgroup (SEA 55Y)
Naval Sea Systems Command

Dr. Donald Liu
Senior Vice President
American Bureau of Shipping

Mr. H. T. Haller
Associate Administrator for Ship-building and Ship Operations
Maritime Administration

Mr. Thomas W. Allen
Engineering Officer (N7)
Military Sealift Command

CDR Michael K. Parmelee, USCG,
Secretary, Ship Structure Committee
U. S. Coast Guard

CONTRACTING OFFICER TECHNICAL REPRESENTATIVES

Mr. William J. Siekierka
SEA 55Y3
Naval Sea Systems Command

Mr. Greg D. Woods
SEA 55Y3
Naval Sea Systems Command

SHIP STRUCTURE SUBCOMMITTEE

The SHIP STRUCTURE SUBCOMMITTEE acts for the Ship Structure Committee on technical matters by providing technical coordination for determinating the goals and objectives of the program and by evaluating and interpreting the results in terms of structural design, construction, and operation.

AMERICAN BUREAU OF SHIPPING

Mr. Stephen G. Arntson (Chairman)
Mr. John F. Conlon
Mr. William Hanzalek
Mr. Philip G. Rynn

MILITARY SEALIFT COMMAND

Mr. Albert J. Attermeyer
Mr. Michael W. Touma
Mr. Jeffery E. Beach

MARITIME ADMINISTRATION

Mr. Frederick Seibold
Mr. Norman O. Hammer
Mr. Chao H. Lin
Dr. Walter M. Maclean

NAVAL SEA SYSTEMS COMMAND

Mr. Robert A. Sielski
Mr. Charles L. Null
Mr. W. Thomas Packard
Mr. Allen H. Engle

U. S. COAST GUARD

CAPT T. E. Thompson
CAPT Donald S. Jensen
CDR Mark E. Noll

SHIP STRUCTURE SUBCOMMITTEE LIAISON MEMBERS

U. S. COAST GUARD ACADEMY

LT Bruce Mustain

U. S. MERCHANT MARINE ACADEMY

Dr. C. B. Kim

U. S. NAVAL ACADEMY

Dr. Ramswar Bhattacharyya

STATE UNIVERSITY OF NEW YORK MARITIME COLLEGE

Dr. W. R. Porter

WELDING RESEARCH COUNCIL

Dr. Martin Prager

NATIONAL ACADEMY OF SCIENCES - MARINE BOARD

Mr. Alexander B. Stavovy

NATIONAL ACADEMY OF SCIENCES - COMMITTEE ON MARINE STRUCTURES

Mr. Stanley G. Stiansen

SOCIETY OF NAVAL ARCHITECTS AND MARINE ENGINEERS - HYDRODYNAMICS COMMITTEE

Dr. William Sandberg

AMERICAN IRON AND STEEL INSTITUTE

Mr. Alexander D. Wilson

Member Agencies:

United States Coast Guard
Naval Sea Systems Command
Maritime Administration
American Bureau of Shipping
Military Sealift Command

Ship Structure Committee

An Interagency Advisory Committee
Dedicated to the Improvement of Marine Structures

Address Correspondence to:

Secretary, Ship Structure Committee
U.S. Coast Guard (G-MTH)
2100 Second Street S.W.
Washington, D.C. 20593-0001
PH: (202) 267-0003
FAX: (202) 267-0025

SSC-338
SR-1297

December 3, 1990

FATIGUE ANALYSIS PREDICTION VALIDATION FROM SL-7 HATCH CORNER STRAIN DATA

The ability to predict the fatigue life of structural details is an essential element in the design of modern ships. Fatigue analyses are frequently performed to ensure the safety and reliability of these structures. There are very few instances, however, where full scale testing and instrumentation was used to validate fatigue analysis predictions. This report provides a well-documented case history of fatigue cracking experienced on the SL-7 Class container ships. Using hatch corner strain gage data obtained while the vessels were in service, fatigue damage evaluations were made for the original structural design and for subsequent modifications. The evaluation methods and results and relevant sea state and strain data are provided.

J. D. SIPES
Rear Admiral, U.S. Coast Guard
Chairman, Ship Structure Committee

Technical Report Documentation Page

1. Report No.	2. Government Accession No.	3. Recipient's Catalog No.
SSC-338		

4. Title and Subtitle	5. Report Date
Fatigue Prediction Analysis Validation From SL-7 Hatch Corner Strain Data	December 1985
	6. Performing Organization Code
7. Author(s)	8. Performing Organization Report No.
Jeng-Wen Chiou and Yung-Kuang Chen	RD-85027 SR-1297
9. Performing Organization Name and Address	10. Work Unit No. (TRAIS)
American Bureau of Shipping 45 Eisenhower Drive Paramus, NJ 07653-0910	11. Contract or Grant No.
	13. Type of Report and Period Covered
12. Sponsoring Agency Name and Address	Final Report
Ship Structure Committee U.S. Coast Guard 2100 Second Street, SW Washington, DC 20593	14. Sponsoring Agency Code G-M

15. Supplementary Notes

16. Abstract

The objective of this report is to provide a comparison of the hatch corner fatigue cracking experience of the SL-7 container ships with theoretical fatigue calculations. The fatigue study was based on hatch corner strain gage data collected from two of the vessels in transoceanic service. Strain histories for the hatch corners as originally designed and as modified are included. Fatigue damage evaluations were carried out using: a) deterministic fatigue life calculations, b) probabilistic fatigue life calculations, and c) fracture mechanic calculations.

17. Key Words		18. Distribution Statement
Fatigue	Strain Gage	Available to the public from National Technical Information Service Springfield, VA 22161 or Marine Technical Information Facility National Maritime Research Center Kings Point, NY 10024-1699
Fatigue Cracking	Fatigue Damage	
Fatigue Life	Hatch Corner	
Deterministic Methods		
Probabilistic Methods		

19. Security Classif. (of this report)	20. Security Classif. (of this page)	21. No. of Pages	22. Price
UNCLASSIFIED	UNCLASSIFIED	170	

Form DOT F 1700.7 (8-72) Reproduction of completed page authorized

METRIC CONVERSION FACTORS

Approximate Conversions to Metric Measures

Symbol	When You Know	Multiply by	To Find	Symbol
LENGTH				
in	inches	*2.5	centimeters	cm
ft	feet	30	centimeters	cm
yd	yards	0.9	meters	m
mi	miles	1.6	kilometers	km
AREA				
in^2	square inches	6.5	square centimeters	cm^2
ft^2	square feet	0.09	square meters	m^2
yd^2	square yards	0.8	square meters	m^2
mi^2	square miles	2.6	square kilometers	km^2
	acres	0.4	hectares	ha
MASS (weight)				
oz	ounces	28	grams	g
lb	pounds	0.45	kilograms	kg
	short tons (2000 lb)	0.9	tonnes	t
VOLUME				
tsp	teaspoons	5	milliliters	ml
Tbsp	tablespoons	15	milliliters	ml
fl oz	fluid ounces	30	milliliters	ml
c	cups	0.24	liters	l
pt	pints	0.47	liters	l
qt	quarts	0.96	liters	l
gal	gallons	3.8	liters	l
ft^3	cubic feet	0.03	cubic meters	m^3
yd^3	cubic yards	0.76	cubic meters	m^3
TEMPERATURE (exact)				
°F	Fahrenheit temperature	5/9 (after subtracting 32)	Celsius temperature	°C

*1 in. = 2.54 cm (exactly). For other exact conversions and more detail tables see NBS Misc. Publ. 286, Units of Weight and Measures. Price $2.25 SD Catalog No. C13 10 286.

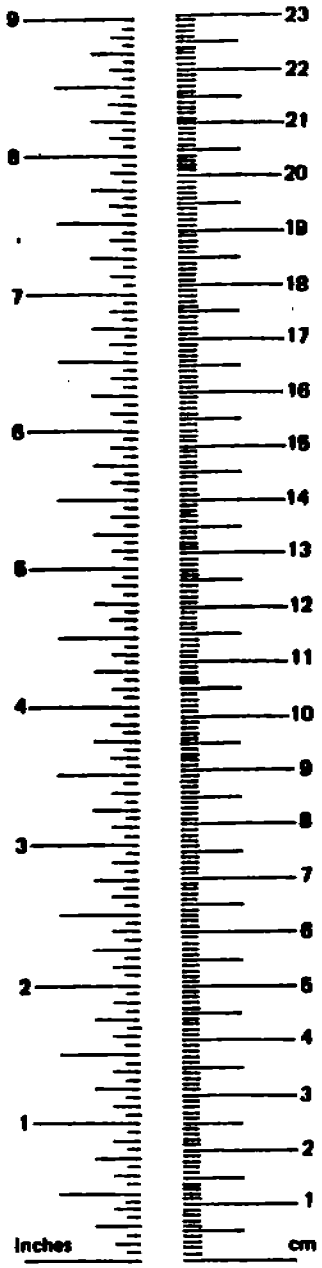

Approximate Conversion

Symbol	When You Know	Multipl
LENG		
mm	millimeters	0.04
cm	centimeters	0.4
m	meters	3.3
m	meters	1.1
km	kilometers	0.6
ARE		
cm^2	square centimeters	0.16
m^2	square meters	1.2
km^2	square kilometers	0.4
ha	hectares (10,000 m^2)	2.5
MASS (		
g	grams	0.03
kg	kilograms	2.2
t	tonnes (1000 kg)	1.1
VOLU		
ml	milliliters	0.03
l	liters	2.1
l	liters	1.06
l	liters	0.26
m^3	cubic meters	36
m^3	cubic meters	1.3
TEMPERATU		
°C	Celsius temperature	9/5 (add 3

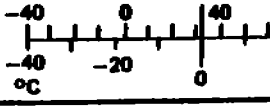

TABLE OF CONTENTS

TABLE OF CONTENTS (continued)

I. INTRODUCTION

The objective of this study is to compare the hatch corner cracking experience of the SL-7 containerships with theoretical fatigue calculations. To accomplish this, a fatigue study was performed based on the hatch corner strain-gauge data collected on the SEALAND McLEAN and the SEALAND MARKET at the various stages of service and fix-ups related to hatch corner cracking experienced during their first five years of service.

The need to publish well-documented case histories of service failures is well recognized. The series of SL-7 containerships represent a major innovation in the field of ship design (see Figures 1.1 and 1.2). Because its design departs from the traditional practice in many aspects, several local structural problems arose which conventional designs had not experienced. In particular, the cracking at the hatch corners is perhaps unique in that it occurred in one of the most intensely analyzed and instrumented ships afloat. Thus, with some additional effort, the SL-7 service experience could yield invaluable information for both designers and theoreticians.

The SEALAND McLEAN was delivered in 1972, and the first season of instrumentation was the winter of 1972-73. Although no hatch corner cracks were observed during this season, strain-gauge data were obtained within 9-12 inches of the radius out of hatch corner No. 1.

During the second winter season, on December 19, 1973, a crack was discovered at hatch corner No. 1, after a severe storm. The strain-gauge records bear the notation "Have to, wind speed 100 knots, wave height (est.) 50 ft.", and show stress excursions of up to 51.4 ksi.

The initiation site was covered by light plating, so that the crack was not visible until it had extended some 3-6 inches. During this same period, there was also green-water damage to the forecastle and flare plating.

The crack was welded, a new extension of the box girder was constructed, and additional strain gauges were installed. Their output was recorded during the third season, 1974-75, during which time additional cracking occurred at the edge of the weld. During the 1975-76 season, a doubler was added locally, which also cracked.

The final fix was designed based on the results of both global and local finite element analyses performed by ABS for the ship structure and hatch corner. Additional data were recorded during the winter of 1977-78. No further cracking occurred.

In this study, the history of the SL-7 containerships is briefly documented, with particular emphasis on the circumstances attending the hatch-corner cracks in the McLean. The occurrence or non-occurrence of similar cracks in sister ships is also noted. For purposes of evaluating the hatch corner fatigue performance, relevant ABS finite element analyses are also retrieved and summarized.

Using measured hatch-corner strain data, fatigue damage evaluations for the hatch corner, reflecting the original structure and various modifications are made based on the following three methods:

(a) Deterministic fatigue life calculations using the stress life (S-N) curves of the American Welding Society (AWS) and the American Society of Mechanical engineers (ASME).

(b) Probabilistic fatigue life calculations, using S-N curve based methods developed by Prof. Munse under the auspices of the ship Structure Committee (the Ang-Munse Model, Reference 1.1), and by Prof. Wirsching under the sponsorship of the American Petroleum Institute (the Lognormal Model, Reference 1.2).

(c) Fracture mechanics calculations of fatigue life, following an approach developed by Prof. Wirsching under ABS sponsorship, Reference 1.3.

II.HISTORY OF THE SL-7 CONTAINERSHIPS

Hatch corner damage due to stress concentration on decks of many containerships has been a well recognized problem, since the era of containership design started. With large hatch openings and usually slender fine hull form, the hull girder of a containership is subjected to torsional moment, in addition to vertical and horizontal bending moments, when the ship is heading into an oblique wave. Due attention had been given to this problem. Before the more sophisticated finite element analysis method became popular, analytical studies in this respect were limited to simplified analysis typically those performed by de Wilde and Roren based on thin-walled beam theory.

In order to meet the commercial demand of fast-going cargo ships and strong competition of sea trades, at the beginning of the 1970s, a series of eight containerships, SL-7, were built. The design of the SL-7 was started in October of 1968. Since eight ships of similar design were to be constructed during the same period of time, a great deal of effort was devoted in setting the design requirements which not only were considered to meet the need then, but also to remain competitive on the basis of speed in later years. The original design requirements as reported are as follows:

1) Speed: 33 knots (maximum sustained)
2) Breadth: to be compatible with regular Panama Canal transit
3) Number of shafts: 2
4) Draft: 30 to 34 ft, depending on particular port
5) Stability: consistent with the requirements of smaller feeder vessels

6) Port turnaround time: 24 hours (that is, discharged and load over 2000 containers in 24 hours)

A good ship design is usually a good compromise of all technical parameters and economical conditions involved. In fulfilling the above set design requirements, the designer had carried out a quite extensive study in selecting the hull form and other geometric properties in connection with optimization of speed/power and stability/trim relationships. The principal characteristics of SL-7 are:

Length overall, ft-in	946-1 1/2	(288.38 m)
Length between perpendiculars, ft-in	880-6	(268.38 m)
Length on 30-ft Waterline, ft-in	900-0	(274.32 m)
Beam, molded, ft-in	105-6	(32.1 m)
Depth to main deck, forward at side, ft-in	64-0	(19.51 m)
Depth to main deck, aft at side, ft-in	68-6	(20.84 m)
Draft, scantling, ft-in	34-8	(10.57 m)
Draft, design, ft-in	30-0	(9.14 m)
Displacement at 34 ft-8 in. LT	51,815	
Light ship weight, LT	22,915	
Ballast, crew, stores, and lube oil, LT	1,756	
Operating light ship weight, LT	24,671	
Deadweight, LT	27,144	
Shaft horsepower	120,000	
Speed, maximum knots at 30-ft draft	33	
Gross tonnage, U.S.	41,127	
Net tonnage, U.S.	25,385	

The structural design of the vessel followed well accepted structural analysis methods then available. The analysis of the initial design resulted in very high stresses and shape distortion. After analyzing several modifications, the most effective one chosen was to install a substantial full-width deck structure in way of the engine

room. Another structural feature worth mentioning is the longitudinal hatch girder. After careful evaluation by the designer, it was decided to install at the main deck a girder with a flexible end connection by welding the girder to the transverse hatch coaming at the upper end only and by eliminating the hatch coaming bracket at this location. The intention was to isolate the girder from the ship's strain. In addition, a longitudinal girder was installed at the second deck level. At that location, the girder is close to the ship's neutral axis so that the hull girder stresses are relatively low. As will be indicated later, even with this arrangement, fractures occurred on two of the SL-7 containerships at the welded connection of longitudinal girders on the main deck to the transverse bulkhead.

Among the eight SL-7 containerships, SEALAND McLEAN was one of the first two ships delivered in 1972 and the Ship Structure Committee's SL-7 Containership Instrumentation Program was initiated on this ship during the winter of 1972-73. Although no hatch corner cracks were observed during the first winter season, many occurred just one year after, repeating mostly in the same locations. In what follows, the occurrences of hatch corner or related cracks on the SEALAND McLEAN are listed in chronological order. The dates given are the survey dates, when the ship was examined and the cracks were discovered. After each occurrence, the cracks were repaired to the satisfaction of the attending surveyor of ABS. As noted later in some cases, temporary repairs were performed, with more permanent repairs being subsequently performed at a more convenient date. Summaries of hatch corner fractures and repairs are herewith described:

(1) October 31, 1973

The plating of the main deck was found cracked in the No. 1 hatch forward corners, port and starboard, and in the No. 2 hatch corner portside forward. Over the 4" to 6" length of the cracks, plating has been chipped in order to achieve a proper preparation for electric welding under pre-heated conditions. Six inch vertical cracks were found in plating of the transverse bulkhead at frame 290, just below the main deck in way of the No. 1 hatch.

The upper part of the bulkhead plating had been released from the main deck and cut-out over the width of the hatch corner. The tightness of the bulkhead was subsequently retrieved by fitting new steel boxes between frames Nos. 290/1, welded to both the bulkhead and the main deck.

(2) March 14, 1974

Cracks were found at the main deck in way of the port and starboard forward corners of the No. 1 hatch. The fractures were terminal drilled. The cracked plating was properly prepared for welding, pre-heated to 170F and welded.

The No. 1 hatch coaming was found to be fractured horizontally and vertically in way of the above deck fractures. The cracks were repaired by terminal drilling, and welding as before.

(3) March 25, 1974

The main deck in way of No. 2 hatch was found to be fractured with a 7" length crack in way of the port forward corner. The fracture was terminal drilled and repaired.

(4) April 4, 1974

A crack was found in the main deck, inboard of the coaming at the port side forward hatch corner No. 2. It was veed out, arrestor holes drilled and rewelded.

(5) October 8, 1974

The forward port and starboard corners of the No. 1 hatch coaming were found fractured at the weld connection to the main deck. The areas were veed out on both sides and rewelded.

(6) May 8, 1975

The main deck plating were found fractured at the No. 1 hatch corners, port and starboard. The fractures extended from the edge of the main deck and hatch opening outboard approximated 12" starboard side and 3" forward of the previously welded fracture. The port fracture was approximately 4-1/2" long and was 5" forward of the previously welded fracture. The longitudinal hatch girders on both sides were also found fractured at the welded connection at the transverse bulkhead.

The deck fractures were drilled at ends and veed out. The areas were pre-heated to 175F and welded. The longitudinal hatch girders at the No. 1 hatch forward port and starboard, which were fractured at the welded connection, were properly rewelded and new collars fitted and welded on newly installed section of bulkhead plating.

Upon completion of all deck repairs at the No. 1 hatch port and starboard, the reinforcing welds were ground flush and adjacent areas of deck scaled and cleaned. A new doubler plate of

1" thickness was installed on main deck at the forward corners of the hatch and plug welded, as shown in Fig. 2.1.

(7) October 7, 1976

A fracture was found inside the coaming at the port forward corner of the No. 2 hatch. The fracture started in the curved edge of the main deck at the edge of the hatch opening and extended obliquely for approximately 8". It was found that the fracture was in the weld of a previous welded repair.

As a temporary measure, a stopper hole was drilled at each end of the crack. Subsequent examinations on November 11, 1976 and December 17, 1976 by a crack detection method showed fracture to have terminated in stopper holes and no further propagation. The final repair of this crack was carried out in April 1977, while the vessel was drydocked.

(8) December 17, 1976

Fractures were found in the main deck at the port forward corner of hatch No. 1 at frame 290. Specifically,

a) The one inch reinforcing doubler was fractured from the curved corner extending approximately 19" outboard to a plug weld in the doubler.

b) Main deck fracture started at the curved corner in line with the doubler fracture, and extended approximately 4" outboard to the hatch coaming.

As a temporary measure, the deck and doubler fractures were properly prepared and welded. Radiographic examination revealed an additional fracture in the main deck, approximately 3" aft of those first noted, starting 2" outboard of the main deck corner

radius and extending outboard approximately 4". This appeared to be an old fracture and was temporarily repaired by drilling arrestor holes at each end. The underdeck longitudinal hatch girder at intersection with bulkhead 290 was fractured vertically. The fracture was properly veed out and welded.

(9) January 15, 1977

Fracture was found in the lower port forward corner of No. 1 hatch coaming, approximately 3" long and ending in the weld connecting the coaming to deck doubler.

Repairs were made by arresting fracture, scarphing out and welding.

(10) May 3, 1977

While the ship was drydocking during April 1977, the hatch corner fractures of No. 1 and No. 2 hatches, which were only temporarily repaired as described in (8) and (9) above, were dealt with as follows:

a) No. 1 Hatch Repairs

Main deck plating at forward port corner fractured in two areas for a maximum length of approximately 20", commencing at the curved portion of the hatch opening. A section of the doubler plate was removed and the fractures veed, and welded using suitable preheat and post-heat and welding procedures. The doubler plate was renewed. The under-deck longitudinal hatch girder, found fractured at the intersection with bulkhead at frame 290, was cropped and repaired.

b) No. 2 Hatch Repairs

Main deck plating at forward port and starboard corners had fractured, with the cracks being approximately 12" long starting at the curved portion of the hatch opening. Both cracks were veed and welded using suitable preheat and post-heat and welding procedures.

c) No. 1 Hatch Modification

The forward, port and starboard main deck openings at the No. 1 hatch were additionally strengthened by fitting and welding two 12" x 1-7/8" face plates of EH32 at the main deck, as shown in Figure 2.2.

(11) February 9, 1978

a) The main deck plating was found fractured in the curved corners of the No. 2 hatch at the port forward corner and at the starboard forward corner as follows:

i) Port fracture extending outboard obliquely approximately 4-3/4".

ii) Starboard fracture extending outboard obliquely approximately 9-1/2".

The areas surrounding both fractures were dye checked to determine the extent of each fracture. An additional crack was found underdeck approximately 1" inboard of the above port fracture, starting 1-1/2" from curved corner and extending outboard obliquely approximately 2".

As temporary repairs, stopper holes were drilled at the ends of each fracture, properly prepared and welded using suitable preheat, post-heat and welding procedures.

b) The starboard forward corner of No. 3 hatch was found fractured near the main deck just inboard of the welded connection of the transverse box girder and the longitudinal hatch side girder.

The area surrounding the vertical crack was dye checked to determine the end of the crack and a temporary arrestor hole drilled to allow the vessel to proceed on its current voyage. A proper repair was done in April 1978, at which time the crack was veed out and rewelded using approved procedures.

(12) March 16, 1978

The main deck plating was found fractured in the starboard forward corner of the No. 1 hatch at frame 287 in way of the fillet weld of the toe of the face plate to the main deck. The fracture extended outboard obliquely approximately 1-1/2".

A stoppper hole was drilled at the end of the fracture, the fractured area was properly prepared and welded using suitable preheat, postheat and welding procedures.

(13) April 15, 1978

Examination of the area surrounding the fracture described in (11) (b) was carried out and a small crack in the hatch coaming directly above the fracture noted in (11) (b) was dye checked to determine its end. It was veed out and rewelded.

(14) October 8, 1981

Upon examination, cracked welding of 20" was found at portside forward No. 1 hatch corner doubler plate and hatch coaming reinforcement face bar alongside the coaming. A crack in

the doubler plate was found in way of the middle of the hatch coaming corner, vertical to the first crack in the horizontal plane, extending into the main deck about 4".

The cracks were veed out and rewelded after preheating welding area. Hatch coaming was partly cropped to enable repair to be carried out. After repairs the cropped coaming part was refitted.

(15) October 15, 1981

A crack of approximately 7" on the main deck was found at port side forward corner of the No. 2 hatch, inside the hatch coaming and diagonally towards the vertical coaming but not under the coaming.

The end of the crack was located by dye check and drilled. The deck was pre-heated and the crack was welded.

(16) December 7, 1981

The deck plate in way of the starboard forward corner of hatch No. 2 was found fractured over a length of approximately 10". The crack was drilled off, veed out and ground smooth. The plating was pre-heated up to 100 C and welded with low hydrogen electrodes type and slowly cooled down. Before repair the hatch coaming plate in way of the hatch corner had been cropped and partly removed. Upon completion, the removed plate of the hatch coaming had been rewelded in place, tested and proven tight.

Based on available information, the occurrence and non-occurrence of similar hatch corner cracks in other SL-7 class ships, SEALAND GALLOWAY, SEALAND COMMERCE, SEALAND EXCHANGE, SEALAND TRADE, SEALAND FINANCE, SEALAND MARKET and SEALAND RESOURCE have been reviewed. The

hatch corner damages on these vessels and the SEALAND McLEAN are summarized in Table 2.1. The data shown indicate that:

1. The first two hatch openings, No. 1 and No. 2, particularly No. 1, were vulnerable to hatch corner damages.
2. The forward hatch corners of No. 1 and No. 2 hatch openings are far more vulnerable than the aft corners.
3. The forward hatch corners of No. 1 hatch opening reinforced with doublers were almost equally vulnerable as the as-built ones.
4. After the final fix, with the forward hatch corners reinforced with a face plate and doubler, further cracking at No. 1 hatch corner was found on the SEALAND McLEAN. Some further cracking at No. 1 hatch corner was also found on the SEALAND GALLOWAY.
5. Experience with the other SL-7 class containerships in general, as described in Items 1 through 4, are quite similar to the damage occurrences on the SEALAND McLEAN.
6. The SEALAND FINANCE had no reported local damage and the SEALAND EXCHANGE had but one reported damage occurrence which is much less than that of their sisterships. One possible reason for this may be that their trade routes were more favorable than that of the other sisterships.

III. FULL-SCALE INSTRUMENTATION PROGRAM

III.1 Full-Scale Instrumentation of the SL-7 Class of Containerships

Immediately after the S.S. SEALAND McLEAN, the first SL-7 containership, was delivered in 1972, a multifaceted program of data collection and analysis, coordinated by the Ship Structure Committee, was instituted to study this ship's structure and its response to imposed loading. One important facet of this program was an extensive onboard instrumentation system with strain gauges located in various areas of interest throughout the vessel. Details of this strain gauge system are given in Reference [3.1]. In addition, a microwave radar was developed and installed to measure wave elevations. After the installation of the instrumentation was completed, a deckside calibration was carried out by Teledyne Materials Research Company and reported in Reference [3.2]. Subsequently, a large amount of stress data has been acquired for three consecutive winter seasons of operation on North Atlantic voyages between September 1972 and March 1975. Some sample results are presented in References [3.3, 3.4, and 3.5]. The wave meter data was analyzed by Dalzell [3.6].

It is noted that a significant amount of new strain gauge instrumentation was installed for the third season data acquisition program. The location of these gauges were selected based on observation of any local damage that may have occurred in the first two years of vessel operation. Specifically, radial cracks from the forward and some aft hatch corners and green water set-down of the forecastle and flare plating had been experienced. It is noted that the instrumentation at hatch corner No. 1 was not installed until 1975, the

year in which the McLEAN's third season data acquisition program was conducted.

In 1976, in order to evaluate the effects of the final fix of the crack of the hatch corner No. 1 designed according to recommendations of ABS, installation of instrumentation was made on both hatch corners of the SEALAND MARKET with one side so modified and the other unmodified. The data acquisition was carried out on the vessel's North Atlantic voyages during the last quarter of 1976. Sample results are presented in Reference [3.7].

In 1977, new gauges were reinstalled onboard the McLEAN at both hatch corners with the final fix [3.8]. This time, the measurement was conducted during the vessel's North Pacific voyages to evaluate the effect of one modified side on the other. The first set of measurements was taken during the period May 1977 to July 1977. The results were reported in Reference [3.8]. Subsequently, in order to further study the effectiveness of the improvement and facilitate comparisons between finite element calculations and full-scale strain measurements, ABS requested that strain data be acquired at several additional locations around the hatch corner modification. In September 1977, Teledyne appropriately re-configured the instrumentation on the hatch corner. The data was collected on the subsequent Pacific voyages during the period September 1977 to January 1978. Some measured results are presented in Reference [3.9].

III.2 Strain Gauge Data for Hatch Corner No. 1

The strain gauge data collected at the hatch corner as well as the other locations of the SL-7 class of containerships were obtained from an automatic turn-on every four hours with the recording lasting 32

minutes. The recording consists of 30-minutes of data recorded automatically, preceded by a one-minute electrical zero and a one-minute period of calibration signals (see Fig. 3.1). Provisions were made to carry out continuous recording during periods of rough seas.

The bulk of the data have never been reduced or analyzed prior to the present fatigue study. Data available include the following:

1. SEALAND McLEAN (original design), January to March 1975, approximately 300 intervals. (Gauges mounted on port side only as shown in Fig. 3.2.)
2. SEALAND MARKET, October to December 1976, 300-350 intervals. (Hatch modified on one side, with gauges mounted on both sides as shown in Fig. 3.3.)
3. SEALAND McLEAN, May to July 1977, approximately 300 intervals. (Hatch modified on both sides with gauges mounted on both sides as shown in Fig. 3.4.)
4. SEALAND McLEAN, September 1977 to January 1978, 499 intervals. (Hatch modification and gauge locations as shown in Figure 3.5, similar to Item 3.)

It is noted that readings from all gauges were recorded simultaneously for each 30-minute interval. The total number of time history records (equal to the number of gauges multiplied by the number of intervals) exceeds 15,000.

With the intent to present some of the more significant trends derived from each operational season and to facilitate future retrieval of data, Teledyne has performed an analysis of certain segments of the data. The important indications from the sample analysis [3.5, 3.6, 3.7, 3.8 & 3.9] are as follows:

1. The hatch corners exhibit high stress levels (especially in quartering seas) even under moderate wave conditions. The stresses are primarily induced by torsional loads arising in part from roll motions of the vessel.

2. The data indicates that the vessel after docking exhibits stillwater stresses up to about 10 ksi at the gauge locations.

3. The highest circumferential normal stresses around the forward hatch corner occur generally at or near a location 22.5° around the cut-out measured forward from abeam towards the ship centerline on both starboard and port sides (see Fig. 3.2). The gauges at these locations are gauges 2 and 8 of SEALAND MARKET and gauges 2 and 8 of SEALAND McLEAN during the operational period May 1977 to July 1977; and gauges 3 and 8 of SEALAND McLEAN during the period September 1977 to January 1978. The exception during McLEAN's third operational season is the occurrence of the highest stresses at the gauge Fyb located at 45° around the cut-out measured forward from abeam toward the ship's centerline.

4. The reduction in stress, due to the reinforcement recommended by ABS, measured at the deck's median edge is between 10 and 25 percent and it averages about 15 percent.

5. A high degree of correlation exists between dynamic stresses measured at the corresponding port and starboard sides in those cases where both sides were instrumented with strain gauges.

IV. ABS FINITE ELEMENT ANALYSES

IV.1 ABS Finite Element Analyses of the SL-7 Containership

In order to identify critical regions for installation of strain gauges, a finite element analysis of the entire ship hull [4.1], using the ABS/DAISY computer program system [4.2] was carried out at the planning and installation stage of the instrumentation program for SEALAND McLEAN in 1972. In that study [4.1], the deck longitudinal stresses accentuated due to the presence of warping restraint at the locations with abrupt changes in deck stiffness were determined. However, the analysis did not at that time include the locations in way of the forward hatch corners.

Although the predicting of structural response due to quasi-static loads using the finite element method had been well tested and verified with full-scale and model experimental results in the 1960s, it was still desirable to further validate the analysis procedure and modelling techniques in dealing with such a special structure as an open-deck containership. Accordingly, ABS performed a structural analysis of the SL-7 steel model, using a three-dimensional finite element model representing the entire steel model. The calculated results, together with a comparison with experimental data, were presented by Elbatouti, Jan and Stiansen in Reference [4.3]. The predicted hull-girder response to both bending and torsional loads was found to be generally in good agreement with the measured results. This indicated that the modelling technique employed this study were considered satisfactory. In Reference [4.3], the effect of a heavy faceplate, 12" by 2", around the

cut-out of the forward hatch corner with actual ("prototype") ship was also studied.

Wave-load prediction for the SL-7 containership using the shipmotion computer program SCORES had been successfully verified with appropriate model test results [4.4, 4.5, and 4.6]. Subsequently, a correlation study of predicted dynamic stresses with measurements onboard ships at sea was conducted by ABS. Reference [4.7] summarizes the work comparing stresses calculated using the finite element method with those measured onboard the SEALAND McLEAN during both first and second seasons between September 1972 and October 1973. Comparison was made for four different and progressively more severe conditions; namely, dockside calibration, RMS stresses in head seas and instantaneous stresses in head and oblique seas. It is noted that the calculated and measured stress results at the rosette gauge locations in way of the forward hatch corner were also included in this study.

Responding to the request of SEALAND for guidance on eliminating the cracking of the forward hatch corner, ABS performed an extensive 3-D finite element study of the hatch corner. The procedure and results of the analysis of various hatch corner configurations are presented in Reference [4.8]. Nineteen possible designs of hatch corner structural configurations were investigated to determine the most effective design for limiting the stress concentrations occurring at the hatch corner cut-out. The loads on the structure are those resulting from the vessel being subjected separately to a maximum torsional moment and a maximum vertical bending moment. The parameters considered in the models were the shape of the hatch corner cut-out, the scantlings and configuration

of the hatch coaming and hatch girder and the use of doublers or insert plates for the deck.

IV.2 Summary of Results of the Forward Hatch Corner No. 1

According to the review in Section IV.1 of this report, the ABS finite element analyses of the SL-7 class containership include:

(i) Structural analysis of SL-7 containerships under combined loading of vertical, lateral and torsional moments [4.1].

(ii) Structural analysis of a containership steel model and comparison with the test results [4.3].

(iii) Comparison of stresses calculated using the DAISY system to those measured on the SL-7 containership instrumentation program [4.7].

(iv) Hatch corner study for the SL-7 containership. By retrieving both published and unpublished finite element analysis results, it was found that all but item (i) have the results relevant to the forward hatch corner No. 1. The results are summarized as follows:

IV.2.1 Hatch Corner Stress Results from Structural Analysis of a Containership Steel Model [4.3]

In the analysis of the SL-7 steel model [4.3], the hatch corner finite element model was created according to the actual ship's scantlings rather than to the steel model's. Figure 4.1 shows the calculated stress distribution around the contour of the circular cut-out of Frame 290. The stress concentration factor for torsional loading (Loading Case 2) is equal to 2.3 compared with 1.33 for the vertical bending moment (Loading Case 1). Different local structural

modifications were investigated for both loading cases. The addition of a heavy faceplate, 12 x 2 in., around the cut-out, has proven to be most successful in reducing the stress magnitudes. In such a case, the stress concentration factor decreases from 2.3 to 1.73 for torsional loading and from 1.33 to 1.19 for vertical bending, Fig. 4.1.

IV.2.2 Hatch Corner Stresses from Correlation Study of Finite Element Analysis and Onboard Measurements of the SL-7 Containership at Sea [4.7]

In Reference [4.7], the results relevant to the hatch corner at Frame 290 were only selectively presented. Through retrieving the computer print-out of the analysis, a complete set of results has been compiled for the eighteen wave load conditions given in Table 4.1. Stresses along the hatch corner cut-out, expressed in terms of RAO (stress per unit wave height), are shown in Table 4.2 for the 18 loading condition. It is noted that the first 12 wave conditions in head seas are for vertical bending only while the last 6 wave conditions in oblique seas can give rise to substantial torsional and lateral loading. An examination of the results reveals the following:

(i) The calculated RAO stresses from the study are found to vary significantly among the 18 wave conditions considered. The RAO stresses are generally higher in the oblique sea conditions as compared to that for the head sea conditions.

(ii) For head sea conditions (L.C. 1 to L.C. 12) in which the vessel is subjected to vertical bending, the highest stress generally occurs at the cut-out edge between 0^{o} and 30^{o} around the cut-out measured forward from abeam towards the ship centerline and the stress

concentration factor (SCF) for the detail is in the range of 1.48 to 1.9.

(iii) For oblique sea conditions (L.C. 13 to L.C. 18) in which the vessel is mainly subjected to torsion, the highest stress occurs at the cut-out edge between 30^{o} and 60^{o} around the cut-out measured from abeam towards the ship centerline, and the SCFs are in general higher than that in head seas, with the highest SCF equal to 2.6.

IV.3 Hatch Corner Stress Results from Hatch Corner Study of the SL-7 Containership [4.8]

The hatch corner stress results in Reference [4.8] are obtained for the vessel subjected separately to a maximum torsional moment and a maximum vertical bending moment. Nineteen possible designs of the hatch corner structure as shown in Table 4.3 were investigated. Model 5 represents the original design and Model 13 is the design used for the "final fix" of the hatch corner crack. The stress results are given in Figure 4.2. A comparison of the two sets of results shows the following:

(i) For the detail of original design, the highest stress induced by vertical bending occurs at the cut-out edge between 0^{o} and 30^{o} around the cut-out measured forward from abeam toward the ships centerline while that induced by torsion occurs at the cut-out edge between 15^{o} and 45^{o}.

(ii) In both loading cases, the highest stresses for the detail of "final fix" design occur at the same locations as the highest stresses for the detail of the original design.

(iii) The "final fix" reduces the stress concentration factor from 3.3 to 1.7 for torsional loading and from 2.2 to 1.2 for vertical bending.

In this study [4.8], the effects of the use of a doubler or an insert plate for the deck and the variations in other parameters were obtained. Presented in Table 4.4 is a comparison of the maximum stresses at the cut-out contour for ten of nineteen designs considered in Reference [4.8].

V. REDUCTION AND VERIFICATION OF HATCH CORNER STRAIN DATA

V.1 Hatch Corner Strain Data Retrieval and Reduction

As previously stated, approximately 15,000 30-minute time histories were available for SEALAND McLEAN and SEALAND MARKET for voyages during the period from January 1975 to January 1978. To reduce the data ensemble to a manageable size, it was decided that only the data associated with locations of maximum stresses, would be evaluated. Thus, the data recorded on SEALAND McLEAN corresponding to Gauge F_yB before May 1977, and those corresponding to Gauges 2 and 8 before August 1977 and Gauges 3 and 8 after August 1977, as well as those corresponding to Gauges 2 and 8 on the SEALAND MARKET were acquired for this study. Gauge locations are shown in Figures 3.2 through 3.5.

The total number of the selected time history intervals was about 2600. However, the actual number of intervals processed was 1327 (see Table 5.1). The reason for this, in part, is that some intervals recorded on the SEALAND McLEAN did not have the needed calibration factors on the analog tapes. Furthermore, for about half the intervals, the vessel's log books did not have corresponding Beaufort sea state description indicated. Such data can not be used for construction of the composite histogram. In addition, some intervals were of questionable quality due probably to failure of tranducers during data reduction.

Using a Fast Fourier Transform (FFT) analyzer, Teledyne produced amplitude spectra from the data stored in analog form. Before reducing all needed spectra, a small sample of the selected data was first reduced for inspection.

By examining the general characteristics of the sample amplitude spectra, the required resolution, and range of frequency of interest were redefined. Also, other pertinent information that should be utilized to produce the needed amplitude spectra were specified. It is noted that each spectrum was reduced from an 800-second segment of a 30-minute time history. This was judged adequate by Teledyne in view of the signal stabilization characteristics in the process. Each reduced spectrum contains 256 ordinates in the frequency range of 0 to 0.32 Hertz with a frequency increment equal to 0.00125 Hertz as shown in Figure 5.1. The ordinate is in volts. A one volt RMS sinosoidal wave input to the analyzer will produce a spectral ordinate of 1 volt at the corresponding frequency. The scale factors used to convert the voltage units to stress units are given in Table 5.2. The digitized spectral data was printed in the form as in Table 5.3. It is noted that storing the digitized spectral data on a tape, in addition to plotting and printing on paper, is desirable for such large amount of data, in order to expedite data processing. Accordingly, the data was stored on Hewlett-Packard tapes. A cross reference of the H-P tapes by file number to the analog tapes and interval numbers is presented in Tables 5.4 through 5.7. In the tables, the Beaufort seastate numbers for the intervals reduced are also included. The processed data stored on the H-P tapes were finally transmitted to the IBM computer system at ABS.

V.2 Data Verification

In light of the fact that the measured data, except for limited samples found in the Teledyne reports [3.5, 3.7, 3.8, 3.9], have never been reduced from the analog tapes, a credible verification of the data was judged necessary prior to using such data in the present

investigation. Of particular importance is to ascertain the correctness and interpretation of the scale factor.

The difference between the forms in which the reduced data and the original data were given further manifests the need for verification. In addition, as noted in Section V.1, the reduced data represent just an 800-second segment of the original 30-minute time history in which the location of the segment could not be identified. The following four steps were thus taken for data verification:

(i) Using the spectra, calculate the most probable extreme values

(ii) Generate time history simulation from the spectral data (without phase angles).

(iii) Reconstruct time histories from spectral data with corresponding phase angles.

(iv) Independently produce spectral data from a limited sample of time histories digitized using a different FFT computer program.

The results obtained for the most probable extreme values, the time histories and the spectral data for some selected intervals were respectively compared with the maximum stresses, time histories and the spectral data for the corresponding intervals either shown in Teledyne reports [3.5, 3.7, 3.8, 3.9] or specially requested at that time. The phase angle data required in Item (iii) were also specially requested for the purpose.

V.2.1 Verifying Data Through Calculation of Most Probable Extreme Values

Before the calculation of the most probable extreme values of any interval record, the amplitude spectrum corresponds to the record was converted to an energy spectrum. The conversion method is described in Section VI.1.

The most probable extreme values (peak-to-trough) is given by the following equation [5.1]:

$$S_o = 2\sqrt{2m_o \ell n \left\{ \frac{T}{4\pi} \frac{1 + \sqrt{1 - \varepsilon^2}}{\sqrt{1 - \varepsilon^2}} \sqrt{\frac{m_o}{m_4}} \right\}} \qquad (5.1)$$

where

ε = bandwidth parameter of the energy spectrum equal to

$$\sqrt{1 - \frac{m_2^2}{m_o m_4}}$$

m_o, m_2, m_4 = zeroth, 2nd and 4th moments of the energy spectrum, respectively.

T = time in second

The most probable extreme values calculated for some selected intervals, and the maximum stresses for the corresponding intervals given in the Teledyne reports [3.5, 3.7, 3.8, 3.9] are presented in Table 5.8. Comparison of the results shows that for the same intervals the calculated most probable extreme values are generally less than the measured maximum stresses. The reasons for this are as follows:

(a) The amplitude spectrum may not have been reduced from the 800-second segment containing the highest peak value of the original 30-minute interval record.

(b) Theoretically, the most probable extreme value is likely to be less than the maximum value.

V.2.2 Verifying Data Through Time History Simulation

A computer program was developed which produces a sample time history from a given amplitude spectrum. It is noted that the ordinates of the spectrum are RMS values of a sine wave therefore the simulation is constructed by adding the K harmonic components:

$$y(t) = \sum_{i=1}^{K} \sqrt{2}\, Y_i \cos\,(2\pi\, f_i t + \phi_i) \qquad (5.2)$$

where

f_i = the midpoint of a spectral frequency increment Δf

y_i = ordinate of the amplitude spectrum

and

ϕ_i is a random phase angle having a uniform distribution, between 0 and 2π.

Using Eq. (5.2), time history simulations were generated from the amplitude spectra representing the selected intervals of Table 5.8. A typical time history simulation is given in Fig. 5.2 while the corresponding amplitude spectrum is shown in Fig. 5.1. A sample comparison of the simulation and the corresponding original time history can be seen in Figs. 5.2 and 5.3. Figure 5.3 is obtained from a

Teledyne report [3.5]. In general, the original and regenerated simulation of time histories are similar both in shape and in amplitude.

V.2.3 Verifying Data Through Reconstruction of Time History

Reconstruction of a time history was again based on Eq. (5.2) except that the actual phase angle corresponding to a spectral ordinate for a selected interval as specially provided by Teledyne was used. The reconstructed time history is shown in Fig. 5.4. The reconstructed time history exhibiting a beating phenomenon and does not resemble the original time history.

V.2.4 Verifying Data Through Reconstruction of Amplitude Spectrum by Digitizing Original Time History

An FFT digital computer program was utilized to reconstruct the amplitude spectrum based on the digitized data of an original time history. It should be noted that the amplitude spectrum ordinate in this case is not the RMS value of a sine wave and is an actual amplitude of a sine wave. Figure 5.5 represents a time history plot for a set of data obtained by manually digitizing an 800-second segment from the whole interval time history shown in Fig. 5.3. An amplitude spectrum for the time history of Fig. 5.5 is given in Fig. 5.6. A comparison of the Teledyne provided spectrum shown in Fig. 5.1 and the reconstructed spectrum in Fig. 5.5 reveals that both spectra are similar in both shape and amplitude, with the sine wave amplitude value converted to the sine wave RMS value.

V.3 Experience Related to Data Verification

In the process of data verification some difficulties were encountered arising from the fact that interpretation of the spectral

data was not straightforward, and that incorrect scale factors and substituting data were sometimes provided.

Another point of note, regarding the data verification process, is that the ordinates of the reduced spectral data corresponding to the first two lowest frequencies should be disregarded since they are an aberration due to a mean value present in the analog signals.

VI. FATIGUE STRESS HISTOGRAMS

To obtain stress histograms for the fatigue study, the amplitude spectra provided by Teledyne, as described in Section V.1, were first converted into energy spectra. For a given series of strain gauge data, the number of occurrences of cyclic stresses were then calculated based on the characteristic parameters of the energy spectra. Since no measurement data for the selected intervals in this study refer to high Beaufort sea states, such as seastates No. 10 through 12, curve fitting of a generalized gamma distribution for the number of stress occurrences was performed. The parameters of the distribution obtained from the stress occurrences associated with the lower seastates through curve fittings were then used to extrapolate for the stress occurrences for the high seastates. Subsequently, composite stress histograms were obtained from the cyclic stress occurrences with the corresponding probabilities of occurrence of the various seastates No. 1 through No. 12. Such construction of the required histograms is described in detail below.

VI.1 Data Categorization for Fatigue Load Cases

In order to determine the fatigue damage of the hatch corner of the original design and the "final fix" as accurately as possible, the reduced data were categorized as shown in Table 6.1. Following the data categorization, five load cases were obtained for fatigue damage analysis. It should be noted that the data sets of the two seasonal operations of the SEALAND McLEAN during 1977 and 1978 were combined, since between these two operations the hatch corner cut-out details and the strain measurement system were unchanged, although the gauge numbers

may in some instances differ such as that at the starboard side hatch corner.

VI.2 Conversion of Amplitude Spectrum to Energy Spectrum

As noted in Chapter V, the amplitude spectral data provided were derived from the strain time histories using an FFT analyzer. During data reduction, for a given frequency, a spectral ordinate of one volt is produced for a one volt RMS sine-wave input to the analyzer. Thus, within a resolution bandwidth Vf centered at a frequency f, the RMS value of the time history x(t) is related to the amplitude spectrum by

$$\hat{\psi}_x\ (f,\Delta_f) = [\frac{1}{T} \int_o^T x^2\ (t,f,\Delta_f)dt]^{1/2} \qquad (6.1)$$

where $x(t,f,\Delta_f)$ represents the narrow-band filter output and T is the averaging time interval. The energy or power spectral density function can then be estimated by

$$\hat{G}x\ (f) = \frac{1}{\Delta_f T} \int_o^T x^2\ (t,f,\Delta_f)dt = \frac{\psi_x^2(f,\Delta f)}{\Delta_f} \qquad (6.2)$$

A typical energy spectrum obtained from the amplitude spectrum shown in Fig. 5.1 is given in Fig. 6.1.

VI.3 Estimation of Number of Cyclic Stress Occurrences

For a certain specified level of a Gaussian random process x(t), the number of cyclic stress occurrences can be estimated from only the statistical properties of the maxima with positive value, since the statistical properties of the minima with negative values are the same

as those of the maxima with positive values. The cumulative distribution of the maxima at a specified level, $x(t) = \xi$ can be defined as [5.1].

$$F(\xi) = \frac{2}{1 + \sqrt{1 - \varepsilon^2}}\left[\frac{1}{2}\left(1 - \sqrt{1 - \varepsilon^2} + \phi\left(\frac{\xi}{\varepsilon\sqrt{m_o}}\right) - \sqrt{1 - \varepsilon^2}\exp\left(-\frac{1}{2}\left(\frac{\xi}{\sqrt{m_o}}\right)^2\right)\right.\right.$$

$$\left.\left.\cdot\left(1 - \Phi\left(\frac{-\sqrt{1 - \varepsilon^2}}{\varepsilon}\frac{\xi}{\sqrt{m_o}}\right)\right)\right] \quad , \qquad o \le \xi < \infty \qquad (6.3)$$

where

$$\varepsilon = \sqrt{1 - \frac{m_2^2}{m_o m_4}}$$

$$\Phi(\mu) = \frac{1}{\sqrt{2\pi}}\int_{-\infty}^{u} e^{\frac{-\mu^2}{2}}\, du$$

$$m_o = \int_o^\infty \hat{G}_x(f)df$$

$$m_2 = \int_o^\infty f^2\, \hat{G}_x(f)df$$

$$m_4 = \int_o^\infty f^4\, \hat{G}_x(f)df$$

where ε is the bandwidth parameter of an energy spectrum, $\Phi(\mu)$ is the cumulative normal distribution function and mo, m2 and m4 are the

zeroth, second and fourth moments of the energy spectrum, respectively. Thus, the number of occurrence of maxima above the specified level x(t), ξ can be calculated as:

$$\bar{N}_{\xi} = \bar{N}_{m>o} \cdot F(\xi) \tag{6.4}$$

where $N_{m>o}$, the total expected number of positive maxima per unit time has the expression as

$$\bar{N}_{m>o} = \frac{1}{4\pi} \left(\frac{1 + \sqrt{1 - \varepsilon^2}}{\sqrt{1 - \varepsilon^2}} \right) \sqrt{\frac{m_2}{m_o}} \tag{6.5}$$

In case the random process x(t) has a narrow-band spectrum $\varepsilon = o$, the $F(\xi)$ will become the Rayleigh cumulative distribution function expressed as

$$F(u) = 1 - e^{-\xi^2/2m_o} \tag{6.6}$$

whereas the expression for the total number of expected positive maxima becomes

$$\bar{N}_{m>o} = \frac{1}{2\pi} \sqrt{\frac{m_2}{m_o}} \tag{6.7}$$

In this study, the approach using the "equivalent narrow-band approximation method for calculating fatigue damage in a wide band

proven" [6.1] was utilized. The method utilizes cycle counts based on the Rayleigh cumulative distribution function, Eq. (6.6). A fatigue damage correction factor that depends on the proven bandwidth is used to adjust the damage calculated for the narrow-band case. The correction factors were derived in [6.1] using the rainflow cycle counting technique on simulated wideband time histories.

On the basis of the narrow band stationary Gaussian process assumptions, the results for number of cyclic stress occurrences are obtained and tabulated in Tables 6.2 through 6.6. Beside the number of stress cycles the bandwidth parameter of each interval was also calculated. Its average value was obtained for each sea state for purposes of determining the Bandwidth correction factor in the calculation of the fatigue damage.

VI.4 Extrapolation of Cyclic Stress Occurrences

In Tables 6.2 through 6.6, the number of cyclic stress occurrences for certain Beaufort seastates are not given due to the lack of data. To fill the gap, a statistical analysis of the cyclic stress occurrences shown in the tables is necessary at the first step.

For this purpose, the partial histogram corresponding to a typical seastate is fitted with a generalized gamma density, which is given by,

$$f(s) = \frac{q}{\Gamma(p)} \, r^{qp} s^{qp-1} e^{-(rs)^q} \qquad 0 \le s < \infty \tag{6.8}$$

in which s denotes the stress range which is equal to the double magnitude of stress amplitude, and p, q and r are the three parameters of the distribution function.

A method proposed by Stacy and Mihram [6.2] has been used for estimating the parameters of the generalized gamma distribution. The method determines the parameters by equating the three logrithmic moments of the measured data to the corresponding theoretical moments. A typical curve fitting of partial histograms is shown in Figures 6.2(a) through 6.2(c).

The fitted distribution functions for the partial histograms are then used for purposes of obtaining by extrapolation the parameters of the distribution function for the unknown partial histograms. Table 6.7 presents the values of both the fit and the extrapolated parameters for all cases. Figures 6.3(c)through 6.3(c) represent plots of extrapolating the parameters for a typical case.

The extrapolated partial histogram is given by

$$n_{ij} = n_j \left[F(s_{i+1/2}) - F(s_{i-1/2})\right] \tag{6.9}$$

where

n_{ij} = number of cyclic stress occurrences per interval at a stress range S_i and a Beaufort seastate No. j

n_j = total number of cyclic stress occurrences per interval at a Beaufort seastate No. j

and

$$F(s) = \int_0^s f(s)ds = \frac{1}{\Gamma(p)} \int_0^{(rs)^q} u^{p-1} e^{-u} du = \frac{\Gamma_{(rs)^q}(p)}{\Gamma(p)} \tag{6.10}$$

is the cumulative distribution function of the generalized gamma density as given in Eq. (6.8).

In Eq. (6.9), n_j was obtained through extrapolating the total numbers of cyclic stress occurrences of the known partial histograms. The partial histograms associated with all the Beaufort sea states are obtained and presented in Tables 6.8 through 6.12.

VI.5 Long-Term Composite Histograms

VI.5.1 Probability of Occurrences of Seastates

The probability of occurrence P_j for Beaufort seastate j required in the construction of the fatigue histograms should be developed based on the best available information. In this study, only the North Atlantic route (New York, Northern North Sea) was considered. Due to the lack of established wave climate records, the data reduced from that recorded on SEALAND McLEAN North Pacific voyages after 1975 was utilized together with the probability of occurrence of the North Atlantic route to obtain the composite stress histogram for fatigue analysis.

Wave data and their pattern in the North Atlantic regions are relatively well established and recognized. The principal source, the Navy's Fleet Numerical Weather Central Project [6.3] was used in this study. The Marsden squares along typical shipping routes were identified and the associated probability of occurrence was properly weighed. Results were presented in Fig. 6.4 and Table 6.13, for seastates up to Beaufort 12.

VI.5.2 Construction of Long-Term Composite Stress Histogram

If P_j denotes the probability of occurrence of a Beaufort seastate j, the number of expected long-term composite cyclic stress occurrences

at a stress range level S_i is represented by n_i, which can be obtained as

$$n_i = \sum_{j=1}^{12} n_{ij} P_j \cdot (108\ T) \qquad (6.11)$$

where the number of 108 represents the number of 800-second intervals per day if stress data were measured continuously. T is the total number of ship days in 20 years estimated based on the assumption that the ship operates at sea 75 percent of a year or 272 days per year, (that is, T is the product of 272 and 20).

For the five fatigue load cases, the long-term composite stress histograms calculated based on Eq. (6.11) are given in Tables 6.14 and 6.15. It should be noted that these results are based on the linear elastic theory. To convert them into a stress scale, the stress-strain relationship for the material of the hatch corner details, ABS-EH33 steel, should be employed. In this study, the nonlinear cyclic stress-strain relationship for the ABS-EH36 steel, shown in Fig. 6.5, was used instead, since the relationship for EH33 was not readily available, but the differences, if any, are thought to be small. The results for the long-term composite histograms in a stress scale based on the nonlinear stress-strain relationship are given in Tables 6.16 and 6.17. Figures 6.6 through 6.10 present histograms to which the Weibull and the generalized gamma distributions were fit. The Weibull and the generalized gamma curve fits were used in Munse's method of detail characterization for estimating the fatigue strength of the hatch corner details.

VII. FATIGUE ANALYSIS AND RESULTS

In this study, fatigue damage hindcast for the hatch corner of the SL-7 containerships was pursued using the following methods:

1) AWS and ASME S-N curve based analysis

2) Wirsching's method of reliability-based fatigue analysis

3) Munse's method of ship detail characterization

4) Fracture mechanics based method

A summary of the procedures are presented below together with results obtained and discussion of results.

VII.1 AWS and ASME S-N Curves Based Analysis

AWS Fatigue Stress Provisions [7.11]

The AWS fatigue stress provisions, where applicable, comply with the Highway Bridge Design Standard of the American Association of State Highway and Transportation Officials (AASHTO), and the Specification for Steel Railway Bridge of the American Parkway Engineering Association (AREA). The major specifications are described as follows:

(i) Full use of the live load and impact stress range concept, instead of the maximum allowable stress based on stress ratio R, and tensile strength of steel.

(ii) Material subjected to fluctuating compressive stresses is exempt from fatigue design requirements.

(iii) For bridges subjected to cyclic loading, other than highway or railway applications, stress ranges may be obtained for the appropriate condition and cyclic life using the six basic categories shown in Figs. 7.1(a) and 7.1(b).

It is noted that the S-N curves for redundant structures in Figs. 7.1(a) and those for non-redundant structures in 7.1(b) are valid for constant amplitude loading. In the case of variable amplitude loading, the S-N curves in the figures can be applied disregarding the endurance limit [7.21]. The S-N curves for redundant structures (Fig. 7.1a) represent 95% confidence limits for a 95% survival of test data [7.3], whereas the S-N curves for non-redundant structures (Fig. 7.1b) were obtained from the S-N curves for redundant structures by imposing an additional factor of safety. The factor of safety varies with fatigue stress range; for example, the value decreases from 7.6 at 60 ksi to 3.6 at 24 ksi for "Category A" S-N curve.

ASME Fatigue Stress Provisions [7.4]

The ASME specifications for design based fatigue analysis are mainly applicable to pressure vessels. The given design fatigue strength curves for different materials represent the strain cyclic fatigue data. In these S-N curves, as typical ones shown in Fig. 7.2, the allowable amplitude S_a of the alternating stress component (one-half of the alternating stress range) is plotted against the number of cycles. This stress amplitude is determined based on the assumption of elastic behavior and is given in terms of stress, but it does not represent a real stress when the elastic range is exceeded. The fatigue curves are obtained from uniaxial cyclic strain data in which imposed strains have been multiplied by the modulus of elasticity and a design margin has been provided.

Stresses produced by any load or thermal condition which does not vary from cycle to cycle need not be considered since they are mean

stresses and the maximum possible effect of mean stress is included in the design curves.

It is noted that the effect of cyclic compression loads considered in these provisions is different from that of AWS Code.

Cumulative Damage Hypothesis

With the AWS and ASME S-N curves, the Palmgren-Miner's linear cumulative damage rule is applied for the determination of fatigue damage. The Miner's rule can be expressed as:

$$D = \sum_{i=1}^{I} \frac{n_i}{N_i} \tag{7.1}$$

where n_i is the composite stress cycles and Ni is the stress cycles to failure at a given stress range or stress amplitude.

Selection of S-N Curves

In this study, two S-N curves were utilized in conjunction with the composite stress histograms obtained in Chapter 6. One is the AWS Category A S-N curve for non-redundant structures as shown in Figure 7.1(a). The other is the ASME curve for steel with ultimate strength less than 80 ksi as shown in Fig. 7.2. It is noted that the selected AWS curve gives the fatigue strength of a plain steel member with cleaned surface and oxygen-cut edges subjected to a reversal of end loads, where the member is a non-redundant structure. Although the hatch corner cut-out detail is not a non-redundant structure, to be conservative the S-N curve for non-redundant structures was selected instead of that for redundant structures.

Results of S-N Curve Based Analysis

In the fatigue damage calculation, the composite stress histograms shown in Tables 6.16 and 6.17 were employed in conjunction with the selected AWS S-N curve, while those in Tables 6.14 and 6.15 were used in conjunction with the selected ASME S-N curve. The results for five cases were obtained as shown in Table 7.1. It is noted that the rainflow correction factor λ, which is a function of both the slope of the S-N curve and the bandwidth of the stress energy spectrum (see Fig. 7.3), was used in the calculation to adjust the fatigue damage level.

The adjusted fatigue damage is equivalent to

$$D_R = \lambda D_N \tag{7.2}$$

where

D_R = fatigue damage using rainflow counting method

D_N = fatigue damage using equivalent narrow-band method

Prior to interpreting the results presented in Table 7.1, it should be noted that gauge F_yB of the SEALAND McLEAN and gauge 2 of the SEALAND MARKET were located at the original hatch corner cut-out while all the others were on the modified ("final fix") hatch corner cut-out. Furthermore, as noted in Section VI.1, the data sets of two operational seasons taken on the SEALAND McLEAN during 1977 and 1978 were combined in the calculation, since between these operational seasons the cut-out details and the strain gauge system were unchanged.

The results given in Table 7.1 reveal the following:

(i) The results for fatigue life obtained by using the S-N curve of either AWS or ASME show the trend consistent with the trend of recorded hatch corner crack incidents. The predicted fatigue life in the unmodified case of the SEALAND McLEAN is close to the reported life. The case with the "final fix" design has a fatigue life considerably improved from the original design.

(ii) In all cases, the use of the AWS S-N curve gives fatigue lives of the hatch corner shorter than that of the ASME S-N curve, with the ratio being about 2 to 3.5. This is to be expected, considering the differences in bases and safety margins inherent in the two curves.

(iii) According to the results for both the original design and the "final fix", the fatigue life is higher on the hatch corners of the SEALAND MARKET than on that of the SEALAND McLEAN. This may be due to differences in workmanship and in environmental loads encountered.

VII.2 Wirsching's Method of Reliability-Based Analysis

A reliability-based fatigue analysis method developed by Wirsching [6.1] was employed in this study to cast the results of the Miner's type analysis in a probabilistic context. Wirsching recommended that the log-normal format, a full distributional procedure, in which each random variable is assumed to have a log-normal distribution, be used as a basis for fatigue reliability analysis.

Employing mathematical properties of log-normal variables, an expression for probability of failure P_f can be described as

$$P_f = \phi\ (-\beta) \qquad (7.3)$$

where ϕ is the standard normal, and β is the safety index defined by

$$\beta = \frac{\ell n(\bar{T}/T_s)}{\sigma_{\ell n\, T}} \tag{7.4}$$

T_s is the intended service life, normally set equal to 20 years.

$\tilde{T}$ is the median value of the time to failure T and is equal to,

$$\tilde{T} = \tilde{\Delta}\, \tilde{K}/(\tilde{B}^{m}\Omega) \tag{7.5}$$

the tildes indicating median values, m denoting the negative reciprocal slope of the S-N curve, and Ω being the stress parameter equal to

$$\Omega = \lambda f_o\, E(S^m) \tag{7.6}$$

where λ is the rainflow correction factor, f_o is the average frequency of cyclic stress, and $E(S^m)$ is the expected value of S^m. Also, the standard deviation of ℓnT is given by

$$\sigma_{\ell nT} = (\sigma^2_{\ell n\Delta} + \sigma^2_{\ell nK} + m^2\sigma^2_{\ell nB})^{1/2} \tag{7.7}$$

$$\sigma_{\ell nT} = [\ell n \{(1 + C_\Delta^2)\,(1 + C_K^2\,(1 + C_B^2)m^2)\}]^{1/2} \tag{7.8}$$

where C's are the coefficients of variation of random variables Δ, K and B, which are assumed to have log-normal distributions.

The random variable Δ denoting damage at failure is considered a random variable in order to account for the inaccuracies associated with using a simple model to describe complicated physical phenomena. The random variable K accounts for uncertainties in fatigue strength, as evidenced by scatter in S-N data. The random variable B describes inaccuracies in the process of estimating fatigue stresses from oceanographic data.

Application and Results of Wirshing's Method

Application of Wirshing's reliability-based fatigue analysis was made using Munse's "detail 1F" S-N curve shown in Fig. 7.4 for all loading cases of the hatch corner details. The coefficients of variation and median values of the random variables used are given in Table 7.2. In conjunction with the composite stress histograms shown in Tables 6.16 and 6.17, the design factor values were then employed to calculate median lives and corresponding probabilities of failure. The results obtained from this analysis are given in Table 7.3.

In interpreting the results obtained by using Wirsching's method of reliability-based analysis, it should be noted that because of (a) the assumption that V, K, and B have log-normal distributions, and the usually poor definition of distributions in the critical tail areas resulting from lack of data, computed values of probabilities of failure, p_f, do not necessarily provide precise estimates of risk; these values are however useful in a relative sense.

The results shown in Table 7.3 indicate the following:

(i) The median lives, probabilities of failure and safety indices show the correct trend for the hatch corner fatigue performance, with

the hatch corner with the "final fix" having higher fatigue lives than the original.

(ii) For both the original and the "final fix", the hatch corner of the SEALAND MARKET has higher fatigue strength than that of the SEALAND McLEAN.

(iii) By comparing the results shown in Tables 7.1 and 7.3, the ratio of the median life to the S/N based fatigue life is fairly constant in all cases, about 12 for the ASME curve and 30 for the AWS curve.

VII.3 Munse's Method of Ship Detail Characterization

In Reference [7.5] Munse et al derived a simple method of estimating an allowable stress for specific ships details. The mean fatigue resistance of 69 structural details, which is the basic information used for this design method, were determined based on laboratory test data and presented in terms of stress range; the secondary effects of mean stress and in most cases the type of steel have been neglected except to the extent that they are included in the "Reliability Factors". The "Reliability Factor" and the "Random Load Factor" are two important factors in the development of this ship structure fatigue design criteria. The "Reliability Factor" is a function of the slope of the S-N curve and the required level of reliability and a coefficient of variation, where the values of coefficients of variation were provided for each detail in Reference [7.5]. The "Random Load Factor" is a function of the expected loading history and the slope of the S-N curve.

Reliability-Based Design Criteria

Let N be a random variable denoting the number of cycles to failure in variable amplitude fatigue. It is assumed that N has a Weibull distribution with parameters α and γ and that the coefficient of variation (COV) of N, C_N, is a constant. The parameters of the first two moments are:

$$\alpha \simeq C_N^{-1.08} \qquad \mu_N = \gamma\Gamma(\frac{1}{\alpha} + 1) \tag{7.9}$$

Then the distribution function of N can be written as

$$F_N(n) = 1 - \exp\left\{ - \frac{n\Gamma\ (1 + C_N^{1.08})}{\mu_N} \right\}^{C_N^{-1.08}} \tag{7.10}$$

where n is a specific value of N.

The probability of failure $p_f = p(N \leq n)$ or

$$P_f(n) = - \ell n\ L(n) = \frac{n}{\mu_n} \Gamma(1 + C_N^{1.08})^{C_N^{-1.08}} \tag{7.11}$$

where L(n) denotes the probability of survival.

Thus for small P_f

$$\mu_N = n\gamma_L \qquad \text{where } \gamma_L = \frac{\Gamma\ (1 + C_N^{1.08})}{(P_f)^{C_N^{1.08}}} \tag{7.12}$$

of which γ_L may be called scatter factor.

Then the reliability factor, R_f, is then given by

$$R_f = \left(\frac{1}{\gamma_L}\right)^{1/m} \tag{7.13}$$

Using a concept that for a given detail a random stress range S can be related to a constant-cycle stress range Sc with the same mean fatigue life, the random load factor is obtained by

$$\xi = \frac{S_o}{E\ (S^m)^{1/m}} \tag{7.14}$$

where S_o is the maximum stress range in a random loading. Thus the maximum allowable stress range is then given as

$$S_D = S_{N_T} \cdot \xi \cdot R_f \tag{7.15}$$

This relationship is usually satisfied in design for a desired life of total cycles, N_T, in 20 years, and for a required level of reliability.

Application and Results of Munse's Model

The application of Munse's design method is not of direct relevance of this study. Of more interest, similar to the log-normal model, are mean fatigue lives and associated probabilities of failure. With the applied stresses known, the expected "mean" life in context of the Munse's model is given by

$$\bar{N} = \frac{K}{E(S^m)} \tag{7.16}$$

And the associated reliability is given by

$$L(N) = \exp\ \left[\ -\ \left(\frac{N}{\bar{N}}\Gamma\ (1 + \frac{1}{\alpha})\ \right)^{\alpha}\right] \tag{7.16}$$

the probability of failure being the complement of L (N) and α being the Weibull shape parameter.

Values for $E(S^m)$ were obtained from Weibull distributions fitted to the long-term composite histograms using the method of moments. The Weibull distributions fit the data well, especially at the tail-ends of the composite stress histograms. In all cases, the values of $E(S^m)$ are consistent with those calculated directly from the long-term histograms, the error being less than 6 percent.

Fatigue damage calculations are made based on Munse's "detail 1F" S-N curve shown in Figure 7.4, with rainflow correction factors given by Fig. 7.3. Table 7.4 shows the mean lives and probabilities of failure obtained. The results are similar to those obtained from Wirshing's log-normal reliability model, and are consistent with the trend of observed fatigue behavior.

VII.4 Fracture Mechanics Based Method

The development of fracture mechanics methodology in the last two decades offers considerable promise in improving our understanding of fatigue crack initiation, fatigue crack propagation, unstable propagation and in design against fatigue. Using fracture mechanics concepts, the procedure to analyze the crack-growth behavior of the hatch corner cut-out detail at the hot-spot location is described as follows.

The approach outlined by Wirsching in Reference [7.6] was used in this study. Wirsching makes the following assumptions.

1. Material Behavior (see Fig. 7.6):

   a) The Paris law applies in Region II and extends through Region III.

   b) A threshold stress intensity ΔK_{th} exists.

2. Loading:

   a) Long-term statistical distribution of fatigue loading is known.

   b) Sequences effect are ignored.

   c) Stress ratio R effects are ignored, although they could be introduced through the constant C in the Paris equation and threshold stress intensity ΔK_{th}.

An integration of the Paris equation and the use of equivalent stress concept yields the cycles to failure

$$N = \frac{1}{CS^m} \int_{a_o}^{a_f} \frac{da}{G(a)\, Y^m(a)\, (\pi a)^{m/2}} \qquad (7.17)$$

where

$$\bar{S}^m = E(S^m) = \int_o^\infty s^m f_S(s)ds \qquad (7.18)$$

$$G(a) = \frac{\bar{S}_o^m}{\bar{S}^m} \qquad (7.19)$$

of which

$$\bar{S}^m = \int_{s_o(a)}^\infty s^m f_S(s)ds \qquad (7.20)$$

$$S_o(a) = \Delta k_{th}/Y(a)\ \sqrt{\pi a} \tag{7.21}$$

Also, Y(a) is a geometry related factor and can be estimated from Figure 7.7 and $f_S(s)$ is the probability density function of s.

Equation (7.17) can be reformulated in terms of the characteristic S-N format with the Miner's rule assumption

$$NS^{-m} = A \tag{7.22}$$

where

$$A = \frac{1}{C} \int_{a_o}^{a_f} \frac{da}{G(a)\ Y^m(a)\ (\pi a)^{m/2}} \tag{7.23}$$

Application of Fracture Mechanics Model

In order to apply the fracture mechanics approach derived by Wirsching [7.6] to estimate crack-growth life for the hatch corner, in addition to the composite stress histogram, the suitable da/dn data, geometry factor, Y(a), threshold stress intensity, ΔK_{th}, initial crack, a_o, and final crack, a_f, for the detail conditions should first be selected or determined.

The material used for the main deck and face plate of the hatch corner, where the gauges are located, is ABS EH33 steel. The data for the fatigue crack growth rate of this material was not available. Nevertheless, the steel used for doubler denoted as ABS CS whose yield strength is close to the ABS EH33 has been tested by Teledyne (7.7).

The approximate expression for fatigue crack growth for the ABS CS steel in kip and inch units, is

$$\frac{da}{dn} = .254 \times 10^{-8} (\Delta K)^{2.53} \qquad (7.24)$$

These data are based on constant-amplitude tests at stress ratios R = 0.05, 03 and 0.6.

The geometry factor for the hatch corner can be obtained from Fig. 7.7. Since the cracks of the face plate and the main deck cut-out are different in nature, the geometry factor of the original design detail is obtained from the curve in the figure corresponding to the member with edge crack while that of the "final fix" the curve corresponding to the member with line crack at middle.

The threshold stress intensity ΔK_{th} for CS material determined by Teledyne [7.7] is the magnitude between 10 and 11 ksi $\sqrt{in}$ for a crack growth rate of 10^{-6} in/cycle. The crack growth rate, at which the threshold stress intensity was determined by Teledyne, seems to be faster than that in the region of slow crack growth (see Fig. 7.6) where the threshold stress intensity for steels is usually found. In addition, many references show that typical thresholds for steels are in the range of 2 to 5 ksi $\sqrt{in}$ without much effect due to alloying or strength level [7.8] as shown in Fig. 7.8. In the present investigation, the threshold stress intensity was varied parametrically in the range of 2 and 5 ksi $\sqrt{in}$.

The initial crack length a_o is an important factor in the calculation of crack growth life. A small change in value of a_o could produce large differences in calculated crack growth life. In addition, there is no general agreement on sizes of initial crack to be used in specific situations (see Fig. 7.9). In this connection, the values of 0.00394 in. (0.1 mm), 0.01 in., and 0.1 in. were selected for parametric study of the crack growth life of the hatch corner.

The final crack length a_f which is not important as compared to the initial crack length in this calculation, can be determined when the quantity

$$(N_{i+1} - N_i)/(a_{i+1} - a_i) \leq \epsilon \tag{7.25}$$

ϵ is a small real number where

$$N_i = \frac{1}{CS^m} \int_{a_o}^{a_i} \frac{da}{G(a)\ Y^m(a)\ (\pi a)^{m/2}} \tag{7.26}$$

Results of Fracture Mechanics Model

After the da/dn data, Y(a), ΔK_{th}, a_o and a_f are determined, Eq. (7.20) is used in conjunction with the composite histograms of Tables 6.18 through 6.23 to obtain the crack growth life for the hatch corner. The results for the crack growth life are presented in Table 7.5. As noted in Section VII.3.2 in the calculation, the rainflow correction factor λ was used to adjust the fatigue crack growth life.

In interpreting the obtained results for crack growth, it should be noted that the selected crack grown rate da/dn was obtained by a

constant amplitude test with R = 0.05, 0.3 and 0.6. However, in the structure subjected to load sequences characteristic of those experienced by ocean-going vessels, the crack growth retardation can occur. Since in the present case retardation is not assumed, the calculated results may show shorter crack growth lives. Thus, care should be exercised in interpreting the results given in Table 7.5.

An examination of the results in the table reveals the following:

(i) For each case, as expected, the crack growth life increases as the threshold stress intensity increases or as the initial crack size decreases.

(ii) For all cases, except in the case of initial crack size a_o = 0.00394 in (1 mm) and threshold stress intensity ΔK_{th} = 5 ksi $\sqrt{in}$, the computed crack growth lives are in the same order of magnitude as those determined by using AWS and ASME S-N curves. The results for the crack growth life show the correct trend of the hatch corner fatigue performance.

(iii) In comparing the crack growth lives associated with both threshold stress intensity values ΔK_{th} = 2 and 5 ksi $\sqrt{in}$, it is noted that the difference in magnitudes of crack growth lives is insignificant for an initial crack a_o = 0.1 in. Differences increase as the initial crack size decreases.

VIII GENERAL DISCUSSION AND CONCLUSIONS

In this study, four different approaches to fatigue life determination have been used to assess their ability to predict the trends of fatigue behavior observed at the forward hatch corner of the SL-7 containerships. Through these varied approaches, predictions of fatigue lives were made for the original configuration of the hatch corner, and for a "modified" hatch corner configuration employing doublers at the corners together with face plates. The long term dynamic stress histograms were obtained from actual strain measurements made during operation of two SL-7 vessels with and without the hatch corner modifications. Comparisons can be made of the predicted fatigue lives with observed incidences of hatch corner cracking as indicated by the survey data given in this report.

In making such comparisons, the following sources of uncertainty must be noted.

1) The first source of uncertainty concerns the fatigue stress histograms. In the case of the original unmodified hatch corner, it may be recalled that strain measurements for the highest stressed mid-surface of the hatch corner deck plating were used in the study. In the case of the modified hatch corner, strain measurements for a similar highest stressed location on the face plate was used. While the former measurements can yield direct indications of fatigue behavior, the latter case cannot since the structural detail in the latter instance also contains a weld which has not been considered. Any assessment of fatigue performance of the weld would have been complicated not only by the lack of measured strain data at the appropriate location, but also by local differences in workmanship, etc.

2) As yet another source of uncertainty in the strain data used in the present study, it is of interest to note that the locations of the highest stressed point for identical details (of the original unmodified hatch corner) on two sister vessels operating in the same general area are somewhat different, see figures for the SEA-LAND McLEAN and the SEA-LAND MARKET.

3) An additional source of uncertainty in the fatigue stress histograms arises from the probabilities of occurrences of the Beaufort wind measures used. It is to be noted that while the SEA-LAND McLEAN operated in the Pacific some of the time, it has always been the Beaufort wind probabilities for the North Atlantic that has conservatively been used in this study.

4) Another source of uncertainty in the fatigue stress histograms concerns the use of random process theory related to stationary Gaussian processes with consideration of zero crossing rates for the purpose of obtaining the number of fatigue cycles from the hatch corner stress spectra available. Any approximations in this regard, however, are thought not to be of major consequence. A more direct method would have been to obtain such information from the original strain time histories by a cycle counting procedure.

5) Another broad class of uncertainties concerns certain details of the fatigue life prediction methodologies used. It will be appreciated, for example, that the AWS and ASME S-N curves used are lower bound design curves obtained from different sets of data. The AWS S-N curve used, that for non-redundant structures, contains an additional factor of safety imposed on a lower bound S-N curve obtained from fatigue test data. The use of such lower bound curves in the prediction of actual

fatigue performance is conservative, as the results show. In contrast, the S-N curve used in the fatigue reliability models, namely the Munse "detail 1F" for flame cut plain material, represents mean life on a Log S Log N scale. Also, except for the case of the ASME curve, mean stress effects have been generally neglected.

6) The use of the fatigue damage accumulation model in the case of the variable amplitude loading, including Miner's hypothesis and the rainflow correction factor, has its own uncertainty. Similarly, the fracture mechanics model has its uncertainties, e.g., in neglecting any possible crack growth retardation effects. These uncertainties, namely those related to the treatment of fatigue damage accumulation, as well as the scatter in S-N data, were accounted for in the probabilistic treatment of fatigue damage through the Wirsching and Munse reliability models used in this study. A measure of uncertainty in the fatigue stresses was also included in those models. It is of some interest to note that the two models, although based on different approaches and assumptions, give comparable values for probabilities of failure in the present case. The average lives predicted from these models are considerably higher than those from the AWS and ASME S-N curves reflecting the fact that the latter represent lower bound performance.

As demonstrated in this study both the deterministic S-N and the probabilistic fatigue reliability models adequately predict the general trend of the hatch corner fatigue behavior. The fatigue lives predicted from the deterministic S-N curve approaches in the case of original unmodified design are in line with observed cracking incidents. In addition, a third and entirely different deterministic approach, viz. fracture mechanics based calculations of fatigue performance also yield

lives comparable to those observed for the unmodified hatch corner. This, of course, reflects the fact that the validation study performed is essentially more accurate for the original unmodified case.

In making any comparisons with data related to observed incidences of cracking it should be noted that generally survey dates rather than dates of crack occurrence are reported. Also that the characteristics of the cracks that occurred would normally not be consistent with the definitions of fatigue failure underlying either the S-N curves or the fracture mechanics model. Thus, in summary, it is emphasized that although predictions of fatigue behavior as made in this study do indicate the general trend of observed incidences of hatch corner cracking, any comparisons related to the exact times to crack occurrence are considerably more difficult because of the various uncertainties in fatigue stresses and fatigue strength.

REFERENCES

1.1 Munse, W.H., Wilbur, T.W., Tellalian, M.L., Nicoll, K. and Wilson, K., "Fatigue Characterization of Fabricated Ship Details for Design". Ship Structure Committee Report No. 318, 1983.

1.2 Wirsching, P.H., "Probability Based Fatigue Design Criteria for Offshore Structures". Final Project Report on API PRAC 81-15. University of Arizona, Tucson, 1983.

1.3 Wirsching, P. H., "A Fracture Mechanics Based Life Prediction Model for Components of Marine Structures," Aerospace and Mechanical Engineering Department, University of Arizona, Technical Report No. 9 to ABS, 1984.

3.1 Fain, R.D., "Design and Installation of a Ship Response Instrumentation System Aboard the SL-7 Class Containership S.S. SEALAND McLEAN", Ship Structure Committee Report SSC-238, 1974.

3.2 Boentgen, R.R. and Wheaton, J.W., "Static Structural Calibration of Ship Response Instrumentation System Aboard the SEALAND McLEAN", Ship Structure Committee Report SSC-263, 1976.

3.3 Boentgen, R.R., Fain R.A. and Wheaton, J.W., "First Season Results from Ship Response Instrumentation Aboard the SL-7 Class Containership S.S. SEALAND McLEAN in North Atlantic Service", Ship Structure Committee Report SSC-264, 1976.

3.4 Wheaton, J.W. and Boentgen, R.R., "Second Season Results from Ship Response Instrumentation Aboard the SL-7 Class Containership S.S. SEALAND McLEAN in North Atlantic Service", Teledyne Material Research Technical Report TR-1559, 1975.

3.5 Boentgen, R.R., "Third Season Results from Ship Response Instrumentation Aboard the SL-7 Class Containership S.S. SEALAND McLEAN in North Atlantic Service", Teledyne Materials Research Technical Report TR-2058, 1975.

3.6 Dalzell, J.F., Correlation and Verification of Wave Meter Data from the SL-7", Davidson Laboratory Report Nos. SIT-DL-77-1931, 1933 and 19, January & February 1976.

3.7 Teledyne Engineering Services "Instrumentation of Modified and Unmodified Forward Hatch Corners Aboard the Containership S/L MARKET", Vols. I and II, Teledyne Engineering Services Report TR-2399, April 1977.

3.8 Teledyne Engineering Services, "Instrumentation of Forward Hatch Corner Aboard the SL-7 Containership SEALAND McLEAN in Pacific Service"' Vols. I and II, Teledyne Engineering Services Report TR-2448, Dec. 1977.

3.9 Teledyne Engineering Services, "Modified Instrumentation of the Forward Hatch Corners on the Containership "SEALAND McLEAN", Teledyne Engineering Services Report TR-2719-2.

4.1 Elbatouti, A.M., Liu, D., and Jan, H.Y., "Structural Analysis of SL-7 Containership Under Combined Loading of Vertical, Lateral and Torsional Moments Using Finite Element Techniques", Ship Structure Committee Report SSC-243, 1974.

4.2 American Bureau of Shipping, "ABS/DAISY System of Computer Programs for Ship Structural Analysis", 1975.

4.3 Elbatouti, A.M., Jan, H.Y. and Stiansen, S.G., "Structural Analysis of a Containership Steel Model and Comparison with the Test Results", SNAME Transactions, 1976.

4.4 Dalzell, J.F., and Chiocco, M.J., "Wave Loads in a Model of the SL-7 Containership Running at Oblique Headings in Regular Waves", Ship Structure Committee Report SSC-239, 1974.

4.5 Kaplan, P., Sargent, T.A. and Cilmi, J., "Theoretical Estimates of Wave Loads on the SL-7 Containership in Regular and Irregular Seas", Ship Structure Committee Report SSC-246, 1974.

4.6 Kaplan, P., Sargent, T.A. and Silbert, M., "A Correlation Study of SL-7 Containership Loads and Motions - Model Test and Computer Simulation", Ship Structure Committee Report SSC-271, 1977.

4.7 Jan, H.Y., Chang, K.T., and Wojnarowski, M.E., "Comparison of Stresses Calculated Using the DAISY System to Those Measured on the SL-7 Containership Program", Ship Structure Committee Report SSC-282, 1979.

4.8 Chiou, J., "Hatch Corner Study for the SL-7 Containerships", American Bureau of Shipping, Technical Report OE-79001, January 1979.

5.1 Ochi, M.K., "On the Prediction of Extreme Values", Journal of Ship Research, Vol. 17, No. 1, March 1973, pp 29-37.

6.1 Wirsching, P.H. "Probability-based Fatigue Design Criteria for Offshore Structures", API-PRAC Project No. 81-15 Report, January 1983.

6.2 Stacy, E.W. and Mihram, G.A., "Parameter Estimation for a Generalized Gamma Distribution", Technometrics, Vol. 7, No. 3, 1965, pp. 349-358.

7.1 Structural Welding Code-Steel, American Welding Society ANSI/AWS D1.1-8, 1982.

7.2 Bridge Fatigue Guide/Design and Details, American Institute of Steel Construction, 1221 Avenue of The Americas, New York, NY, 10020, 1977.

7.3 Fisher, J.W., et.al., "Fatigue Strength of Steel Beam with Transverse Stiffeners and Attachments, National Cooperative Highway Research Program Report 147, 1974.

7.4 Pressure Vessel Code, American Society of Mechanical Engineering Section, VIII, Division 2, 1983.

7.5 Munse, et.al. "Fatigue Characterization of Fabricated Ship Details for Design", Ship Structure Committee Report SSC-318, 1983.

7.6 Wirsching, P.H., "A Fracture Mechanics Based Life Prediction Model for Components of Marine Structures", Aerospace and Mechanical Engineering Department, University of Arizona, Technical Report No. 9 to ABS, 1984.

7.7 "Fatigue Consideration in View of Measured Load Spectra, Vol. I", Teledyne Engineering Service Technical Report TR-3049-5, December 1980.

7.8 Barsom, J.M., Novak, S.R., "Subcritical Crack Growth and Fracture of Bridge Steels", National Cooperative Highway Research Program Report 181, Transportation Research Board, Washington, DC 1977

7.9 Wirsching, P.H., "A First Iteration of Developing Probability Based Fatigue Design Rules for TLP Components Using Lognormal Format", Aerospace and Mechanical Engineering Dept., University of Arizona, Technical Report No. 1, January 1985.

Table 2.1 Damage at Hatch Corners of SL-7 Containerships

NAME OF SL-7 CONTAINERSHIP	REPORT DATE	FIRST HATCH		SECOND HATCH		OTHER HATCH	REMARKS
		FORWARD	AFT	FORWARD	AFT		
MCLEAN	7311	X					AS BUILT
	7403	X					AS BUILT
	7410	X					AS BUILT
	7610			X			AS BUILT
	7612	X					DOUBLER
	7701	X					DOUBLER
COMMERCE	7501	X					AS BUILT
	7502	X					AS BUILT
	7611			X			AS BUILT
	8003			X			AS BUILT
TRADE	7501	X					AS BUILT
	7610	X					AS BUILT
	7803	X				X	AS BUILT
	7805			X	X		AS BUILT
	7810	X					DOUBLER
EXCHANGE	7502	X					AS BUILT
MARKET	7309	X					AS BUILT
	7506			X			AS BUILT
	7509	X					AS BUILT
	7602			X			AS BUILT
RESOURCE	7312	X	X				AS BUILT
	7504	X					AS BUILT
	7602			X			AS BUILT
	7801	X					DOUBLER
	8001			X		X	AS BUILT
	8104			X	X	X	AS BUILT
GALLOWAY	7404	X					AS BUILT
	7502	X					AS BUILT
	7802	X					DOUBLER
	8105	X	X				FP/DBLR*
	8105			X	X	X	AS BUILT

* FACE PLATE AND DOUBLER WERE ADDED

Table 4.1 Wave Characteristics and Ship Motions of the 18 Loading Conditions Analized in [4.7]

Loading Condition	Ship Speed (knots)	Wave Frequency (Rad/Sec)	Wave Length (ft)	Wave Height (P-T) (ft)	d = distance from Wave Crest to AP (ft)	ABS/SHIPMOTION Calculation		
						Heave (ft.)	Pitch (Degrees)	Roll (Degrees)
1	Stillwater Condition (Mean Draft = 30.57 ft.)							
2	10.9	0.50	808.5	20.92	473.14	-3.931	2.06	0
3	"	0.35	165.1	51.2	253.08	-15.87	-2.80	0
4	"	"	"	"	473.14	-20.36	1.482	0
5	18.7	0.50	808.5	21.97	693.23	-7.3	3.27	0
6	28.1	1.60	561.5	16.47	473.14	-0.84	0.01	0
7	"	0.50	808.5	30.6	693.23	-15.64	-1.988	0
8	"	"	"	"	473.14	4.64	5.4	0
9	10.9	0.606	550.4	19.68	"	-1.74	0.96	0
10	18.7	0.56	644.56	"	"	-2.14	1.97	0
11	28.1	0.539	695.7	"	"	1.52	1.3	0
12	"	0.65	478.4	"	"	-1.03	-0.01	0
13	32.3	0.435	540.15	30.18	253.08	-21.46	3.145	-0.27
14	"	"	"	"	473.14	-3.99	5.76	1.412
15	"	"	"	"	693.23	18.0	1.85	1.495
16	31.8	0.344	880.29	33.46	253.08	-17.5	-0.944	-0.457
17	"	"	"	"	473.14	-20.35	5.317	1.252
18	"	"	"	"	693.23	1.8	5.048	1.421

Table 4.2 Stress RAO (in psi) along Hatch-corner Cut-out

L.C. \ Point	1	2	3	4	5	6	7	8	SCF
1	197	224	409	401	44	-53	-108	-19	1.8
2	222	252	438	415	33	-67	-119	-20	1.7
3	219	249	444	428	41	-61	-118	-20	1.8
4	247	281	489	465	39	-73	-133	-22	1.8
5	141	161	286	269	21	-42	-75	-12	1.8
6	209	239	422	405	36	-62	-114	-19	1.8
7	269	309	606	616	89	-61	-154	-29	1.9
8	83	97	171	159	11	-25	-43	-7	1.8
9	188	214	376	357	29	-57	-102	-17	1.8
10	63	73	108	76	14	-27	-28	-3	1.5
11	182	208	355	327	18	-60	-98	-16	1.6
12	196	224	401	387	37	-57	-109	-19	1.8
13	50	59	71	60	27	24	24	6	1.2
14	167	222	417	577	310	193	88	8	2.6
15	327	400	776	919	300	86	-70	-21	2.3
16	264	294	518	482	24	-93	-152	-25	1.8
17	186	230	393	467	186	87	14	-1	2.0
18	131	171	311	400	184	98	30	1	2.6

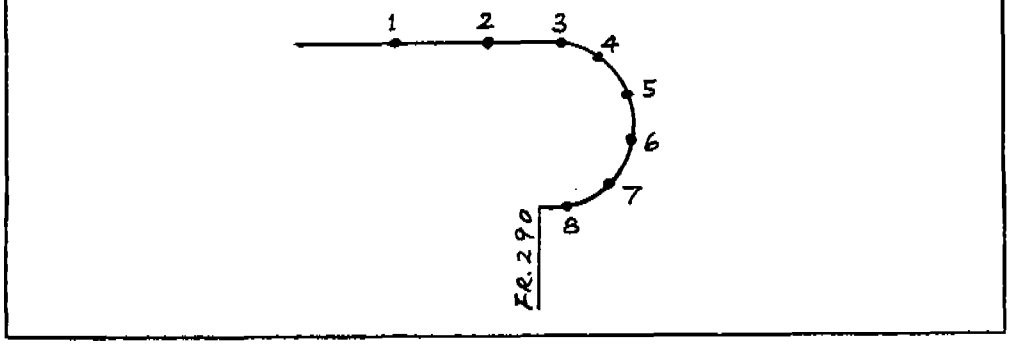

Table 4.3 Special Features of Models

Model No.	Cut-out		Main Deck Reinforcement		Hatch Coaming			Hatch Girder		
	Shape	Size in radius	Insert Plate	Doubler	Type	Modeling Element		Type	Modeling E	
						Beam	Plate		Beam	
1	Circular	610mm			As built	✓		As built	✓	
2	"	"			"	✓		Extended	✓	
3	"	"			"	✓		Longit. bulkhead		
4	"	"			"	✓		Deep girder		
5	"	400mm			"	✓		As built	✓	
6	"	"			Partially reinforced setback		✓	With tapered extension		
7	"	"	✓		"		✓	"		
8	"	"		✓	As built	✓		As built	✓	
9	"	"			Extended to Fr. 291		✓	Deep girder		
10	"	"			Reinforced & extended		✓	With tapered extension		
11	"	"	✓		Ext. to Fr.291		✓	"		
12	Parabolic		✓		"		✓	"		
13	Circular	400mm	✓		"		✓	"		
14	"	"	✓		Bracket added		✓	"		
15	"	"			Partially reinforced		✓	"		
16	"				Extended		✓	"		
17	Parabolic				"		✓	"		
18	"				"		✓	"		
19	"				"		✓	"		

Table 4.4 Comparison of Maximum Stresses at Hatch Corner Cut-Out Contour

A (BASE) \ B	MODEL 6 (T)-2226 (B) 889	MODEL 7 -1883 687	MODEL 8 -2009 986	MODEL 9 -2423 1013	MODEL 10 -1877 605	MODEL 12 -2355 895	MODEL 13 -1286 539	MODEL 14 -1910 662
MODEL 5 -2580(T) 1332(B)	(1) -14% -33%		(2) -22% -26%				(3) -50% -60%	
MODEL 6 -2226(T) 889(B)		(4) -15% -23%		(5) 9% 14%				
MODEL 7 1883(T) 687(B)					(6) 0% -12%			
MODEL 11 -1953(T) 734(B)		(7) -4% -7%				(8) 21% 22%	(9) -34% -27%	(10) -2% -10%
MODEL 15 -2580(T) 1332(B)	(11) -3% -3%							

Remarks:

(1) Effect of stiffened coaming and tapered extended girder
(2) Effect of doubler
(3) Total effect of insert plate, face plate, extended coaming and tapered extended girder
(4) Effect of insert plate
(5) Effect of deep girder while compared to tapered extended girder
(6) Effect of extended stiffened coaming
(7) Effect of stiffened coaming
(8) Effect of parabolic cut-out
(9) Effect of face plate
(10) Effect of bracket
(11) Effect of discontinuity of hatch coaming

Table 5.1 Data of Selected Intervals and for this Study

Ship	Date Recorded	Gage	Total Intervals	
			Est.	Act.
SEALAND McLEAN	Jan-Mar 75	F_yB	300	214
	May-Jul 77	2&8	600	400
	Sep-Jan 78	3&8	1000	425
SEALAND MARKET	Oct-Dec 76	2&8	700	288

Table 5.2 Scale Factors for Reduced Data

SHIP	DATE RECORDED	GAUGE	HP FILE	
			FROM	TO
SEALAND McLEAN	Jan - March 75	F_yB	F_yB-1	F_yB-22
" "	May - July 77	2 & 8	MCL-1A	MCL-40A
" "	Sept. 77 - Jan. 78	3	SLM-1A Int. 1 & 2 SLM-3A Int. 7 & 8 SLM-16A Int. 3 & 4 SLM-27A Int. 7 & 8	SLM-3A Int. 5 & SLM-16A Int. 1 & SLM-27A Int. 5 & SLM-43A Int. 5
		8	SLM-1A Int. 1 & 2 SLM-16A Int. 3 & 4 SLM-27A Int. 7 & 8	SLM-16A Int. 1 & SLM-27A Int. 5 & SLM-43S Int. 5
SEALAND MARKET	Oct. - Dec. 76	2 & 8	MKT-1	MKT-29

Table 5.3 Digital Data for File No. F_yB-15 Interval 9

.423217773438	.207057572351	2.78116701242E-02	1.64400436593E-02
3.95855323705E-02	3.98784299527E-02	5.70650832255E-02	.055437874932
4.81570450382E-02	2.59375941393E-02	1.94566853071E-02	1.38257362501E-0_
3.00471795045E-02	1.70173300837E-02	4.34446253612E-02	3.05359537263E-02
3.15717915335E-02	2.06229328095E-02	2.74302824899E-02	3.86728101691E-02
4.09855697103E-02	.035966584745	4.90803813143E-02	5.26215109326E-02
4.00917670645E-02	7.81364317085E-02	8.96276884467E-02	4.68190245539E-02
9.03452025939E-02	.174108664792	.20861056815	.118655566156
9.64357340635E-02	.196493057185	.178558370635	.222594955994
8.91363380108E-02	.141823058167	8.94567249439E-03	.148135128433
.137769622399	.124323847454	3.47811524567E-02	9.41507916677E-02
9.91062068[illegible]3E-02	.066382337247	4.12932125374E-02	.059700458269
3.99331103[illegible]8E-02	7.49674854697E-02	6.56779423802E-02	6.28062722019E-02
3.87634956241E-02	2.17003908195E-02	3.35084311187E-02	1.23935375426E-02
3.[illegible]3809909157E-02	9.83241325432E-02	.122764343455	9.28735595293E-02
7.72177301203E-02	6.90673838279E-02	4.41303200004E-02	3.34663054396E-02
3.91[illegible]97621E-02	4.22042300678E-02	2.76035817252E-02	1.04552644184E-02
[illegible] 18[illegible] 593049E-02	1.24835150666E-02	3.28582531255E-02	4.61[illegible]3110384E-02
3.[illegible]5188E-02	2.26309447951E-02	.017799991323	3.0[illegible] 227865E-02
2.[illegible]319E-02	3.06132495573E-02	.015313119494	2.[illegible]40952E-02
2.[illegible]e821E-02	1.83369926432E-02	1.69895018774E-02	3.21469239716E-02
2.76796939724E-02	1.59806773598E-02	2.45210045355E-02	2.15454686456E-02
1.59480343829E-02	1.44888208312E-02	1.23251106656E-03	8.53836838984E-03
1.62492057547E-02	.016137747541	1.58227149876E-02	8.82554059734E-03
2.17691320493E-02	.023163088715	2.48343850006E-02	2.28761501664E-02
9.97993174594E-03	3.65847790237E-03	7.44543341821E-03	1.43241470964E-02
1.46542125561E-02	8.05628119702E-03	7.72357036677E-03	1.41353405222E-02
1.12777626735E-02	8.92961232045E-03	2.53849086119E-02	2.14257361222E-02
2.09820376017E-02	1.41264585491E-02	2.72570864363E-03	8.42440638857E-03
3.81381913050E-03	1.34423003522E-02	9.44685921532E-03	8.11772600204E-03
7.33503642391E-03	3.43861739875E-03	6.42805240781E-03	7.64316865260E-03
2.79958173986E-03	3.62588128936E-03	3.59608847816E-03	8.07324508589E-03
1.08667050111E-02	2.82618869791E-03	5.47314247519E-03	7.56911304781E-03
4.37170542070E-03	7.15781362438E-03	1.52184525448E-02	.016817671802
1.22358386798E-02	8.67748517796E-04	9.74224989683E-03	9.44764964052E-03
4.53993771675E-03	6.98448099625E-03	3.60176314410E-03	5.58342293434E-03
8.88013839722E-03	.01100473482	1.75865249915E-03	4.43498548279E-03
4.46520336511E-03	5.39582557531E-03	1.08337509801E-02	1.13838454346E-02
.015076639205	1.33311485911E-02	6.63292382172E-03	1.31329498849E-02
1.12191537167E-02	5.66575062376E-03	5.67281365428E-03	3.63632853119E-03
1.36041394957E-02	1.37029511799E-02	9.69511896683E-03	8.23864797401E-03
3.09456368061E-03	6.35387873891E-03	5.23545485361E-03	1.39256828593E-03
4.83118721065E-03	5.05792611242E-03	6.57141313638E-03	4.39627599679E-03
5.31133000731E-03	6.92999738517E-03	6.12073377025E-03	7.25891822685E-03
5.86487591335E-03	5.53329267881E-03	7.54399714704E-03	1.65080060134E-03
4.66833928147E-04	7.02413667607E-04	2.42641198904E-03	1.03063297104E-03
7.12822246201E-03	1.32229937041E-02	1.12230863642E-02	6.00141236163E-03
5.50692212908E-03	3.75560191274E-03	2.18380757361E-03	2.76188362473E-03
3.18514201187E-03	3.70121629046E-03	1.89928148893E-03	1.07529750153E-03
1.52442863211E-03	3.69452494908E-03	5.55507422972E-03	4.99151351569E-03
3.57890375084E-03	4.13344584819E-03	6.54371511212E-03	5.55649647510E-03
4.53676414407E-03	2.78507322241E-03	8.82667286321E-03	7.30888766375E-03
7.70190637874E-03	8.09672527508E-03	5.52759901508E-03	4.58165985537E-03
4.25368675360E-03	3.04342802251E-03	3.41875215199E-03	4.50506541313E-03
4.71274778037E-03	6.58908375773E-03	7.32730463099E-03	5.20262297582E-03
3.68247300066E-03	4.61353452740E-03	7.17988657717E-03	7.80162717634E-03
6.34780411813E-03	6.14306037113E-03	5.58449954764E-03	5.82844816195E-03
5.40425332855E-03	2.69580162563E-03	3.63341854536E-03	6.22898481759E-03
6.15253791551E-03	1.76007629425E-03	6.17388807026E-03	4.43009713081E-03
6.82919779354E-03	4.11998607339E-03	3.02182418363E-03	3.48253343168E-03
8.92997734887E-04	5.61873699909E-03	5.31164522601E-03	3.79469059916E-03
3.64107758428E-03	4.47748618890E-03	4.05029176620E-03	3.83915499371E-03
5.63973061246E-03	5.41289277534E-03	1.05550805065E-03	1.23238975344E-03
7.23249198196E-03	6.56548465204E-03	3.20398237801E-03	2.32435640752E-03

Table 5.4 Reference of H.P. File to Analog Tape, F_{yB}

H.P. TAPE			ANALOG TAPE	
FILE	INT#	BEAUFORT	TAPE	INDEX
FYB-1	1	1	202	1
FYB-1	2	4	202	2
FYB-1	3	5	202	3
FYB-1	4	6	202	4
FYB-1	5	7	202	5
FYB-1	6	7	202	6
FYB-1	7	7	202	7
FYB-1	8	7	202	8
FYB-1	9	7	202	9
FYB-1	10	7	202	10
FYB-2	1	7	202	11
FYB-2	2	7	202	12
FYB-2	3	6	202	13
FYB-2	4	6	202	14
FYB-2	5	6	202	15
FYB-2	6	3	204	16
FYB-2	7	2	204	17
FYB-2	8	3	204	18
FYB-2	9	2	204	19
FYB-2	10	4	204	20
FYB-3	1	3	204	21
FYB-3	2	1	204	22
FYB-3	3	1	204	23
FYB-3	4	1	204	24
FYB-3	5	1	204	25
FYB-3	6	2	204	26
FYB-3	7	3	204	27
FYB-3	8	5	204	28
FYB-3	9	5	204	29
FYB-3	10	5	204	30
FYB-4	1	5	206	31
FYB-4	2	5	206	32
FYB-4	3	7	206	33
FYB-4	4	6	206	34
FYB-4	5	2	206	35
FYB-4	6	4	206	36
FYB-4	7	3	206	37
FYB-4	8	2	206	38
FYB-4	9	4	206	39
FYB-4	10	3	206	40
FYB-5	1	5	206	41
FYB-5	2	5	206	42
FYB-5	3	4	206	43
FYB-5	4	5	208	5
FYB-5	5	7	208	6
FYB-5	6	7	208	7
FYB-5	7	6	208	8

Table 5.4 (continued)

H.P. TAPE			ANALOG TAPE	
FILE	INT#	BEAUFORT	TAPE	INDEX
FYB-5	8	6	208	9
FYB-5	9	7	208	10
FYB-5	10	7	208	11
FYB-6	1	7	208	12
FYB-6	2	7	208	13
FYB-6	3	7	208	14
FYB-6	4	7	208	15
FYB-6	5	5	208	16
FYB-6	6	6	208	17
FYB-6	7	6	208	18
FYB-6	8	4	210	19
FYB-6	9	6	210	20
FYB-6	10	8	210	21
FYB-7	1	8	210	22
FYB-7	2	9	210	23
FYB-7	3	7	210	24
FYB-7	4	5	210	25
FYB-7	5	7	210	26
FYB-7	6	7	210	27
FYB-7	7	7	210	28
FYB-7	8	6	210	29
FYB-7	9	6	210	30
FYB-7	10	6	210	31
FYB-8	1	6	210	32
FYB-8	2	6	210	33
FYB-8	3	6	210	34
FYB-8	4	3	214	16
FYB-8	5	4	214	17
FYB-8	6	3	214	18
FYB-8	7	2	214	19
FYB-8	8	4	214	20
FYB-8	9	4	214	21
FYB-8	10	2	214	22
FYB-9	1	3	214	23
FYB-9	2	3	214	24
FYB-9	3	3	214	25
FYB-9	4	5	214	26
FYB-9	5	6	214	27
FYB-9	6	5	214	28
FYB-9	7	6	214	29
FYB-9	8	5	216	31
FYB-9	9	5	216	32
FYB-9	10	6	216	33
FYB-10	1	3	216	34
FYB-10	2	5	216	35
FYB-10	3	5	216	36
FYB-10	4	4	216	37

Table 5.4 (continued)

H.P. TAPE			ANALOG TAPE	
FILE	INT#	BEAUFORT	TAPE	INDEX
FYB-10	5	5	216	38
FYB-10	6	5	216	39
FYB-10	7	5	216	40
FYB-10	8	4	216	41
FYB-10	9	3	216	42
FYB-10	10	4	216	43
FYB-11	1	2	216	44
FYB-11	2	2	218	1
FYB-11	3	5	218	2
FYB-11	4	4	218	3
FYB-11	5	2	218	4
FYB-11	6	2	218	5
FYB-11	7	5	218	6
FYB-11	8	2	218	7
FYB-11	9	6	218	8
FYB-11	10	6	218	9
FYB-12	1	2	218	10
FYB-12	2	0	218	11
FYB-12	3	4	218	12
FYB-12	4	5	218	13
FYB-12	5	7	218	14
FYB-12	6	6	218	15
FYB-12	7	6	220	16
FYB-12	8	8	220	17
FYB-12	9	7	220	18
FYB-12	10	1	220	19
FYB-13	1	1	220	20
FYB-13	2	3	220	21
FYB-13	3	2	220	22
FYB-13	4	2	220	23
FYB-13	5	7	220	24
FYB-13	6	8	220	25
FYB-13	7	8	220	26
FYB-13	8	4	220	27
FYB-13	9	6	220	28
FYB-13	10	2	220	29
FYB-14	1	5	220	30
FYB-14	2	5	222	31
FYB-14	3	3	222	32
FYB-14	4	0	222	33
FYB-14	5	0	222	34
FYB-14	6	0	222	35
FYB-14	7	2	224	1
FYB-14	8	2	224	2
FYB-14	9	2	224	3
FYB-14	10	2	224	4

Table 5.4 (continued)

H.P. TAPE			ANALOG TAPE	
FILE	INT#	BEAUFORT	TAPE	INDEX
FYB-15	1	4	224	5
FYB-15	2	7	224	6
FYB-15	3	8	224	7
FYB-15	4	8	224	8
FYB-15	5	8	224	9
FYB-15	6	6	224	10
FYB-15	7	6	224	11
FYB-15	8	6	224	11
FYB-15	9	6	224	12
FYB-15	10	3	224	13
FYB-16	1	4	224	14
FYB-16	2	4	224	15
FYB-16	3	6	226	16
FYB-16	4	6	226	17
FYB-16	5	3	226	18
FYB-16	6	3	226	19
FYB-16	7	4	226	20
FYB-16	8	3	226	21
FYB-16	9	4	226	22
FYB-16	10	4	226	23
FYB-17	1	3	226	24
FYB-17	2	3	226	25
FYB-17	3	3	226	26
FYB-17	4	2	226	27
FYB-17	5	2	226	28
FYB-17	6	4	226	29
FYB-17	7	4	226	30
FYB-17	8	3	228	31
FYB-17	9	3	228	32
FYB-17	10	3	228	33
FYB-18	1	3	228	34
FYB-18	2	3	228	35
FYB-18	3	3	228	36
FYB-18	4	3	228	37
FYB-18	5	3	228	38
FYB-18	6	2	228	39
FYB-18	7	2	230	1
FYB-18	8	4	230	2
FYB-18	9	2	230	3
FYB-18	10	3	230	4
FYB-19	1	4	230	5
FYB-19	2	4	230	6
FYB-19	3	4	230	7
FYB-19	4	1	230	8
FYB-19	5	4	230	9
FYB-19	6	1	230	11

Table 5.4 (continued)

H.P. TAPE			ANALOG TAPE	
FILE	INT#	BEAUFORT	TAPE	INDEX
FYB-19	7	3	230	12
FYB-19	8	3	230	13
FYB-19	9	2	230	14
FYB-19	10	2	230	15
FYB-20	1	2	230	16
FYB-20	2	2	232	17
FYB-20	3	2	232	18
FYB-20	4	1	232	19
FYB-20	5	5	232	20
FYB-20	6	5	232	21
FYB-20	7	5	232	22
FYB-20	8	3	232	23
FYB-20	9	2	232	24
FYB-20	10	5	232	25
FYB-21	1	6	232	26
FYB-21	2	7	232	27
FYB-21	3	7	232	28
FYB-21	4	7	232	29
FYB-21	5	9	232	30
FYB-21	6	8	234	31
FYB-21	7	7	234	32
FYB-21	8	6	234	33
FYB-21	9	6	234	34
FYB-21	10	5	234	35
FYB-22	1	4	234	36
FYB-22	2	3	234	37
FYB-22	3	1	234	38
FYB-22	4	1	234	39

Table 5.5 Reference of H.P. File to Analog Tape, MKT

H.P. TAPE			ANALOG TAPE	
FILE	INT#	BEAUFORT	TAPE	INTERVAL
MKT-1	1&2	6	1	1
MKT-1	3&4	7	1	2
MKT-1	5&6	7	1	3
MKT-1	7&8	7	1	4
MKT-1	9&10	7	1	5
MKT-2	1&2	7	1	6
MKT-2	3&4	8	1	7
MKT-2	5&5	7	1	8
MKT-2	7&8	7	1	9
MKT-2	9&10	7	1	10
MKT-3	1&2	7	1	11
MKT-3	3&4	7	1	12
MKT-3	5&6	8	1	13
MKT-3	7&8	7	1	14
MKT-3	9&10	6	1	15
MKT-4	1&2	6	1	16
MKT-4	3&4	6	1	18
MKT-4	5&6	6	1	19
MKT-4	7&8	6	1	20
MKT-4	9&10	6	1	21
MKT-5	1&2	7	1	22
MKT-5	3&4	7	1	23
MKT-5	5&6	8	1	24
MKT-5	7&8	8	1	25
MKT-5	9&10	8	1	26
MKT-6	1&2	8	1	27
MKT-6	3&4	7	1	28
MKT-6	5&6	7	1	29
MKT-6	7&8	7	1	30
MKT-6	9&10	8	1	31
MKT-7	1&2	7	1	32
MKT-7	3&4	7	1	33
MKT-7	5&6	8	1	34
MKT-7	7&8	7	1	35
MKT-7	9&10	7	1	36
MKT-8	1&2	5	2	13
MKT-8	3&4	5	2	14
MKT-8	5&6	5	2	15
MKT-8	7&8	4	2	21
MKT-8	9&10	5	2	22
MKT-9	1&2	5	2	23
MKT-9	3&4	6	2	25
MKT-9	5&6	7	2	26
MKT-9	7&8	7	2	28
MKT-9	9&10	6	2	29

Table 5.5 (Continued)

H.P. TAPE			ANALOG TAPE	
FILE	INT#	BEAUFORT	TAPE	INTERVAL
MKT-10	1&2	5	2	32
MKT-10	3&4	5	2	33
MKT-10	5&6	4	2	41
MKT-10	7&8	5	2	42
MKT-10	9&10	5	2	44
MKT-11	1&2	6	2	45
MKT-11	3&4	5	2	46
MKT-11	5&6	8	2	47
MKT-11	7&8	9	2	48
MKT-11	9&10	5	2	49
MKT-12	1&2	6	2	50
MKT-12	3&4	3	2	51
MKT-12	5&6	2	2	52
MKT-12	7&8	2	2	54
MKT-12	9&10	2	2	55
MKT-13	1&2	2	2	56
MKT-13	3&4	3	2	57
MKT-13	5&6	3	2	58
MKT-13	7&8	3	2	59
MKT-13	9&10	6	2	60
MKT-14	1&2	6	2	61
MKT-14	3&4	3	2	62
MKT-14	5&6	5	2	63
MKT-14	7&8	5	2	64
MKT-14	9&10	9	2	66
MKT-15	1&2	4	3	7
MKT-15	3&4	2	3	17
MKT-15	5&6	2	3	23
MKT-15	7&8	2	3	24
MKT-15	9&10	2	3	25
MKT-16	1&2	2	3	26
MKT-16	3&4	3	3	28
MKT-16	5&6	2	3	29
MKT-16	7&8	2	3	30
MKT-16	9&10	2	3	31
MKT-17	1&2	3	3	32
MKT-17	3&4	4	3	33
MKT-17	5&6	5	3	34
MKT-17	7&8	5	3	35
MKT-17	9&10	4	3	36
MKT-18	1&2	3	3	37
MKT-18	3&4	4	3	38
MKT-18	5&6	5	3	40
MKT-18	7&8	5	3	41
MKT-18	9&10	4	3	42

Table 5.5 (Continued)

H.P. TAPE			ANALOG TAPE	
FILE	INT#	BEAUFORT	TAPE	INTERVAL
MKT-19	1&2	5	3	43
MKT-19	3&4	5	3	44
MKT-19	5&6	6	3	45
MKT-19	7&8	5	3	46
MKT-19	9&10	5	3	47
MKT-20	1&2	5	3	48
MKT-20	3&4	6	3	49
MKT-20	5&6	6	3	50
MKT-20	7&8	7	3	51
MKT-20	9&10	4	4	15
MKT-21	1&2	4	4	17
MKT-21	3&4	4	4	18
MKT-21	5&6	2	4	19
MKT-21	7&8	2	4	20
MKT-21	9&10	8	4	23
MKT-22	1&2	5	4	49
MKT-22	3&4	5	4	50
MKT-22	5&6	5	4	51
MKT-22	7&8	6	4	55
MKT-22	9&10	6	4	56
MKT-23	1&2	7	4	57
MKT-23	3&4	8	4	60
MKT-23	5&6	7	4	62
MKT-23	7&8	3	5	1
MKT-23	9&10	3	5	2
MKT-24	1&2	2	5	3
MKT-24	3&4	3	5	4
MKT-24	5&6	3	5	5
MKT-24	7&8	2	5	6
MKT-24	9&10	3	5	7
MKT-25	1&2	4	6	19
MKT-25	3&4	5	6	24
MKT-25	5&6	7	6	25
MKT-25	7&8	9	6	26
MKT-25	9&10	10	6	27
MKT-26	1&2	10	6	29
MKT-26	3&4	9	6	31
MKT-26	5&6	8	6	32
MKT-26	7&8	6	6	44
MKT-26	9&10	3	6	46
MKT-27	1&2	3	6	47
MKT-27	3&4	6	6	48
MKT-27	5&6	6	6	49
MKT-27	7&8	4	6	51
MKT-27	9&10	3	6	52

Table 5.5 (Continued)

H.P. TAPE			ANALOG TAPE	
FILE	INT#	BEAUFORT	TAPE	INTERVAL
MKT-28	1&2	2	6	53
MKT-28	3&4	6	6	54
MKT-28	5&6	6	6	56
MKT-28	7&8	7	6	57
MKT-28	9&10	7	6	58
MKT-29	1&2	6	7	1
MKT-29	3&4	7	7	2
MKT-29	5&6	7	7	3
MKT-29	7&8	7	7	4

Table 5.6 Reference of U.P. File To Analog Tape, MCL

H.P. TAPE			ANALOG TAPE	
FILE	INT#	BEAUFORT	TAPE	INTERVAL
MCL-1	1&2	3	1	18
MCL-1	3&4	3	1	19
MCL-1	5&6	4	1	20
MCL-1	7&8	3	1	21
MCL-1	9&10	6	1	22
MCL-2	1&2	4	1	23
MCL-2	3&4	4	1	24
MCL-2	5&6	4	1	25
MCL-2	7&8	3	1	26
MCL-2	9&10	3	1	32
MCL-3	1&2	2	1	33
MCL-3	3&4	2	1	34
MCL-3	5&6	3	2	6
MCL-3	7&8	3	2	7
MCL-3	9&10	3	2	8
MCL-4	1&2	3	2	9
MCL-4	3&4	3	2	10
MCL-4	5&6	5	2	11
MCL-4	7&8	5	2	12
MCL-4	9&10	5	2	13
MCL-5	1&2	4	2	14
MCL-5	3&4	5	2	15
MCL-5	5&6	4	2	16
MCL-5	7&8	2	2	17
MCL-5	9&10	4	2	18
MCL-6	1&2	2	2	19
MCL-6	3&4	2	2	20
MCL-6	5&6	2	2	21
MCL-6	7&8	2	2	22
MCL-6	9&10	2	2	23
MCL-7	1&2	2	2	24
MCL-7	3&4	2	2	25
MCL-7	5&6	2	2	26
MCL-7	7&8	6	2	27
MCL-7	9&10	3	2	28
MCL-8	1&2	3	2	29
MCL-8	3&4	5	2	30
MCL-8	5&6	4	2	31
MCL-8	7&8	5	2	32
MCL-8	9&10	4	2	33
MCL-9	1&2	6	2	34
MCL-9	3&4	6	2	35
MCL-9	5&6	6	2	36
MCL-9	7&8	7	2	37
MCL-9	9&10	6	2	38

Table 5.6 (Continued)

H.P. TAPE			ANALOG TAPE	
FILE	INT#	BEAUFORT	TAPE	INTERVAL
MCL-10	1&2	4	2	39
MCL-10	3&4	2	2	40
MCL-10	5&6	5	2	41
MCL-10	7&8	6	2	42
MCL-10	9&10	7	2	43
MCL-11	1	5	2	44
MCL-11	2	2	2	49
MCL-11	3	2	2	50
MCL-11	4	3	2	51
MCL-11	5	2	2	58
MCL-11	6	3	2	59
MCL-11	7	3	2	60
MCL-11	8	1	2	61
MCL-11	9	1	2	62
MCL-11	10	3	2	63
MCL-12	1	5	2	64
MCL-12	2	3	2	65
MCL-12	3	3	2	66
MCL-12	4	3	2	67
MCL-12	5	3	2	68
MCL-12	6	3	2	69
MCL-12	7	2	3	9
MCL-12	8	4	3	10
MCL-12	9	5	3	11
MCL-12	10	5	3	12
MCL-13	1	4	3	13
MCL-13	2	3	3	14
MCL-13	3	3	3	15
MCL-13	4	3	3	16
MCL-13	5	3	3	17
MCL-13	6	4	3	18
MCL-13	7	5	3	19
MCL-13	8	4	3	20
MCL-13	9	3	3	21
MCL-13	10	6	3	30
MCL-14	1	6	3	31
MCL-14	2	3	3	32
MCL-14	3	2	3	39
MCL-14	4	5	3	40
MCL-14	5	3	3	41
MCL-14	6	3	3	42
MCL-14	7	3	3	43
MCL-14	8	3	3	44
MCL-14	9	2	3	45
MCL-14	10	2	3	46

Table 5.6 (Continued)

H.P. TAPE			ANALOG TAPE	
FILE	INT#	BEAUFORT	TAPE	INTERVAL
MCL-15	1	2	3	47
MCL-15	2	2	3	48
MCL-15	3	1	3	49
MCL-15	4	2	3	50
MCL-15	5	2	3	51
MCL-15	6	2	3	52
MCL-15	7	2	3	53
MCL-15	8	3	3	54
MCL-15	9	3	3	55
MCL-15	10	2	3	56
MCL-16	1	3	3	57
MCL-16	2	3	3	58
MCL-16	3	3	3	59
MCL-16	4	3	3	60
MCL-16	5	3	3	61
MCL-16	6	5	3	62
MCL-16	7	5	3	63
MCL-16	8	5	3	64
MCL-16	9	4	3	65
MCL-16	10	4	3	66
MCL-17	1	4	3	67
MCL-17	2	4	3	68
MCL-17	3	2	3	69
MCL-17	4	2	3	70
MCL-17	5	1	4	1
MCL-17	6	2	4	2
MCL-17	3	2	4	3
MCL-17	8	2	4	4
MCL-17	9	3	4	5
MCL-17	10	4	4	6
MCL-18	1	4	4	7
MCL-18	2	3	4	8
MCL-18	3	3	4	9
MCL-18	4	1	4	22
MCL-18	5	2	4	23
MCL-18	6	3	4	24
MCL-18	7	3	4	25
MCL-18	8	4	4	26
MCL-18	9	4	4	27
MCL-18	10	4	4	28
MCL-19	1	4	4	29
MCL-19	2	4	4	30
MCL-19	3	4	4	31
MCL-19	4	2	4	32
MCL-19	5	0	4	39
MCL-19	6	5	4	40

Table 5.6 (Continued)

H.P. TAPE			ANALOG TAPE	
FILE	INT#	BEAUFORT	TAPE	INTERVAL
MCL-19	7	3	4	41
MCL-19	8	3	4	55
MCL-19	9	4	4	56
MCL-19	10	4	4	57
MCL-20	1	5	4	58
MCL-20	2	6	4	59
MCL-20	3	6	4	60
MCL-20	4	4	4	61
MCL-20	5	2	4	62
MCL-20	6	2	4	63
MCL-20	7	3	4	64
MCL-20	8	4	4	65
MCL-20	9	4	4	66
MCL-20	10	2	4	68
MCL-21	1	4	4	69
MCL-21	2	3	4	70
MCL-21	3	2	5	1
MCL-21	4	5	5	2
MCL-21	5	5	5	3
MCL-21	6	5	5	4
MCL-21	7	7	5	5
MCL-21	8	7	5	6
MCL-21	9	3	5	7
MCL-21	10	3	5	8
MCL-22	1	3	5	9
MCL-22	2	3	5	10
MCL-22	3	3	5	11
MCL-22	4	3	5	12
MCL-22	5	3	5	13
MCL-22	6	3	5	14
MCL-22	7	3	5	15
MCL-22	8	3	5	16
MCL-22	9	2	5	17
MCL-22	10	1	5	18
MCL-23	1	1	5	19
MCL-23	2	3	5	20
MCL-23	3	3	5	21
MCL-23	4	3	5	22
MCL-24	5	2	5	23
MCL-23	6	2	5	24
MCL-23	7	0	5	25
MCL-23	8	2	5	26
MCL-23	9	5	5	27
MCL-23	10	5	5	28
MCL-24	1	4	5	29

Table 5.6 (Continued)

H.P. TAPE			ANALOG TAPE	
FILE	INT#	BEAUFORT	TAPE	INTERVAL
MCL-24	2	4	5	30
MCL-24	3	4	5	31
MCL-24	4	4	5	32
MCL-24	5	6	5	33
MCL-24	6	6	5	34
MCL-24	7	4	5	40
MCL-24	8	3	5	41
MCL-24	9	5	5	51
MCL-24	10	5	5	52
MCL-25	1	6	5	53
MCL-25	2	6	5	54
MCL-25	3	5	5	55
MCL-25	4	5	5	56
MCL-25	5	4	5	57
MCL-25	6	4	5	58
MCL-25	7	3	5	59
MCL-25	8	5	5	60
MCL-25	9	5	5	61
MCL-25	10	3	5	62
MCL-26	1&2	3	6	3
MCL-26	3&4	3	6	4
MCL-26	5&6	3	6	5
MCL-26	7&8	3	6	6
MCL-26	9&10	3	6	7
MCL-27	1&2	2	6	8
MCL-27	3&4	3	6	9
MCL-27	5&6	3	6	10
MCL-27	7&8	3	6	11
MCL-27	9&10	3	6	12
MCL-28	1&2	4	6	13
MCL-28	3&4	3	6	14
MCL-28	5&6	3	6	15
MCL-28	7&8	3	6	16
MCL-28	9&10	3	6	25
MCL-29	1&2	3	6	26
MCL-29	3&4	3	6	27
MCL-29	5&6	2	6	32
MCL-29	7&8	5	6	33
MCL-29	9&10	5	6	34
MCL-30	1&2	5	6	35
MCL-30	3&4	6	6	36
MCL-30	5&6	5	6	37
MCL-30	7&8	5	6	38
MCL-30	9&10	5	6	39
MCL-31	1&2	4	6	40

Table 5.6 (Continued)

H.P. TAPE			ANALOG TAPE	
FILE	INT#	BEAUFORT	TAPE	INTERVAL
MCL-31	3&4	3	6	41
MCL-31	5&6	4	6	42
MCL-31	7&8	4	6	43
MCL-31	9&10	2	6	44
MCL-32	1&2	4	6	45
MCL-32	3&4	4	6	46
MCL-32	5&6	3	6	47
MCL-32	7&8	3	6	48
MCL-32	9&10	3	6	49
MCL-33	1&2	3	6	50
MCL-33	3&4	3	6	51
MCL-33	5&6	4	6	52
MCL-33	7&8	5	6	53
MCL-33	9&10	4	6	54
MCL-34	1&2	3	6	55
MCL-34	3&4	4	6	56
MCL-34	5&6	4	6	57
MCL-34	7&8	4	6	58
MCL-34	9&10	5	6	59
MCL-35	1&2	4	6	60
MCL-35	3&4	4	6	61
MCL-35	5&6	4	6	62
MCL-35	7&8	4	6	63
MCL-35	9&10	5	6	64
MCL-36	1&2	5	6	65
MCL-36	3&4	4	6	66
MCL-36	5&6	3	6	67
MCL-36	7&8	3	6	68
MCL-36	9&10	2	6	69
MCL-37	1&2	2	6	70
MCL-37	3&4	2	6	71
MCL-37	5&6	2	6	72
MCL-37	7&8	2	6	73
MCL-37	9&10	2	7	12
MCL-38	1&2	2	7	13
MCL-38	3&4	3	7	14
MCL-38	5&6	3	7	15
MCL-38	7&8	4	7	16
MCL-38	9&10	7	7	17
MCL-39	1&2	7	7	18
MCL-39	3&4	6	7	19
MCL-39	5&6	1	7	20
MCL-39	7&8	0	7	21
MCL-39	9&10	0	7	22
MCL-40	1&2	2	7	23
MCL-40	3&4	1	7	31
MCL-40	5&6	1	7	32
MCL-40	7&8	1	7	33
MCL-40	9&10	3	7	34

Table 5.7 Reference of H.P. File To Analog Tape, SLM

H.P. TAPE			ANALOG TAPE	
FILE	INT#	BEAUFORT	TAPE	INTERVAL
SLM-1A	1&2	4	11	8
SLM-1A	3&4	4	11	9
SLM-1A	5&6	5	11	10
SLM-1A	7&8	5	11	11
SLM-1A	9&10	5	11	12
SLM-2A	1&2	5	11	13
SLM-2A	3&4	3	11	14
SLM-2A	5&6	2	11	15
SLM-2A	7&8	2	11	16
SLM-2A	9&10	3	11	25
SLM-3A	1&2	4	11	26
SLM-3A	3&4	4	11	27
SLM-3A	5&6	4	11	35
SLM-3A	7&8	2	11	36
SLM-3A	9&10	3	11	37
SLM-4A	1&2	3	11	38
SLM-4A	3&4	4	11	39
SLM-4A	5&6	4	11	40
SLM-4A	7&8	4	11	41
SLM-4A	9&10	4	11	42
SLM-5A	1&2	3	11	44
SLM-5A	3&4	3	11	45
SLM-5A	5&6	3	11	46
SLM-5A	7&8	4	11	47
SLM-5A	9&10	5	11	48
SLM-6A	1&2	5	11	49
SLM-6A	3&4	4	11	50
SLM-6A	5&6	4	11	51
SLM-6A	7&8	3	11	52
SLM-6A	9&10	2	11	53
SLM-7A	1&2	2	11	54
SLM-7A	3&4	4	11	55
SLM-7A	5&6	4	11	56
SLM-7A	7&8	4	11	57
SLM-7A	9&10	4	11	58
SLM-8A	1&2	5	11	59
SLM-8A	3&4	6	11	60
SLM-8A	5&6	5	11	61
SLM-8A	7&8	4	11	62
SLM-8A	9&10	3	11	63
SLM-9A	1&2	2	11	64
SLM-9A	3&4	2	11	65
SLM-9A	5&6	3	11	66
SLM-9A	7&8	4	11	68
SLM-9A	9&10	3	11	69

Table 5.7 (Continued)

H.P. TAPE			ANALOG TAPE	
FILE	INT#	BEAUFORT	TAPE	INTERVAL
SLM-10A	1&2	3	11	70
SLM-10A	3&4	3	11	71
SLM-10A	5&6	3	11	72
SLM-10A	7&8	4	11	73
SLM-10A	9&10	5	12	8
SLM-11A	1&2	4	12	9
SLM-11A	3&4	5	12	10
SLM-11A	5&6	5	12	11
SLM-11A	7&8	4	12	12
SLM-11A	9&10	5	12	13
SLM-12A	1&2	6	12	14
SLM-12A	3&4	5	12	15
SLM-12A	5&6	6	12	16
SLM-12A	7&8	6	12	17
SLM-12A	9&10	7	12	18
SLM-13A	1&2	8	12	19
SLM-13A	3&4	3	12	37
SLM-13A	5&6	3	12	38
SLM-13A	7&8	7	12	39
SLM-13A	9&10	8	12	40
SLM-14A	1&2	6	12	41
SLM-14A	3&4	6	12	42
SLM-14A	5&6	6	12	43
SLM-14A	7&8	4	12	44
SLM-14A	9&10	5	12	45
SLM-15A	1&2	5	12	46
SLM-15A	3&4	5	12	47
SLM-15A	5&6	4	12	48
SLM-15A	7&8	6	12	49
SLM-15A	9&10	4	12	50
SLM-16A	1&2	2	12	56
SLM-16A	3&4	1	12	62
SLM-16A	5&6	4	12	64
SLM-16A	7&8	2	12	65
SLM-16A	9&10	4	12	66
SLM-17A	1&2	2	12	67
SLM-17A	3&4	5	12	70
SLM-17A	5&6	6	13	1
SLM-17A	7&8	6	13	2
SLM-17A	9&10	5	13	3
SLM-18A	1&2	6	13	4
SLM-18A	3&4	6	13	5
SLM-18A	5&6	5	13	6
SLM-18A	7&8	6	13	7
SLM-18A	9&10	6	13	8

Table 5.7 (Continued)

H.P. TAPE			ANALOG TAPE	
FILE	INT#	BEAUFORT	TAPE	INTERVAL
SLM-19A	1&2	4	13	9
SLM-19A	3&4	3	13	10
SLM-19A	5&6	5	13	11
SLM-19A	7&8	4	13	12
SLM-19A	9&10	4	13	13
SLM-20A	1&2	5	13	14
SLM-20A	3&4	3	13	15
SLM-20A	5&6	3	13	16
SLM-20A	7&8	4	13	17
SLM-20A	9&10	3	13	18
SLM-21A	1&2	7	13	19
SLM-21A	3&4	7	13	20
SLM-21A	5&6	7	13	21
SLM-21A	7&8	8	13	22
SLM-21A	9&10	9	13	23
SLM-22A	1&2	7	13	24
SLM-22A	3&4	7	13	25
SLM-22A	5&6	7	13	26
SLM-22A	7&8	6	13	27
SLM-22A	9&10	6	13	28
SLM-23A	1&2	5	13	29
SLM-23A	3&4	2	13	30
SLM-23A	5&6	4	13	31
SLM-23A	7&8	5	13	32
SLM-23A	9&10	5	13	33
SLM-24A	1&2	6	13	35
SLM-24A	3&4	2	14	9
SLM-24A	5&6	4	14	10
SLM-24A	7&8	5	14	11
SLM-24A	9&10	3	14	12
SLM-25A	1&2	3	14	13
SLM-25A	3&4	3	14	14
SLM-25A	5&6	3	14	15
SLM-25A	7&8	4	14	16
SLM-25A	9&10	6	14	17
SLM-26A	1&2	2	14	18
SLM-26A	3&4	3	14	19
SLM-26A	5&6	3	14	20
SLM-26A	7&8	0	14	21
SLM-26A	9&10	6	14	30
SLM-27A	1&2	5	14	31
SLM-27A	3&4	4	14	32
SLM-27A	5&6	5	14	33
SLM-27A	7&8	2	15	7
SLM-27A	9&10	2	15	8

Table 5.7 (Continued)

H.P. TAPE			ANALOG TAPE	
FILE	INT#	BEAUFORT	TAPE	INTERVAL
SLM-28A	1&2	4	15	9
SLM-28A	3&4	4	15	10
SLM-28A	5&6	3	15	11
SLM-28A	7&8	4	15	12
SLM-28A	9&10	4	15	13
SLM-29A	1	3	15	14
SLM-29A	2	4	15	15
SLM-29A	3	4	15	16
SLM-29A	4	3	15	17
SLM-29A	5	5	15	18
SLM-29A	6	6	15	19
SLM-29A	7	6	15	20
SLM-29A	8	9	15	21
SLM-29A	9	9	15	22
SLM-29A	10	8	15	23
SLM-30A	1	7	15	24
SLM-30A	2	4	15	25
SLM-30A	3	4	15	26
SLM-30A	4	6	15	27
SLM-30A	5	7	15	28
SLM-30A	6	7	15	29
SLM-30A	7	8	15	30
SLM-30A	8	8	15	31
SLM-30A	9	7	15	32
SLM-30A	10	7	15	33
SLM-31A	1	5	15	34
SLM-31A	2	4	15	35
SLM-31A	3	4	15	36
SLM-31A	4	5	15	37
SLM-31A	5	4	15	38
SLM-31A	6	4	15	39
SLM-31A	7	4	15	40
SLM-31A	8	4	15	41
SLM-31A	9	4	15	42
SLM-31A	10	8	15	43
SLM-32A	1	4	15	44
SLM-32A	2	2	15	45
SLM-32A	3	7	15	46
SLM-32A	4	9	15	47
SLM-32A	5	9	15	48
SLM-32A	6	9	15	49
SLM-32A	7	8	15	50
SLM-32A	8	6	15	51
SLM-32A	9	5	15	52
SLM-32A	10	7	15	53

Table 5.7 (Continued)

H.P. TAPE			ANALOG TAPE	
FILE	INT#	BEAUFORT	TAPE	INTERVAL
SLM-33A	1	7	15	54
SLM-33A	2	6	15	55
SLM-33A	3	7	15	56
SLM-33A	4	4	15	57
SLM-33A	5	2	15	58
SLM-33A	6	6	15	63
SLM-33A	7	5	15	64
SLM-33A	8	4	16	1
SLM-33A	9	3	16	2
SLM-33A	10	4	16	3
SLM-34A	1	6	16	4
SLM-34A	2	4	16	5
SLM-34A	3	3	16	6
SLM-34A	4	3	16	7
SLM-34A	5	3	16	8
SLM-34A	6	3	16	9
SLM-34A	7	3	16	10
SLM-34A	8	3	16	11
SLM-34A	9	3	16	12
SLM-34A	10	2	16	13
SLM-35A	1	0	16	14
SLM-35A	2	0	16	15
SLM-35A	3	4	16	29
SLM-35A	4	6	16	30
SLM-35A	5	5	16	31
SLM-35A	6	4	16	32
SLM-35A	7	4	16	33
SLM-35A	8	5	16	34
SLM-35A	9	2	16	35
SLM-35A	10	4	16	36
SLM-36A	1	4	16	37
SLM-36A	2	3	16	38
SLM-36A	3	4	16	39
SLM-36A	4	4	16	40
SLM-36A	5	4	16	41
SLM-36A	6	5	16	42
SLM-36A	7	4	16	47
SLM-36A	8	4	16	48
SLM-36A	9	3	16	49
SLM-36A	10	5	16	50
SLM-37A	1	3	16	54
SLM-37A	2	4	16	55
SLM-37A	3	4	16	56
SLM-37A	4	3	16	57
SLM-37A	5	4	16	58

Table 5.7 (Continued)

H.P. TAPE			ANALOG TAPE	
FILE	INT#	BEAUFORT	TAPE	INTERVAL
SLM-37A	6	5	16	59
SLM-37A	7	5	16	60
SLM-37A	8	5	16	61
SLM-37A	9	6	16	62
SLM-37A	10	6	16	63
SLM-38A	1	8	16	64
SLM-38A	2	8	16	65
SLM-38A	3	8	16	66
SLM-38A	4	9	16	67
SLM-38A	5	10	16	68
SLM-38A	6	10	16	69
SLM-38A	7	10	16	70
SLM-38A	8	9	16	71
SLM-38A	9	9	16	72
SLM-38A	10	10	16	73
SLM-39A	1	10	16	74
SLM-39A	2	9	16	75
SLM-39A	3	9	17	1
SLM-39A	4	6	17	2
SLM-39A	5	5	17	3
SLM-39A	6	7	17	4
SLM-39A	7	8	17	5
SLM-39A	8	8	17	6
SLM-39A	9	9	17	7
SLM-39A	10	8	17	8
SLM-40A	1	7	17	9
SLM-40A	2	6	17	10
SLM-40A	3	4	17	11
SLM-40A	4	2	17	12
SLM-40A	5	2	17	13
SLM-40A	6	5	17	14
SLM-40A	7	2	17	15
SLM-40A	8	3	17	16
SLM-40A	9	4	17	17
SLM-40A	10	4	17	18
SLM-41A	1	4	17	19
SLM-41A	2	4	17	20
SLM-41A	3	3	17	21
SLM-41A	4	4	17	22
SLM-41A	5	5	17	33
SLM-41A	6	5	17	34
SLM-41A	7	5	17	35
SLM-41A	8	5	17	36
SLM-41A	9	5	17	37
SLM-41A	10	5	17	38

Table 5.7 (Continued)

H.P. TAPE			ANALOG TAPE	
FILE	INT#	BEAUFORT	TAPE	INTERVAL
SLM-42A	1	5	17	39
SLM-42A	2	5	17	40
SLM-42A	3	4	17	41
SLM-42A	4	5	17	42
SLM-42A	5	2	17	43
SLM-42A	6	3	17	55
SLM-42A	7	5	17	56
SLM-42A	8	5	17	57
SLM-42A	9	5	17	58
SLM-42A	10	3	17	69
SLM-43A	1	5	17	70
SLM-43A	2	7	17	71
SLM-43A	3	5	17	72
SLM-43A	4	4	17	73
SLM-43A	5	4	18	1

Table 5.8 Calculated and Measured Extreme Values for 30 Minutes

SHIP	GAUGE	H.P. TAPE		ANALOG TAPE		MOST PROBABLE VALUE FOR FOR 800-SEC INTERVAL (ksi)	MAX
		FILE	INT. NO.	TAPE	INDEX		
McLEAN 1975	F_yB	F_yB-9	5	214	27	45	
			6	"	28	37	
		F_yB-15	8	224	11	47	
			9	"	12	65	
McLEAN May-June 1977	2	MCL-1	1	1	18	31	
	8	"	2	1	18	34	
	2	"	3	1	19	26	
	8	"	4	1	20	27	
McLEAN Sept. 77-Jan. 78	3	SLM-1	7	11	11	22	
	8	"	8	11	11	25	
MARKET 1976	2	MKT-19	5	3	45	39	
	8	"	6	3	45	33	

Table 6.1 **Cases Studied for Fatigue Damage**

SHIP	PERIOD	GAUGE	NUMBER OF 800-SEC INTERVALS SELECTED	REMARKS
SEA-LAND McLEAN	Jan.-March 1975	FyB	214	Gauge on unmodified hatch corners, North Altantic Data
	May-July 1977 Sept.77-Jan. 1978	2 3	265	Gauge on modified hatch corners, Pacific Data.
	May-July 1977 Sept.77-Jan. 1978	8 8	560	Gauge on modified hatch corners, Pacific Data.
SEA-LAND MARKET	Oct.-Dec. 1976	2	144	Gauge on unmodified side of hatch corner, North Atlantic Data.
	Oct.-Dec. 1976	8	144	Gauge on modified side of hatch corner, North Atlantic Data

Table 6.2 Cyclic Stress Occurrences, Gage F_yB on McLean, 1975

STRS. AMPL. (KSI)	S.S. 1	S.S. 2	S.S. 3	S.S. 4	S.S. 5	S.S. 6	S.S. 7	S.S. 8	S.S. 9
1	354.9	414.1	207.2	106.7	413.3	175.3	184.9	24.9	2.8
2	245.5	402.5	271.6	228.8	341.8	279.8	185.2	64.9	8.0
3	164.6	344.8	266.5	219.0	284.5	236.3	233.1	83.5	12.6
4	101.6	228.1	222.3	172.1	196.0	224.0	249.6	84.4	16.1
5	56.9	138.6	163.6	138.2	137.3	207.4	234.4	77.9	18.4
6	29.3	85.2	118.0	116.6	105.1	182.9	205.7	70.7	19.6
7	16.2	55.9	90.0	100.4	86.7	159.2	175.8	64.5	19.6
8	11.3	40.0	73.4	86.2	74.7	139.1	150.4	58.7	18.7
9	10.1	31.1	62.4	73.1	65.8	122.6	130.4	52.9	17.3
10	10.1	25.8	54.1	61.0	58.5	108.4	114.9	47.0	15.5
11	10.3	22.5	47.3	50.4	52.1	95.8	102.4	41.3	13.7
12	10.4	20.1	41.4	41.4	46.6	84.3	91.7	35.9	11.9
13	10.5	18.2	36.3	33.9	41.7	73.9	82.1	30.9	10.2
14	10.4	16.7	32.0	27.9	37.3	64.5	73.3	26.4	8.7
15	10.1	15.3	28.3	23.0	33.4	56.0	65.1	22.3	7.4
16	9.8	14.1	25.1	19.2	29.9	48.5	57.4	18.7	6.2
17	9.4	13.1	22.4	16.2	26.9	41.9	50.3	15.5	5.2
18	8.9	12.1	19.9	13.8	24.2	36.0	43.9	12.8	4.4
19	8.3	11.1	17.8	11.8	21.9	30.9	38.1	10.5	3.6
20	7.7	10.3	15.9	10.2	19.9	26.4	32.9	8.5	3.0
21	7.1	9.5	14.3	8.9	18.1	22.6	28.4	6.8	2.4
22	6.5	8.7	12.8	7.8	16.5	19.2	24.4	5.4	2.0
23	5.9	8.0	11.4	6.9	15.0	16.4	20.9	4.2	1.6
24	5.3	7.3	10.2	6.2	13.7	14.0	17.9	3.3	1.2
25	4.7	6.7	9.1	5.5	12.5	12.0	15.4	2.5	0.9
26	4.1	6.1	8.1	4.9	11.3	10.3	13.2	1.9	0.7
27	3.6	5.6	7.3	4.5	10.3	8.8	11.3	1.4	0.5
28	3.1	5.1	6.5	4.0	9.4	7.6	9.7	1.1	0.4
29	2.7	4.6	5.8	3.7	8.5	6.6	8.4	0.8	0.3
30	2.3	4.2	5.2	3.3	7.7	5.7	7.2	0.6	0.2
31	2.0	3.8	4.6	3.0	6.9	5.0	6.2	0.4	0.1
32	1.7	3.4	4.1	2.8	6.3	4.4	5.4	0.3	0.1
33	1.4	3.1	3.7	2.5	5.6	3.8	4.6	0.2	0.1
34	1.2	2.8	3.3	2.3	5.1	3.3	4.0	0.1	0.1
35	1.0	2.5	3.0	2.1	4.6	2.9	3.5	0.1	0.0
36	0.8	2.3	2.7	1.9	4.1	2.6	3.0	0.1	0.0
37	0.6	2.1	2.4	1.8	3.8	2.3	2.6	0.1	0.0
38	0.5	1.9	2.2	1.6	3.4	2.0	2.3	0.0	0.0
39	0.4	1.7	2.0	1.5	3.1	1.8	2.0	0.0	0.0
40	0.3	1.5	1.8	1.3	2.8	1.6	1.8	0.0	0.0
41	0.3	1.4	1.6	1.2	2.5	1.4	1.6	0.0	0.0
42	0.2	1.3	1.5	1.1	2.3	1.3	1.4	0.0	0.0
43	0.2	1.1	1.3	1.0	2.1	1.1	1.2	0.0	0.0
44	0.1	1.0	1.2	0.9	1.9	1.0	1.1	0.0	0.0
45	0.1	0.9	1.1	0.8	1.7	0.9	0.9	0.0	0.0
46	0.1	0.9	1.0	0.7	1.5	0.8	0.8	0.0	0.0
47	0.1	0.8	0.9	0.6	1.4	0.7	0.8	0.0	0.0
48	0.1	0.7	0.9	0.6	1.3	0.6	0.7	0.0	0.0
49	0.0	0.6	0.8	0.5	1.1	0.6	0.6	0.0	0.0
50	0.0	0.6	0.7	0.4	1.0	0.5	0.5	0.0	0.0
51	0.0	0.5	0.7	0.4	0.9	0.4	0.5	0.0	0.0
52	0.0	0.5	0.6	0.3	0.9	0.4	0.4	0.0	0.0
53	0.0	0.4	0.6	0.3	0.8	0.3	0.4	0.0	0.0
54	0.0	0.4	0.5	0.3	0.7	0.3	0.4	0.0	0.0
55	0.0	0.3	0.5	0.2	0.6	0.3	0.3	0.0	0.0
56	0.0	0.3	0.5	0.2	0.6	0.2	0.3	0.0	0.0
57	0.0	0.3	0.4	0.2	0.5	0.2	0.3	0.0	0.0
58	0.0	0.2	0.4	0.1	0.5	0.2	0.2	0.0	0.0
59	0.0	0.2	0.4	0.1	0.4	0.2	0.2	0.0	0.0
60	0.0	0.2	0.3	0.1	0.4	0.1	0.2	0.0	0.0
61	0.0	0.2	0.3	0.1	0.4	0.1	0.2	0.0	0.0
62	0.0	0.1	0.3	0.1	0.3	0.1	0.1	0.0	0.0
63	0.0	0.1	0.3	0.1	0.3	0.1	0.1	0.0	0.0
64	0.0	0.1	0.2	0.1	0.3	0.1	0.1	0.0	0.0
65	0.0	0.1	0.2	0.1	0.2	0.1	0.1	0.0	0.0
66	0.0	0.1	0.2	0.0	0.2	0.1	0.1	0.0	0.0
67	0.0	0.1	0.2	0.0	0.2	0.1	0.1	0.0	0.0
68	0.0	0.1	0.2	0.0	0.2	0.1	0.1	0.0	0.0
69	0.0	0.1	0.1	0.0	0.2	0.0	0.1	0.0	0.0
70	0.0	0.1	0.1	0.0	0.1	0.0	0.1	0.0	0.0
TOTAL INT.	16	31	35	29	30	33	29	9	2

Table 6 3(a) Cyclic Stress Occurrences, Gage 2 on McLean, May-July 1977

STRS. AMPL. (KSI)	S.S. 1	S.S. 2	S.S. 3	S.S. 4	S.S. 5	S.S. 6	S.S. 7
1	121.6	590.4	1191.9	512.0	363.1	124.6	4.7
2	115.4	599.7	999.0	564.6	505.5	155.9	12.7
3	41.9	319.9	426.3	262.9	271.8	71.1	17.5
4	22.5	188.8	193.4	116.5	118.7	45.0	18.4
5	13.2	115.1	100.4	51.4	48.5	37.2	16.4
6	6.5	70.0	56.8	23.5	18.3	29.5	12.9
7	2.6	42.2	34.3	12.8	6.8	22.2	9.3
8	0.9	25.2	21.9	8.3	2.9	16.5	6.5
9	0.2	14.8	14.5	5.7	1.4	12.6	4.6
10	0.1	8.4	9.7	3.8	0.8	10.0	3.5
11	0.0	4.5	6.5	2.4	0.4	8.3	2.8
12	0.0	2.3	4.3	1.4	0.2	7.0	2.3
13	0.0	1.1	2.8	0.8	0.1	6.0	1.9
14	0.0	0.5	1.8	0.5	0.0	5.1	1.6
15	0.0	0.2	1.1	0.3	0.0	4.3	1.3
16	0.0	0.1	0.7	0.1	0.0	3.7	1.1
17	0.0	0.0	0.4	0.1	0.0	3.1	0.9
18	0.0	0.0	0.2	0.0	0.0	2.6	0.7
19	0.0	0.0	0.1	0.0	0.0	2.1	0.5
20	0.0	0.0	0.1	0.0	0.0	1.7	0.4
21	0.0	0.0	0.0	0.0	0.0	1.4	0.3
22	0.0	0.0	0.0	0.0	0.0	1.1	0.2
23	0.0	0.0	0.0	0.0	0.0	0.9	0.1
24	0.0	0.0	0.0	0.0	0.0	0.7	0.1
25	0.0	0.0	0.0	0.0	0.0	0.6	0.1
26	0.0	0.0	0.0	0.0	0.0	0.4	0.0
27	0.0	0.0	0.0	0.0	0.0	0.4	0.0
28	0.0	0.0	0.0	0.0	0.0	0.3	0.0
29	0.0	0.0	0.0	0.0	0.0	0.2	0.0
30	0.0	0.0	0.0	0.0	0.0	0.1	0.0
31	0.0	0.0	0.0	0.0	0.0	0.1	0.0
32	0.0	0.0	0.0	0.0	0.0	0.1	0.0
33	0.0	0.0	0.0	0.0	0.0	0.1	0.0
34	0.0	0.0	0.0	0.0	0.0	0.1	0.0
35	0.0	0.0	0.0	0.0	0.0	0.0	0.0
36	0.0	0.0	0.0	0.0	0.0	0.0	0.0
37	0.0	0.0	0.0	0.0	0.0	0.0	0.0
38	0.0	0.0	0.0	0.0	0.0	0.0	0.0
39	0.0	0.0	0.0	0.0	0.0	0.0	0.0
40	0.0	0.0	0.0	0.0	0.0	0.0	0.0
41	0.0	0.0	0.0	0.0	0.0	0.0	0.0
42	0.0	0.0	0.0	0.0	0.0	0.0	0.0
43	0.0	0.0	0.0	0.0	0.0	0.0	0.0
44	0.0	0.0	0.0	0.0	0.0	0.0	0.0
45	0.0	0.0	0.0	0.0	0.0	0.0	0.0
46	0.0	0.0	0.0	0.0	0.0	0.0	0.0
47	0.0	0.0	0.0	0.0	0.0	0.0	0.0
48	0.0	0.0	0.0	0.0	0.0	0.0	0.0
49	0.0	0.0	0.0	0.0	0.0	0.0	0.0
50	0.0	0.0	0.0	0.0	0.0	0.0	0.0
51	0.0	0.0	0.0	0.0	0.0	0.0	0.0
52	0.0	0.0	0.0	0.0	0.0	0.0	0.0
53	0.0	0.0	0.0	0.0	0.0	0.0	0.0
54	0.0	0.0	0.0	0.0	0.0	0.0	0.0
55	0.0	0.0	0.0	0.0	0.0	0.0	0.0
56	0.0	0.0	0.0	0.0	0.0	0.0	0.0
57	0.0	0.0	0.0	0.0	0.0	0.0	0.0
58	0.0	0.0	0.0	0.0	0.0	0.0	0.0
59	0.0	0.0	0.0	0.0	0.0	0.0	0.0
60	0.0	0.0	0.0	0.0	0.0	0.0	0.0
61	0.0	0.0	0.0	0.0	0.0	0.0	0.0
62	0.0	0.0	0.0	0.0	0.0	0.0	0.0
63	0.0	0.0	0.0	0.0	0.0	0.0	0.0
64	0.0	0.0	0.0	0.0	0.0	0.0	0.0
65	0.0	0.0	0.0	0.0	0.0	0.0	0.0
66	0.0	0.0	0.0	0.0	0.0	0.0	0.0
67	0.0	0.0	0.0	0.0	0.0	0.0	0.0
68	0.0	0.0	0.0	0.0	0.0	0.0	0.0
69	0.0	0.0	0.0	0.0	0.0	0.0	0.0
70	0.0	0.0	0.0	0.0	0.0	0.0	0.0
TOTAL INT.	5	32	41	20	16	9	2

Table 6 . 3(b) Cyclic Stress Occurrences, Gage 3 on McLean, Sep-Jan 1978

STRS. AMPL. (KSI)	S.S. 1	S.S. 2	S.S. 3	S.S. 4	S.S. 5	S.S. 6	S.S. 7	S.S. 8	S.S. 9
1	111.2	309.0	341.9	650.4	340.5	183.6	21.2	13.8	1.9
2	52.0	202.0	498.2	819.3	371.4	289.3	57.9	36.4	5.3
3	31.5	189.3	385.7	655.5	341.0	270.3	80.0	47.1	8.1
4	10.4	136.1	266.8	414.1	277.7	209.8	84.9	45.8	9.9
5	1.9	82.6	175.6	235.5	209.7	150.8	76.3	37.6	10.6
6	0.2	46.6	112.0	130.7	147.7	105.0	60.8	27.9	10.3
7	0.0	25.8	70.1	74.5	100.8	72.3	44.5	19.6	9.3
8	0.0	14.3	43.4	44.2	68.8	49.5	31.1	13.5	7.8
9	0.0	8.1	26.5	27.2	47.8	33.8	21.8	9.1	6.1
10	0.0	4.9	15.9	17.2	33.8	23.3	16.0	6.0	4.5
11	0.0	3.2	9.5	11.1	24.3	16.4	12.7	3.8	3.2
12	0.0	2.4	5.6	7.1	17.6	12.0	10.9	2.3	2.1
13	0.0	1.9	3.3	4.6	12.9	9.1	9.8	1.3	1.3
14	0.0	1.6	2.0	3.0	9.5	7.2	9.0	0.7	0.8
15	0.0	1.4	1.3	1.9	7.0	5.8	8.4	0.4	0.4
16	0.0	1.2	0.8	1.2	5.1	4.8	7.8	0.2	0.2
17	0.0	1.0	0.5	0.8	3.8	4.1	7.2	0.1	0.1
18	0.0	0.8	0.3	0.5	2.8	3.5	6.5	0.0	0.1
19	0.0	0.6	0.2	0.3	2.0	3.0	5.9	0.0	0.0
20	0.0	0.5	0.1	0.2	1.4	2.6	5.3	0.0	0.0
21	0.0	0.4	0.1	0.1	1.0	2.2	4.6	0.0	0.0
22	0.0	0.3	0.0	0.1	0.7	1.9	4.0	0.0	0.0
23	0.0	0.2	0.0	0.0	0.5	1.6	3.5	0.0	0.0
24	0.0	0.1	0.0	0.0	0.4	1.4	3.0	0.0	0.0
25	0.0	0.1	0.0	0.0	0.3	1.2	2.5	0.0	0.0
26	0.0	0.1	0.0	0.0	0.2	1.0	2.1	0.0	0.0
27	0.0	0.1	0.0	0.0	0.1	0.9	1.7	0.0	0.0
28	0.0	0.0	0.0	0.0	0.1	0.8	1.4	0.0	0.0
29	0.0	0.0	0.0	0.0	0.1	0.7	1.2	0.0	0.0
30	0.0	0.0	0.0	0.0	0.0	0.6	0.9	0.0	0.0
31	0.0	0.0	0.0	0.0	0.0	0.5	0.8	0.0	0.0
32	0.0	0.0	0.0	0.0	0.0	0.4	0.6	0.0	0.0
33	0.0	0.0	0.0	0.0	0.0	0.4	0.5	0.0	0.0
34	0.0	0.0	0.0	0.0	0.0	0.3	0.4	0.0	0.0
35	0.0	0.0	0.0	0.0	0.0	0.3	0.3	0.0	0.0
36	0.0	0.0	0.0	0.0	0.0	0.2	0.2	0.0	0.0
37	0.0	0.0	0.0	0.0	0.0	0.2	0.2	0.0	0.0
38	0.0	0.0	0.0	0.0	0.0	0.1	0.1	0.0	0.0
39	0.0	0.0	0.0	0.0	0.0	0.1	0.1	0.0	0.0
40	0.0	0.0	0.0	0.0	0.0	0.1	0.1	0.0	0.0
41	0.0	0.0	0.0	0.0	0.0	0.1	0.1	0.0	0.0
42	0.0	0.0	0.0	0.0	0.0	0.1	0.0	0.0	0.0
43	0.0	0.0	0.0	0.0	0.0	0.1	0.0	0.0	0.0
44	0.0	0.0	0.0	0.0	0.0	0.1	0.0	0.0	0.0
45	0.0	0.0	0.0	0.0	0.0	0.0	0.0	0.0	0.0
46	0.0	0.0	0.0	0.0	0.0	0.0	0.0	0.0	0.0
47	0.0	0.0	0.0	0.0	0.0	0.0	0.0	0.0	0.0
48	0.0	0.0	0.0	0.0	0.0	0.0	0.0	0.0	0.0
49	0.0	0.0	0.0	0.0	0.0	0.0	0.0	0.0	0.0
50	0.0	0.0	0.0	0.0	0.0	0.0	0.0	0.0	0.0
51	0.0	0.0	0.0	0.0	0.0	0.0	0.0	0.0	0.0
52	0.0	0.0	0.0	0.0	0.0	0.0	0.0	0.0	0.0
53	0.0	0.0	0.0	0.0	0.0	0.0	0.0	0.0	0.0
54	0.0	0.0	0.0	0.0	0.0	0.0	0.0	0.0	0.0
55	0.0	0.0	0.0	0.0	0.0	0.0	0.0	0.0	0.0
56	0.0	0.0	0.0	0.0	0.0	0.0	0.0	0.0	0.0
57	0.0	0.0	0.0	0.0	0.0	0.0	0.0	0.0	0.0
58	0.0	0.0	0.0	0.0	0.0	0.0	0.0	0.0	0.0
59	0.0	0.0	0.0	0.0	0.0	0.0	0.0	0.0	0.0
60	0.0	0.0	0.0	0.0	0.0	0.0	0.0	0.0	0.0
61	0.0	0.0	0.0	0.0	0.0	0.0	0.0	0.0	0.0
62	0.0	0.0	0.0	0.0	0.0	0.0	0.0	0.0	0.0
63	0.0	0.0	0.0	0.0	0.0	0.0	0.0	0.0	0.0
64	0.0	0.0	0.0	0.0	0.0	0.0	0.0	0.0	0.0
65	0.0	0.0	0.0	0.0	0.0	0.0	0.0	0.0	0.0
66	0.0	0.0	0.0	0.0	0.0	0.0	0.0	0.0	0.0
67	0.0	0.0	0.0	0.0	0.0	0.0	0.0	0.0	0.0
68	0.0	0.0	0.0	0.0	0.0	0.0	0.0	0.0	0.0
69	0.0	0.0	0.0	0.0	0.0	0.0	0.0	0.0	0.0
70	0.0	0.0	0.0	0.0	0.0	0.0	0.0	0.0	0.0
TOTAL INT.	2	15	27	38	27	19	8	3	1

Table 6. 4(a) Cyclic Stress Occurrences, Gage 8 on McLean, May-July 1977

STRS. AMPL. (KSI)	S.S. 1	S.S. 2	S.S. 3	S.S. 4	S.S. 5	S.S. 6	S.S. 7
1	572.1	1221.0	2886.3	1325.0	999.6	215.0	25.7
2	279.9	1224.6	2205.0	1360.8	1007.0	276.2	54.6
3	95.5	498.0	798.9	716.4	626.4	194.6	53.7
4	40.2	180.8	299.0	359.1	338.0	136.7	44.4
5	15.5	81.1	119.7	179.2	172.9	98.9	33.9
6	4.8	46.3	54.5	89.0	89.0	70.6	23.3
7	1.2	30.5	30.8	45.3	48.4	49.4	14.7
8	0.3	20.7	20.5	24.1	28.8	34.7	8.9
9	0.0	13.6	14.6	13.3	18.3	24.8	5.6
10	0.0	8.5	10.5	7.4	12.0	18.1	3.8
11	0.0	5.0	7.6	4.1	8.1	13.6	2.9
12	0.0	2.8	5.3	2.2	5.5	10.4	2.4
13	0.0	1.4	3.7	1.2	3.9	8.1	2.0
14	0.0	0.7	2.5	0.6	2.9	6.4	1.7
15	0.0	0.3	1.6	0.3	2.2	5.2	1.5
16	0.0	0.1	1.1	0.2	1.7	4.2	1.2
17	0.0	0.1	0.7	0.1	1.3	3.5	1.0
18	0.0	0.0	0.4	0.0	1.0	2.9	0.8
19	0.0	0.0	0.2	0.0	0.8	2.4	0.6
20	0.0	0.0	0.1	0.0	0.6	2.0	0.5
21	0.0	0.0	0.1	0.0	0.5	1.6	0.4
22	0.0	0.0	0.0	0.0	0.4	1.4	0.3
23	0.0	0.0	0.0	0.0	0.3	1.1	0.2
24	0.0	0.0	0.0	0.0	0.2	0.9	0.1
25	0.0	0.0	0.0	0.0	0.1	0.7	0.1
26	0.0	0.0	0.0	0.0	0.1	0.6	0.1
27	0.0	0.0	0.0	0.0	0.1	0.5	0.1
28	0.0	0.0	0.0	0.0	0.0	0.4	0.0
29	0.0	0.0	0.0	0.0	0.0	0.3	0.0
30	0.0	0.0	0.0	0.0	0.0	0.2	0.0
31	0.0	0.0	0.0	0.0	0.0	0.2	0.0
32	0.0	0.0	0.0	0.0	0.0	0.1	0.0
33	0.0	0.0	0.0	0.0	0.0	0.1	0.0
34	0.0	0.0	0.0	0.0	0.0	0.1	0.0
35	0.0	0.0	0.0	0.0	0.0	0.1	0.0
36	0.0	0.0	0.0	0.0	0.0	0.0	0.0
37	0.0	0.0	0.0	0.0	0.0	0.0	0.0
38	0.0	0.0	0.0	0.0	0.0	0.0	0.0
39	0.0	0.0	0.0	0.0	0.0	0.0	0.0
40	0.0	0.0	0.0	0.0	0.0	0.0	0.0
41	0.0	0.0	0.0	0.0	0.0	0.0	0.0
42	0.0	0.0	0.0	0.0	0.0	0.0	0.0
43	0.0	0.0	0.0	0.0	0.0	0.0	0.0
44	0.0	0.0	0.0	0.0	0.0	0.0	0.0
45	0.0	0.0	0.0	0.0	0.0	0.0	0.0
46	0.0	0.0	0.0	0.0	0.0	0.0	0.0
47	0.0	0.0	0.0	0.0	0.0	0.0	0.0
48	0.0	0.0	0.0	0.0	0.0	0.0	0.0
49	0.0	0.0	0.0	0.0	0.0	0.0	0.0
50	0.0	0.0	0.0	0.0	0.0	0.0	0.0
51	0.0	0.0	0.0	0.0	0.0	0.0	0.0
52	0.0	0.0	0.0	0.0	0.0	0.0	0.0
53	0.0	0.0	0.0	0.0	0.0	0.0	0.0
54	0.0	0.0	0.0	0.0	0.0	0.0	0.0
55	0.0	0.0	0.0	0.0	0.0	0.0	0.0
56	0.0	0.0	0.0	0.0	0.0	0.0	0.0
57	0.0	0.0	0.0	0.0	0.0	0.0	0.0
58	0.0	0.0	0.0	0.0	0.0	0.0	0.0
59	0.0	0.0	0.0	0.0	0.0	0.0	0.0
60	0.0	0.0	0.0	0.0	0.0	0.0	0.0
61	0.0	0.0	0.0	0.0	0.0	0.0	0.0
62	0.0	0.0	0.0	0.0	0.0	0.0	0.0
63	0.0	0.0	0.0	0.0	0.0	0.0	0.0
64	0.0	0.0	0.0	0.0	0.0	0.0	0.0
65	0.0	0.0	0.0	0.0	0.0	0.0	0.0
66	0.0	0.0	0.0	0.0	0.0	0.0	0.0
67	0.0	0.0	0.0	0.0	0.0	0.0	0.0
68	0.0	0.0	0.0	0.0	0.0	0.0	0.0
69	0.0	0.0	0.0	0.0	0.0	0.0	0.0
70	0.0	0.0	0.0	0.0	0.0	0.0	0.0
TOTAL INT.	15	52	90	56	39	17	6

Table 6.4(b) Cyclic Stress Occurrences, Gage 8 on McLean, Sep-Jan 1978

STRS. AMPL. (KSI)	S.S. 1	S.S. 2	S.S. 3	S.S. 4	S.S. 5	S.S. 6	S.S. 7	S.S. 8	S.S. 9	S.S. 10
1	256.7	461.2	1035.9	1558.8	610.7	252.7	30.6	20.2	4.9	1.1
2	55.4	253.7	755.4	1204.3	728.7	330.6	85.3	54.8	14.4	3.1
3	35.1	207.6	518.5	896.1	652.8	325.3	123.2	75.9	22.8	5.1
4	17.6	176.0	354.9	621.3	526.4	288.0	140.1	82.9	29.8	6.9
5	5.8	128.3	243.1	410.8	404.9	233.7	138.3	80.6	34.9	8.6
6	1.3	84.5	162.7	271.4	298.0	180.7	124.2	74.7	38.1	10.0
7	0.2	52.6	105.9	184.9	211.6	136.3	104.7	68.1	39.5	11.1
8	0.0	32.2	68.1	131.6	148.3	101.8	84.9	61.8	39.4	12.0
9	0.0	19.9	43.8	97.2	105.0	75.9	67.8	55.7	38.2	12.6
10	0.0	12.7	28.3	73.4	76.2	56.8	54.3	49.7	36.1	12.9
11	0.0	8.5	18.2	55.9	57.0	42.9	44.1	43.9	33.6	13.0
12	0.0	6.0	11.8	42.6	43.8	32.8	36.6	38.4	31.0	12.9
13	0.0	4.5	7.6	32.2	34.4	25.5	31.0	33.4	28.3	12.6
14	0.0	3.5	4.9	24.1	27.5	20.2	26.8	28.8	25.8	12.1
15	0.0	2.8	3.2	17.8	22.3	16.3	23.5	24.6	23.5	11.6
16	0.0	2.2	2.1	13.1	18.2	13.4	20.7	20.9	21.4	11.0
17	0.0	1.8	1.4	9.4	15.0	11.2	18.3	17.7	19.5	10.3
18	0.0	1.4	1.0	6.8	12.3	9.4	16.1	14.9	17.8	9.6
19	0.0	1.1	0.7	4.8	10.2	8.1	14.2	12.4	16.2	8.9
20	0.0	0.9	0.5	3.3	8.4	6.9	12.5	10.3	14.8	8.2
21	0.0	0.7	0.3	2.3	6.9	6.0	10.9	8.4	13.5	7.6
22	0.0	0.6	0.2	1.6	5.7	5.3	9.5	6.9	12.4	6.9
23	0.0	0.4	0.1	1.1	4.7	4.6	8.3	5.6	11.3	6.4
24	0.0	0.3	0.1	0.7	3.9	4.0	7.1	4.5	10.3	5.8
25	0.0	0.2	0.1	0.5	3.2	3.6	6.1	3.6	9.4	5.3
26	0.0	0.2	0.0	0.3	2.6	3.1	5.3	2.9	8.5	4.8
27	0.0	0.1	0.0	0.2	2.1	2.8	4.5	2.3	7.7	4.4
28	0.0	0.1	0.0	0.1	1.7	2.4	3.8	1.8	7.0	4.0
29	0.0	0.1	0.0	0.1	1.4	2.1	3.2	1.4	6.4	3.6
30	0.0	0.1	0.0	0.1	1.1	1.9	2.7	1.1	5.7	3.3
31	0.0	0.0	0.0	0.0	0.9	1.6	2.3	0.9	5.2	3.0
32	0.0	0.0	0.0	0.0	0.7	1.4	1.9	0.7	4.7	2.7
33	0.0	0.0	0.0	0.0	0.6	1.3	1.6	0.5	4.2	2.5
34	0.0	0.0	0.0	0.0	0.4	1.1	1.3	0.4	3.8	2.3
35	0.0	0.0	0.0	0.0	0.4	1.0	1.1	0.3	3.4	2.1
36	0.0	0.0	0.0	0.0	0.3	0.8	0.9	0.2	3.0	1.9
37	0.0	0.0	0.0	0.0	0.2	0.7	0.7	0.2	2.7	1.7
38	0.0	0.0	0.0	0.0	0.2	0.6	0.6	0.1	2.4	1.6
39	0.0	0.0	0.0	0.0	0.1	0.5	0.5	0.1	2.1	1.4
40	0.0	0.0	0.0	0.0	0.1	0.4	0.4	0.1	1.9	1.3
41	0.0	0.0	0.0	0.0	0.1	0.4	0.3	0.1	1.7	1.2
42	0.0	0.0	0.0	0.0	0.1	0.3	0.2	0.0	1.5	1.1
43	0.0	0.0	0.0	0.0	0.0	0.3	0.2	0.0	1.4	1.0
44	0.0	0.0	0.0	0.0	0.0	0.2	0.1	0.0	1.2	0.9
45	0.0	0.0	0.0	0.0	0.0	0.2	0.1	0.0	1.1	0.8
46	0.0	0.0	0.0	0.0	0.0	0.2	0.1	0.0	0.9	0.7
47	0.0	0.0	0.0	0.0	0.0	0.1	0.1	0.0	0.8	0.6
48	0.0	0.0	0.0	0.0	0.0	0.1	0.1	0.0	0.7	0.6
49	0.0	0.0	0.0	0.0	0.0	0.1	0.0	0.0	0.6	0.5
50	0.0	0.0	0.0	0.0	0.0	0.1	0.0	0.0	0.6	0.5
51	0.0	0.0	0.0	0.0	0.0	0.1	0.0	0.0	0.5	0.4
52	0.0	0.0	0.0	0.0	0.0	0.1	0.0	0.0	0.4	0.4
53	0.0	0.0	0.0	0.0	0.0	0.0	0.0	0.0	0.4	0.3
54	0.0	0.0	0.0	0.0	0.0	0.0	0.0	0.0	0.3	0.3
55	0.0	0.0	0.0	0.0	0.0	0.0	0.0	0.0	0.3	0.3
56	0.0	0.0	0.0	0.0	0.0	0.0	0.0	0.0	0.3	0.2
57	0.0	0.0	0.0	0.0	0.0	0.0	0.0	0.0	0.2	0.2
58	0.0	0.0	0.0	0.0	0.0	0.0	0.0	0.0	0.2	0.2
59	0.0	0.0	0.0	0.0	0.0	0.0	0.0	0.0	0.2	0.1
60	0.0	0.0	0.0	0.0	0.0	0.0	0.0	0.0	0.1	0.1
61	0.0	0.0	0.0	0.0	0.0	0.0	0.0	0.0	0.1	0.1
62	0.0	0.0	0.0	0.0	0.0	0.0	0.0	0.0	0.1	0.1
63	0.0	0.0	0.0	0.0	0.0	0.0	0.0	0.0	0.1	0.1
64	0.0	0.0	0.0	0.0	0.0	0.0	0.0	0.0	0.1	0.1
65	0.0	0.0	0.0	0.0	0.0	0.0	0.0	0.0	0.1	0.1
66	0.0	0.0	0.0	0.0	0.0	0.0	0.0	0.0	0.1	0.1
67	0.0	0.0	0.0	0.0	0.0	0.0	0.0	0.0	0.1	0.1
68	0.0	0.0	0.0	0.0	0.0	0.0	0.0	0.0	0.0	0.0
69	0.0	0.0	0.0	0.0	0.0	0.0	0.0	0.0	0.0	0.0
70	0.0	0.0	0.0	0.0	0.0	0.0	0.0	0.0	0.0	0.0
TOTAL INT.	4	23	45	76	55	31	20	14	12	5

Table 6.5 Cyclic Stress Occurrences, Gage 2 on MARKET, 1976

STRS. AMPL. (KSI)	S.S. 1	S.S. 2	S.S. 3	S.S. 4	S.S. 5	S.S. 6	S.S. 7	S.S. 8	S.S. 9	S.S. 10
1	0.0	493.9	152.0	332.4	601.1	141.6	40.4	12.1	7.0	0.8
2	0.0	352.7	225.5	178.3	266.4	327.5	108.4	32.8	19.5	2.5
3	0.0	183.1	209.3	133.7	218.7	348.2	148.0	45.4	28.0	4.0
4	0.0	109.4	176.8	98.1	182.6	286.7	161.0	50.2	31.7	5.4
5	0.0	67.0	130.4	66.6	148.1	214.8	158.1	49.5	31.3	6.6
6	0.0	41.1	86.3	41.9	115.2	153.5	148.2	46.0	28.3	7.6
7	0.0	23.8	53.9	24.5	87.3	106.2	135.7	40.9	24.5	8.3
8	0.0	12.7	33.3	13.7	65.9	72.2	122.1	35.2	20.9	8.8
9	0.0	6.3	20.9	7.6	50.1	49.0	108.1	29.9	18.0	9.0
10	0.0	3.0	13.5	4.4	38.6	33.5	94.1	25.3	15.7	9.0
11	0.0	1.3	9.0	2.6	29.8	23.0	80.9	21.8	13.8	8.7
12	0.0	0.5	6.1	1.6	22.9	15.9	68.7	19.1	12.1	8.3
13	0.0	0.2	4.2	1.0	17.5	11.1	57.8	17.1	10.6	7.8
14	0.0	0.1	2.9	0.6	13.1	7.8	48.4	15.6	9.1	7.1
15	0.0	0.0	2.1	0.3	9.7	5.4	40.3	14.4	7.7	6.4
16	0.0	0.0	1.4	0.2	7.0	3.8	33.5	13.4	6.4	5.6
17	0.0	0.0	0.9	0.1	4.9	2.7	27.8	12.4	5.3	4.9
18	0.0	0.0	0.6	0.1	3.4	1.9	23.1	11.4	4.4	4.2
19	0.0	0.0	0.4	0.0	2.3	1.3	19.1	10.5	3.6	3.5
20	0.0	0.0	0.3	0.0	1.5	0.9	15.8	9.6	2.9	2.9
21	0.0	0.0	0.1	0.0	1.0	0.6	13.1	8.7	2.3	2.4
22	0.0	0.0	0.1	0.0	0.6	0.4	10.8	7.8	1.9	1.9
23	0.0	0.0	0.1	0.0	0.4	0.3	9.0	7.0	1.5	1.5
24	0.0	0.0	0.0	0.0	0.2	0.2	7.4	6.2	1.3	1.2
25	0.0	0.0	0.0	0.0	0.1	0.1	6.1	5.5	1.0	0.9
26	0.0	0.0	0.0	0.0	0.1	0.1	5.1	4.8	0.8	0.7
27	0.0	0.0	0.0	0.0	0.0	0.0	4.2	4.2	0.7	0.5
28	0.0	0.0	0.0	0.0	0.0	0.0	3.5	3.7	0.6	0.4
29	0.0	0.0	0.0	0.0	0.0	0.0	2.9	3.2	0.5	0.3
30	0.0	0.0	0.0	0.0	0.0	0.0	2.4	2.8	0.4	0.2
31	0.0	0.0	0.0	0.0	0.0	0.0	2.0	2.4	0.3	0.1
32	0.0	0.0	0.0	0.0	0.0	0.0	1.7	2.1	0.3	0.1
33	0.0	0.0	0.0	0.0	0.0	0.0	1.4	1.8	0.2	0.1
34	0.0	0.0	0.0	0.0	0.0	0.0	1.1	1.5	0.2	0.0
35	0.0	0.0	0.0	0.0	0.0	0.0	0.9	1.3	0.1	0.0
36	0.0	0.0	0.0	0.0	0.0	0.0	0.8	1.1	0.1	0.0
37	0.0	0.0	0.0	0.0	0.0	0.0	0.6	0.9	0.1	0.0
38	0.0	0.0	0.0	0.0	0.0	0.0	0.5	0.8	0.1	0.0
39	0.0	0.0	0.0	0.0	0.0	0.0	0.4	0.7	0.1	0.0
40	0.0	0.0	0.0	0.0	0.0	0.0	0.4	0.6	0.0	0.0
41	0.0	0.0	0.0	0.0	0.0	0.0	0.3	0.5	0.0	0.0
42	0.0	0.0	0.0	0.0	0.0	0.0	0.2	0.4	0.0	0.0
43	0.0	0.0	0.0	0.0	0.0	0.0	0.2	0.3	0.0	0.0
44	0.0	0.0	0.0	0.0	0.0	0.0	0.2	0.3	0.0	0.0
45	0.0	0.0	0.0	0.0	0.0	0.0	0.1	0.2	0.0	0.0
46	0.0	0.0	0.0	0.0	0.0	0.0	0.1	0.2	0.0	0.0
47	0.0	0.0	0.0	0.0	0.0	0.0	0.1	0.1	0.0	0.0
48	0.0	0.0	0.0	0.0	0.0	0.0	0.1	0.1	0.0	0.0
49	0.0	0.0	0.0	0.0	0.0	0.0	0.1	0.1	0.0	0.0
50	0.0	0.0	0.0	0.0	0.0	0.0	0.0	0.1	0.0	0.0
51	0.0	0.0	0.0	0.0	0.0	0.0	0.0	0.1	0.0	0.0
52	0.0	0.0	0.0	0.0	0.0	0.0	0.0	0.1	0.0	0.0
53	0.0	0.0	0.0	0.0	0.0	0.0	0.0	0.0	0.0	0.0
54	0.0	0.0	0.0	0.0	0.0	0.0	0.0	0.0	0.0	0.0
55	0.0	0.0	0.0	0.0	0.0	0.0	0.0	0.0	0.0	0.0
56	0.0	0.0	0.0	0.0	0.0	0.0	0.0	0.0	0.0	0.0
57	0.0	0.0	0.0	0.0	0.0	0.0	0.0	0.0	0.0	0.0
58	0.0	0.0	0.0	0.0	0.0	0.0	0.0	0.0	0.0	0.0
59	0.0	0.0	0.0	0.0	0.0	0.0	0.0	0.0	0.0	0.0
60	0.0	0.0	0.0	0.0	0.0	0.0	0.0	0.0	0.0	0.0
61	0.0	0.0	0.0	0.0	0.0	0.0	0.0	0.0	0.0	0.0
62	0.0	0.0	0.0	0.0	0.0	0.0	0.0	0.0	0.0	0.0
63	0.0	0.0	0.0	0.0	0.0	0.0	0.0	0.0	0.0	0.0
64	0.0	0.0	0.0	0.0	0.0	0.0	0.0	0.0	0.0	0.0
65	0.0	0.0	0.0	0.0	0.0	0.0	0.0	0.0	0.0	0.0
66	0.0	0.0	0.0	0.0	0.0	0.0	0.0	0.0	0.0	0.0
67	0.0	0.0	0.0	0.0	0.0	0.0	0.0	0.0	0.0	0.0
68	0.0	0.0	0.0	0.0	0.0	0.0	0.0	0.0	0.0	0.0
69	0.0	0.0	0.0	0.0	0.0	0.0	0.0	0.0	0.0	0.0
70	0.0	0.0	0.0	0.0	0.0	0.0	0.0	0.0	0.0	0.0
TOTAL INT.	0	17	16	12	26	24	31	12	4	2

Table 6.6 Cyclic Stress Occurrences, Gage 8 on MARKET, 1976

STRS. AMPL. (KSI)	S.S. 1	S.S. 2	S.S. 3	S.S. 4	S.S. 5	S.S. 6	S.S. 7	S.S. 8	S.S. 9	S.S. 10
1	0.0	561.4	192.4	350.2	621.1	177.1	54.5	17.4	8.9	0.9
2	0.0	342.7	268.4	172.1	285.1	392.4	141.2	45.0	24.2	2.8
3	0.0	172.0	240.4	138.0	233.4	390.4	183.4	57.9	33.5	4.5
4	0.0	98.1	181.9	96.4	192.6	299.5	191.2	59.8	36.0	6.0
5	0.0	59.8	116.7	62.1	147.9	209.3	182.4	56.0	33.6	7.2
6	0.0	35.6	68.0	37.8	107.3	139.8	166.5	49.5	28.9	8.2
7	0.0	19.4	38.5	21.7	76.2	90.4	147.3	42.0	24.2	8.9
8	0.0	9.6	22.2	11.9	54.6	57.2	126.9	34.9	20.4	9.2
9	0.0	4.2	13.1	6.3	39.6	35.8	106.6	29.0	17.5	9.3
10	0.0	1.7	8.0	3.2	28.9	22.3	87.7	24.5	15.2	9.1
11	0.0	0.6	5.0	1.6	20.7	13.9	71.0	21.3	13.1	8.8
12	0.0	0.2	3.1	0.8	14.6	8.8	56.9	18.9	11.2	8.2
13	0.0	0.1	2.0	0.4	9.9	5.6	45.2	17.0	9.4	7.6
14	0.0	0.0	1.2	0.2	6.5	3.5	35.8	15.4	7.8	6.8
15	0.0	0.0	0.7	0.1	4.1	2.2	28.4	13.9	6.4	6.1
16	0.0	0.0	0.4	0.0	2.5	1.4	22.4	12.4	5.2	5.3
17	0.0	0.0	0.2	0.0	1.5	0.9	17.8	11.1	4.2	4.6
18	0.0	0.0	0.1	0.0	0.9	0.5	14.1	9.8	3.4	3.9
19	0.0	0.0	0.1	0.0	0.5	0.3	11.1	8.6	2.8	3.3
20	0.0	0.0	0.0	0.0	0.3	0.2	8.8	7.4	2.3	2.7
21	0.0	0.0	0.0	0.0	0.1	0.1	7.0	6.4	1.9	2.2
22	0.0	0.0	0.0	0.0	0.1	0.1	5.5	5.4	1.6	1.8
23	0.0	0.0	0.0	0.0	0.0	0.0	4.4	4.6	1.4	1.5
24	0.0	0.0	0.0	0.0	0.0	0.0	3.5	3.9	1.1	1.2
25	0.0	0.0	0.0	0.0	0.0	0.0	2.8	3.2	1.0	0.9
26	0.0	0.0	0.0	0.0	0.0	0.0	2.2	2.7	0.8	0.7
27	0.0	0.0	0.0	0.0	0.0	0.0	1.8	2.2	0.7	0.6
28	0.0	0.0	0.0	0.0	0.0	0.0	1.4	1.8	0.6	0.4
29	0.0	0.0	0.0	0.0	0.0	0.0	1.1	1.5	0.5	0.3
30	0.0	0.0	0.0	0.0	0.0	0.0	0.9	1.2	0.4	0.3
31	0.0	0.0	0.0	0.0	0.0	0.0	0.7	1.0	0.4	0.2
32	0.0	0.0	0.0	0.0	0.0	0.0	0.5	0.8	0.3	0.1
33	0.0	0.0	0.0	0.0	0.0	0.0	0.4	0.6	0.2	0.1
34	0.0	0.0	0.0	0.0	0.0	0.0	0.3	0.5	0.2	0.1
35	0.0	0.0	0.0	0.0	0.0	0.0	0.3	0.4	0.1	0.1
36	0.0	0.0	0.0	0.0	0.0	0.0	0.2	0.3	0.1	0.0
37	0.0	0.0	0.0	0.0	0.0	0.0	0.1	0.2	0.1	0.0
38	0.0	0.0	0.0	0.0	0.0	0.0	0.1	0.2	0.1	0.0
39	0.0	0.0	0.0	0.0	0.0	0.0	0.1	0.1	0.1	0.0
40	0.0	0.0	0.0	0.0	0.0	0.0	0.1	0.1	0.0	0.0
41	0.0	0.0	0.0	0.0	0.0	0.0	0.1	0.1	0.0	0.0
42	0.0	0.0	0.0	0.0	0.0	0.0	0.0	0.1	0.0	0.0
43	0.0	0.0	0.0	0.0	0.0	0.0	0.0	0.0	0.0	0.0
44	0.0	0.0	0.0	0.0	0.0	0.0	0.0	0.0	0.0	0.0
45	0.0	0.0	0.0	0.0	0.0	0.0	0.0	0.0	0.0	0.0
46	0.0	0.0	0.0	0.0	0.0	0.0	0.0	0.0	0.0	0.0
47	0.0	0.0	0.0	0.0	0.0	0.0	0.0	0.0	0.0	0.0
48	0.0	0.0	0.0	0.0	0.0	0.0	0.0	0.0	0.0	0.0
49	0.0	0.0	0.0	0.0	0.0	0.0	0.0	0.0	0.0	0.0
50	0.0	0.0	0.0	0.0	0.0	0.0	0.0	0.0	0.0	0.0
51	0.0	0.0	0.0	0.0	0.0	0.0	0.0	0.0	0.0	0.0
52	0.0	0.0	0.0	0.0	0.0	0.0	0.0	0.0	0.0	0.0
53	0.0	0.0	0.0	0.0	0.0	0.0	0.0	0.0	0.0	0.0
54	0.0	0.0	0.0	0.0	0.0	0.0	0.0	0.0	0.0	0.0
55	0.0	0.0	0.0	0.0	0.0	0.0	0.0	0.0	0.0	0.0
56	0.0	0.0	0.0	0.0	0.0	0.0	0.0	0.0	0.0	0.0
57	0.0	0.0	0.0	0.0	0.0	0.0	0.0	0.0	0.0	0.0
58	0.0	0.0	0.0	0.0	0.0	0.0	0.0	0.0	0.0	0.0
59	0.0	0.0	0.0	0.0	0.0	0.0	0.0	0.0	0.0	0.0
60	0.0	0.0	0.0	0.0	0.0	0.0	0.0	0.0	0.0	0.0
61	0.0	0.0	0.0	0.0	0.0	0.0	0.0	0.0	0.0	0.0
62	0.0	0.0	0.0	0.0	0.0	0.0	0.0	0.0	0.0	0.0
63	0.0	0.0	0.0	0.0	0.0	0.0	0.0	0.0	0.0	0.0
64	0.0	0.0	0.0	0.0	0.0	0.0	0.0	0.0	0.0	0.0
65	0.0	0.0	0.0	0.0	0.0	0.0	0.0	0.0	0.0	0.0
66	0.0	0.0	0.0	0.0	0.0	0.0	0.0	0.0	0.0	0.0
67	0.0	0.0	0.0	0.0	0.0	0.0	0.0	0.0	0.0	0.0
68	0.0	0.0	0.0	0.0	0.0	0.0	0.0	0.0	0.0	0.0
69	0.0	0.0	0.0	0.0	0.0	0.0	0.0	0.0	0.0	0.0
70	0.0	0.0	0.0	0.0	0.0	0.0	0.0	0.0	0.0	0.0
TOTAL INT.	0	17	16	12	26	24	31	12	4	2

Table 6.7 Generalized Gamma Parameters for Partial Stress Histograms

Data Set				Generalized Gamma Parameters	Beaufort Sea State No.									
Ship	Sea Trail Period	Gage	Total Interval		1	2	3	4	5	6	7	8	9	
Sealand McLean	Jan-Mar 1975	FyB	214	p	4.82	6.60	8.20	9.25	5.40	3.21	2.23	2.10	1.46	1
				q	.403	.363	.332	.347	.363	.596	.750	.942	1.39	1
				r	9.01	27.5	55.6	56.6	11.0	.509	.182	.140	.067	.
	May-Jul 1977 Sep-Jan 1978	2 3	265	p	13.3	11.1	8.77	9.50	8.43	8.08	5.58	1.77	.994	.
				q	.361	.323	.368	.376	.365	.362	.531	1.22	1.97	2
				r	501.	501.	101.	100.	75.9	51.5	2.25	.177	.074	.
	May-Jul 1977 Sep-Jan 1978	8 8	560	p	12.7	10.0	9.01	8.52	8.46	8.08	5.58	2.16	258.	1
				q	.340	.347	.375	.370	.360	.361	.511	.946	.870	1
				r	955.	240.	120.	83.2	74.6	48.2	2.25	.133	.109	.
Sealand Market	Oct-Dec 1976	2	144	p	4.85	8.82	3.79	8.44	8.81	3.46	2.39	4.01	2.68	.
				q	.685	.376	.653	.374	.349	.737	.887	.599	.841	2
				r	4.46	105.	1.18	79.4	97.7	.701	.165	.555	.206	.
		8	144	p	8.00	10.1	4.67	8.76	8.46	3.34	2.26	3.67	3.42	1
				q	.530	.375	.593	.370	.370	.767	.932	.632	.771	1
				r	31.6	161.	2.45	100.	79.4	.710	.175	.505	.400	.

Note: The figures underlined are extrapolated values.

Table 6.8 Cyclic Stress Occurrences per interval, Gage F_yB on McLean, 1975

STRS. AMPL. (KSI)	S.S. 1	S.S. 2	S.S. 3	S.S. 4	S.S. 5	S.S. 6	S.S. 7	S.S. 8	S.S. 9	S.S. 10	S.S. 11	S.S. 12
1	22.2	13.4	5.9	3.7	13.8	5.3	6.4	2.8	1.4	0.6	0.3	0.1
2	15.3	13.0	7.8	7.9	11.4	8.5	6.4	7.2	4.0	2.3	1.5	0.6
3	10.3	11.1	7.6	7.6	9.5	7.2	8.0	9.3	6.3	4.3	3.1	1.5
4	6.3	7.4	6.4	5.9	6.5	6.8	8.6	9.4	8.1	6.2	4.9	2.7
5	3.6	4.5	4.7	4.8	4.6	6.3	8.1	8.7	9.2	7.8	6.7	4.2
6	1.8	2.7	3.4	4.0	3.5	5.5	7.1	7.9	9.8	9.0	8.2	5.8
7	1.0	1.8	2.6	3.5	2.9	4.8	6.1	7.2	9.8	9.7	9.5	7.4
8	0.7	1.3	2.1	3.0	2.5	4.2	5.2	6.5	9.4	10.0	10.4	8.8
9	0.6	1.0	1.8	2.5	2.2	3.7	4.5	5.9	8.6	9.9	10.9	10.1
10	0.6	0.8	1.5	2.1	1.9	3.3	4.0	5.2	7.8	9.5	10.9	11.0
11	0.6	0.7	1.2	1.7	1.7	2.9	3.5	4.6	6.8	8.8	10.6	11.5
12	0.7	0.6	1.2	1.4	1.6	2.6	3.2	4.0	5.9	8.0	9.9	11.6
13	0.7	0.6	1.0	1.2	1.4	2.2	2.8	3.4	5.1	7.1	9.0	11.3
14	0.6	0.5	0.9	1.0	1.2	2.0	2.5	2.9	4.3	6.1	8.0	10.6
15	0.6	0.5	0.8	0.8	1.1	1.7	2.2	2.5	3.7	5.2	6.8	9.7
16	0.6	0.5	0.7	0.7	1.0	1.5	2.0	2.1	3.1	4.3	5.7	8.5
17	0.6	0.4	0.6	0.6	0.9	1.3	1.7	1.7	2.6	3.5	4.6	7.3
18	0.6	0.4	0.6	0.5	0.8	1.1	1.5	1.4	2.2	2.8	3.7	6.0
19	0.5	0.4	0.5	0.4	0.7	0.9	1.3	1.2	1.8	2.2	2.9	4.8
20	0.5	0.3	0.5	0.4	0.7	0.8	1.1	0.9	1.5	1.7	2.2	3.7
21	0.4	0.3	0.4	0.3	0.6	0.7	1.0	0.8	1.2	1.3	1.6	2.8
22	0.4	0.3	0.4	0.3	0.5	0.6	0.8	0.6	1.0	1.0	1.1	2.0
23	0.4	0.3	0.3	0.2	0.5	0.5	0.7	0.5	0.8	0.7	0.8	1.4
24	0.3	0.2	0.3	0.2	0.5	0.4	0.6	0.4	0.6	0.5	0.6	1.0
25	0.3	0.2	0.3	0.2	0.4	0.4	0.5	0.3	0.5	0.4	0.4	0.6
26	0.3	0.2	0.2	0.2	0.4	0.3	0.5	0.2	0.4	0.3	0.2	0.4
27	0.2	0.2	0.2	0.2	0.3	0.3	0.4	0.2	0.3	0.2	0.2	0.2
28	0.2	0.2	0.2	0.1	0.3	0.2	0.3	0.1	0.2	0.1	0.1	0.1
29	0.2	0.1	0.2	0.1	0.3	0.2	0.3	0.1	0.1	0.1	0.1	0.1
30	0.1	0.1	0.1	0.1	0.3	0.2	0.2	0.1	0.1	0.1	0.0	0.0
31	0.1	0.1	0.1	0.1	0.2	0.2	0.2	0.0	0.1	0.0	0.0	0.0
32	0.1	0.1	0.1	0.1	0.2	0.1	0.2	0.0	0.1	0.0	0.0	0.0
33	0.1	0.1	0.1	0.1	0.2	0.1	0.2	0.0	0.0	0.0	0.0	0.0
34	0.1	0.1	0.1	0.1	0.2	0.1	0.1	0.0	0.0	0.0	0.0	0.0
35	0.1	0.1	0.1	0.1	0.2	0.1	0.1	0.0	0.0	0.0	0.0	0.0
36	0.0	0.1	0.1	0.1	0.1	0.1	0.1	0.0	0.0	0.0	0.0	0.0
37	0.0	0.1	0.1	0.1	0.1	0.1	0.1	0.0	0.0	0.0	0.0	0.0
38	0.0	0.1	0.1	0.1	0.1	0.1	0.1	0.0	0.0	0.0	0.0	0.0
39	0.0	0.1	0.1	0.1	0.1	0.1	0.1	0.0	0.0	0.0	0.0	0.0
40	0.0	0.0	0.1	0.0	0.1	0.0	0.1	0.0	0.0	0.0	0.0	0.0
41	0.0	0.0	0.0	0.0	0.1	0.0	0.1	0.0	0.0	0.0	0.0	0.0
42	0.0	0.0	0.0	0.0	0.1	0.0	0.0	0.0	0.0	0.0	0.0	0.0
43	0.0	0.0	0.0	0.0	0.1	0.0	0.0	0.0	0.0	0.0	0.0	0.0
44	0.0	0.0	0.0	0.0	0.1	0.0	0.0	0.0	0.0	0.0	0.0	0.0
45	0.0	0.0	0.0	0.0	0.1	0.0	0.0	0.0	0.0	0.0	0.0	0.0
46	0.0	0.0	0.0	0.0	0.1	0.0	0.0	0.0	0.0	0.0	0.0	0.0
47	0.0	0.0	0.0	0.0	0.0	0.0	0.0	0.0	0.0	0.0	0.0	0.0
48	0.0	0.0	0.0	0.0	0.0	0.0	0.0	0.0	0.0	0.0	0.0	0.0
49	0.0	0.0	0.0	0.0	0.0	0.0	0.0	0.0	0.0	0.0	0.0	0.0
50	0.0	0.0	0.0	0.0	0.0	0.0	0.0	0.0	0.0	0.0	0.0	0.0
51	0.0	0.0	0.0	0.0	0.0	0.0	0.0	0.0	0.0	0.0	0.0	0.0
52	0.0	0.0	0.0	0.0	0.0	0.0	0.0	0.0	0.0	0.0	0.0	0.0
53	0.0	0.0	0.0	0.0	0.0	0.0	0.0	0.0	0.0	0.0	0.0	0.0
54	0.0	0.0	0.0	0.0	0.0	0.0	0.0	0.0	0.0	0.0	0.0	0.0
55	0.0	0.0	0.0	0.0	0.0	0.0	0.0	0.0	0.0	0.0	0.0	0.0
56	0.0	0.0	0.0	0.0	0.0	0.0	0.0	0.0	0.0	0.0	0.0	0.0
57	0.0	0.0	0.0	0.0	0.0	0.0	0.0	0.0	0.0	0.0	0.0	0.0
58	0.0	0.0	0.0	0.0	0.0	0.0	0.0	0.0	0.0	0.0	0.0	0.0
59	0.0	0.0	0.0	0.0	0.0	0.0	0.0	0.0	0.0	0.0	0.0	0.0
60	0.0	0.0	0.0	0.0	0.0	0.0	0.0	0.0	0.0	0.0	0.0	0.0
61	0.0	0.0	0.0	0.0	0.0	0.0	0.0	0.0	0.0	0.0	0.0	0.0
62	0.0	0.0	0.0	0.0	0.0	0.0	0.0	0.0	0.0	0.0	0.0	0.0
63	0.0	0.0	0.0	0.0	0.0	0.0	0.0	0.0	0.0	0.0	0.0	0.0
64	0.0	0.0	0.0	0.0	0.0	0.0	0.0	0.0	0.0	0.0	0.0	0.0
65	0.0	0.0	0.0	0.0	0.0	0.0	0.0	0.0	0.0	0.0	0.0	0.0
66	0.0	0.0	0.0	0.0	0.0	0.0	0.0	0.0	0.0	0.0	0.0	0.0
67	0.0	0.0	0.0	0.0	0.0	0.0	0.0	0.0	0.0	0.0	0.0	0.0
68	0.0	0.0	0.0	0.0	0.0	0.0	0.0	0.0	0.0	0.0	0.0	0.0
69	0.0	0.0	0.0	0.0	0.0	0.0	0.0	0.0	0.0	0.0	0.0	0.0
70	0.0	0.0	0.0	0.0	0.0	0.0	0.0	0.0	0.0	0.0	0.0	0.0
TOTAL	71.8	64.8	55.3	56.0	75.9	77.1	92.9	97.8	116.7	124.0	135.0	146.0

Table 6.9 Cyclic Stress occurrences per interval combined data of Gage 2 during May-July 1977 & Gage 3 during Sep-Jan 1978 on McLean

STRS. AMPL. (KSI)	S.S. 1	S.S. 2	S.S. 3	S.S. 4	S.S. 5	S.S. 6	S.S. 7	S.S. 8	S.S. 9	S.S. 10	S.S. 11	S.S. 12
1	33.3	19.1	22.6	20.0	16.4	11.0	2.6	4.6	1.9	0.2	0.1	0.1
2	23.9	17.1	22.0	23.9	20.4	15.9	7.1	12.1	5.3	0.9	0.4	0.3
3	10.5	10.8	11.9	15.8	14.3	12.2	9.7	15.7	8.1	1.9	0.8	0.6
4	4.7	6.9	6.8	9.1	9.2	9.1	10.3	15.3	9.9	3.1	1.4	0.9
5	2.2	4.2	4.1	4.9	6.0	6.7	9.3	12.5	10.5	4.3	2.0	1.4
6	1.0	2.5	2.5	2.7	3.9	4.8	7.4	9.3	10.3	5.5	2.6	1.8
7	0.4	1.4	1.5	1.5	2.5	3.4	5.4	6.5	9.3	6.6	3.4	2.3
8	0.1	0.8	1.0	0.9	1.7	2.4	3.8	4.5	7.8	7.4	4.1	2.8
9	0.0	0.5	0.6	0.6	1.1	1.7	2.6	3.0	6.1	7.9	4.8	3.3
10	0.0	0.3	0.4	0.4	0.8	1.2	2.0	2.0	4.5	8.0	5.4	3.8
11	0.0	0.2	0.2	0.2	0.6	0.9	1.5	1.3	3.2	7.6	5.8	4.3
12	0.0	0.1	0.1	0.1	0.4	0.7	1.3	0.8	2.1	7.0	6.3	4.7
13	0.0	0.1	0.1	0.1	0.3	0.5	1.2	0.4	1.3	6.1	6.5	5.2
14	0.0	0.0	0.1	0.1	0.2	0.4	1.1	0.2	0.8	5.0	6.5	5.5
15	0.0	0.0	0.0	0.0	0.2	0.4	1.0	0.1	0.4	3.9	6.3	5.7
16	0.0	0.0	0.0	0.0	0.1	0.3	0.9	0.1	0.2	2.9	5.9	5.8
17	0.0	0.0	0.0	0.0	0.1	0.3	0.8	0.0	0.1	2.1	5.3	5.8
18	0.0	0.0	0.0	0.0	0.1	0.2	0.7	0.0	0.1	1.4	4.6	5.6
19	0.0	0.0	0.0	0.0	0.0	0.2	0.6	0.0	0.0	0.9	3.8	5.3
20	0.0	0.0	0.0	0.0	0.0	0.2	0.6	0.0	0.0	0.5	3.0	4.8
21	0.0	0.0	0.0	0.0	0.0	0.1	0.5	0.0	0.0	0.3	2.2	4.2
22	0.0	0.0	0.0	0.0	0.0	0.1	0.4	0 0	0.0	0.1	1.6	3.5
23	0.0	0.0	0.0	0.0	0.0	0.1	0.4	0.0	0.0	0.1	1.1	2.8
24	0.0	0.0	0.0	0.0	0.0	0.1	0.3	0.0	0.0	0.0	0.7	2.2
25	0.0	0.0	0.0	0.0	0.0	0.1	0.3	0.0	0.0	0.0	0.4	1.5
26	0.0	0.0	0.0	0.0	0.0	0.1	0.2	0.0	0.0	0.0	0.2	1.1
27	0.0	0.0	0.0	0.0	0.0	0.0	0.2	0.0	0.0	0.0	0.1	0.7
28	0.0	0.0	0.0	0.0	0.0	0.0	0.1	0.0	0.0	0.0	0.1	0.4
29	0.0	0.0	0.0	0.0	0.0	0.0	0.1	0.0	0.0	0.0	0.0	0.2
30	0.0	0.0	0.0	0.0	0.0	0.0	0.1	0.0	0.0	0.0	0.0	0.1
31	0.0	0.0	0.0	0.0	0.0	0.0	0.1	0.0	0.0	0.0	0.0	0.0
32	0.0	0.0	0.0	0.0	0.0	0.0	0.1	0.0	0.0	0.0	0.0	0.0
33	0.0	0.0	0.0	0.0	0.0	0.0	0.0	0.0	0.0	0.0	0.0	0.0
34	0.0	0.0	0.0	0.0	0.0	0.0	0.0	0.0	0.0	0.0	0.0	0.0
35	0.0	0.0	0.0	0.0	0.0	0.0	0.0	0.0	0.0	0.0	0.0	0.0
36	0.0	0.0	0.0	0.0	0.0	0.0	0.0	0.0	0.0	0.0	0.0	0.0
37	0.0	0.0	0.0	0.0	0.0	0.0	0.0	0.0	0.0	0.0	0.0	0.0
38	0.0	0.0	0.0	0.0	0.0	0.0	0.0	0.0	0.0	0.0	0.0	0.0
39	0.0	0.0	0.0	0.0	0.0	0.0	0.0	0.0	0.0	0.0	0.0	0.0
40	0.0	0.0	0.0	0.0	0.0	0.0	0.0	0.0	0.0	0.0	0.0	0.0
41	0.0	0.0	0.0	0.0	0.0	0.0	0.0	0.0	0.0	0.0	0.0	0.0
42	0.0	0.0	0.0	0.0	0.0	0.0	0.0	0.0	0.0	0.0	0.0	0.0
43	0.0	0.0	0.0	0.0	0.0	0.0	0.0	0.0	0.0	0.0	0.0	0.0
44	0.0	0.0	0.0	0.0	0.0	0.0	0.0	0.0	0.0	0.0	0.0	0.0
45	0.0	0.0	0.0	0.0	0.0	0.0	0.0	0.0	0.0	0.0	0.0	0.0
46	0.0	0.0	0.0	0.0	0.0	0.0	0.0	0.0	0.0	0.0	0.0	0.0
47	0.0	0.0	0.0	0.0	0.0	0.0	0.0	0.0	0.0	0.0	0.0	0.0
48	0.0	0.0	0.0	0.0	0.0	0.0	0.0	0.0	0.0	0.0	0.0	0.0
49	0.0	0.0	0.0	0.0	0.0	0.0	0.0	0.0	0.0	0.0	0.0	0.0
50	0.0	0.0	0.0	0.0	0.0	0.0	0.0	0.0	0.0	0.0	0.0	0.0
51	0.0	0.0	0.0	0.0	0.0	0.0	0.0	0.0	0.0	0.0	0.0	0.0
52	0.0	0.0	0.0	0.0	0.0	0.0	0.0	0.0	0.0	0.0	0.0	0.0
53	0.0	0.0	0.0	0.0	0.0	0.0	0.0	0.0	0.0	0.0	0.0	0.0
54	0.0	0.0	0.0	0.0	0.0	0.0	0.0	0.0	0.0	0.0	0.0	0.0
55	0.0	0.0	0.0	0.0	0.0	0.0	0.0	0.0	0.0	0.0	0.0	0.0
56	0.0	0.0	0.0	0.0	0.0	0.0	0.0	0.0	0.0	0.0	0.0	0.0
57	0.0	0.0	0.0	0.0	0.0	0.0	0.0	0.0	0.0	0.0	0.0	0.0
58	0.0	0.0	0.0	0.0	0.0	0.0	0.0	0.0	0.0	0.0	0.0	0.0
59	0.0	0.0	0.0	0.0	0.0	0.0	0.0	0.0	0.0	0.0	0.0	0.0
60	0.0	0.0	0.0	0.0	0.0	0.0	0.0	0.0	0.0	0.0	0.0	0.0
61	0.0	0.0	0.0	0.0	0.0	0.0	0.0	0.0	0.0	0.0	0.0	0.0
62	0.0	0.0	0.0	0.0	0.0	0.0	0.0	0.0	0.0	0.0	0.0	0.0
63	0.0	0.0	0.0	0.0	0.0	0.0	0.0	0.0	0.0	0.0	0.0	0.0
64	0.0	0.0	0.0	0.0	0.0	0.0	0.0	0.0	0.0	0.0	0.0	0.0
65	0.0	0.0	0.0	0.0	0.0	0.0	0.0	0.0	0.0	0.0	0.0	0.0
66	0.0	0.0	0.0	0.0	0.0	0.0	0.0	0.0	0.0	0.0	0.0	0.0
67	0.0	0.0	0.0	0.0	0.0	0.0	0.0	0.0	0.0	0.0	0.0	0.0
68	0.0	0.0	0.0	0.0	0.0	0.0	0.0	0.0	0.0	0.0	0.0	0.0
69	0.0	0.0	0.0	0.0	0.0	0.0	0.0	0.0	0.0	0.0	0.0	0.0
70	0.0	0.0	0.0	0.0	0.0	0.0	0.0	0.0	0.0	0.0	0.0	0.0
TOTAL	76.0	64.0	73.8	80.4	78.2	72.8	72.5	88.5	81.9	83.7	85.2	86.6

Table 6.10 Cyclic Stress Occurrences per interval combined Gage & Data measured on McLean during May-July 1977 and Sep-Jan 1978

STRS. AMPL. (KSI)	S.S. 1	S.S. 2	S.S. 3	S.S. 4	S.S. 5	S.S. 6	S.S. 7	S.S. 8	S.S. 9	S.S. 10	S.S. 11	S.S. 12
1	43.6	22.4	29.1	21.8	17.1	9.7	2.2	1.4	0.4	0.2	0.1	0.0
2	17.7	19.7	21.9	19.4	18.5	12.6	5.4	3.9	1.2	0.6	0.2	0.1
3	6.9	9.4	9.8	12.2	13.6	10.8	6.8	5.4	1.9	1.0	0.4	0.1
4	3.0	4.8	4.8	7.4	9.2	8.8	7.1	5.9	2.5	1.4	0.6	0.2
5	1.1	2.8	2.7	4.5	6.1	6.9	6.6	5.8	2.9	1.7	0.8	0.3
6	0.3	1.7	1.6	2.7	4.1	5.2	5.7	5.3	3.2	2.0	1.0	0.4
7	0.1	1.1	1.0	1.7	2.8	3.9	4.6	4.9	3.3	2.2	1.2	0.6
8	0.0	0.7	0.7	1.2	1.9	2.8	3.6	4.4	3.3	2.4	1.4	0.7
9	0.0	0.4	0.4	0.8	1.3	2.1	2.8	4.0	3.2	2.5	1.5	0.8
10	0.0	0.3	0.3	0.6	0.9	1.6	2.2	3.6	3.0	2.6	1.7	0.9
11	0.0	0.2	0.2	0.5	0.7	1.2	1.8	3.1	2.8	2.6	1.8	1.0
12	0.0	0.1	0.1	0.3	0.5	0.9	1.5	2.7	2.6	2.6	1.9	1.2
13	0.0	0.1	0.1	0.3	0.4	0.7	1.3	2.4	2.4	2.5	2.0	1.3
14	0.0	0.1	0.1	0.2	0.3	0.6	1.1	2.1	2.2	2.4	2.1	1.4
15	0.0	0.0	0.0	0.1	0.3	0.4	1.0	1.8	2.0	2.3	2.1	1.5
16	0.0	0.0	0.0	0.1	0.2	0.4	0.8	1.5	1.8	2.2	2.1	1.5
17	0.0	0.0	0.0	0.1	0.2	0.3	0.7	1.3	1.6	2.1	2.1	1.6
18	0.0	0.0	0.0	0.1	0.1	0.3	0.7	1.1	1.5	1.9	2.1	1.7
19	0.0	0.0	0.0	0.0	0.1	0.2	0.6	0.9	1.4	1.8	2.1	1.7
20	0.0	0.0	0.0	0.0	0.1	0.2	0.5	0.7	1.2	1.6	2.1	1.8
21	0.0	0.0	0.0	0.0	0.1	0.2	0.4	0.6	1.1	1.5	2.0	1.8
22	0.0	0.0	0.0	0.0	0.1	0.1	0.4	0.5	1.0	1.4	1.9	1.8
23	0.0	0.0	0.0	0.0	0.1	0.1	0.3	0.4	0.9	1.3	1.9	1.8
24	0.0	0.0	0.0	0.0	0.0	0.1	0.3	0.3	0.9	1.2	1.8	1.8
25	0.0	0.0	0.0	0.0	0.0	0.1	0.2	0.3	0.8	1.1	1.7	1.8
26	0.0	0.0	0.0	0.0	0.0	0.1	0.2	0.2	0.7	1.0	1.6	1.8
27	0.0	0.0	0.0	0.0	0.0	0.1	0.2	0.2	0.6	0.9	1.5	1.7
28	0.0	0.0	0.0	0.0	0.0	0.1	0.1	0.1	0.6	0.8	1.5	1.7
29	0.0	0.0	0.0	0.0	0.0	0.1	0.1	0.1	0.5	0.7	1.4	1.6
30	0.0	0.0	0.0	0.0	0.0	0.0	0.1	0.1	0.5	0.7	1.3	1.6
31	0.0	0.0	0.0	0.0	0.0	0.0	0.1	0.1	0.4	0.6	1.2	1.5
32	0.0	0.0	0.0	0.0	0.0	0.0	0.1	0.0	0.4	0.5	1.1	1.5
33	0.0	0.0	0.0	0.0	0.0	0.0	0.1	0.0	0.3	0.5	1.0	1.4
34	0.0	0.0	0.0	0.0	0.0	0.0	0.0	0.0	0.3	0.5	0.9	1.3
35	0.0	0.0	0.0	0.0	0.0	0.0	0.0	0.0	0.3	0.4	0.9	1.3
36	0.0	0.0	0.0	0.0	0.0	0.0	0.0	0.0	0.3	0.4	0.8	1.2
37	0.0	0.0	0.0	0.0	0.0	0.0	0.0	0.0	0.2	0.3	0.7	1.1
38	0.0	0.0	0.0	0.0	0.0	0.0	0.0	0.0	0.2	0.3	0.7	1.1
39	0.0	0.0	0.0	0.0	0.0	0.0	0.0	0.0	0.2	0.3	0.6	1.0
40	0.0	0.0	0.0	0.0	0.0	0.0	0.0	0.0	0.2	0.3	0.5	0.9
41	0.0	0.0	0.0	0.0	0.0	0.0	0.0	0.0	0.1	0.2	0.5	0.9
42	0.0	0.0	0.0	0.0	0.0	0.0	0.0	0.0	0.1	0.2	0.4	0.8
43	0.0	0.0	0.0	0.0	0.0	0.0	0.0	0.0	0.1	0.2	0.4	0.7
44	0.0	0.0	0.0	0.0	0.0	0.0	0.0	0.0	0.1	0.2	0.4	0.7
45	0.0	0.0	0.0	0.0	0.0	0.0	0.0	0.0	0.1	0.2	0.3	0.6
46	0.0	0.0	0.0	0.0	0.0	0.0	0.0	0.0	0.1	0.1	0.3	0.6
47	0.0	0.0	0.0	0.0	0.0	0.0	0.0	0.0	0.1	0.1	0.3	0.5
48	0.0	0.0	0.0	0.0	0.0	0.0	0.0	0.0	0.1	0.1	0.2	0.5
49	0.0	0.0	0.0	0.0	0.0	0.0	0.0	0.0	0.1	0.1	0.2	0.4
50	0.0	0.0	0.0	0.0	0.0	0.0	0.0	0.0	0.0	0.1	0.2	0.4
51	0.0	0.0	0.0	0.0	0.0	0.0	0.0	0.0	0.0	0.1	0.2	0.3
52	0.0	0.0	0.0	0.0	0.0	0.0	0.0	0.0	0.0	0.1	0.1	0.3
53	0.0	0.0	0.0	0.0	0.0	0.0	0.0	0.0	0.0	0.1	0.1	0.3
54	0.0	0.0	0.0	0.0	0.0	0.0	0.0	0.0	0.0	0.1	0.1	0.2
55	0.0	0.0	0.0	0.0	0.0	0.0	0.0	0.0	0.0	0.0	0.1	0.2
56	0.0	0.0	0.0	0.0	0.0	0.0	0.0	0.0	0.0	0.0	0.1	0.2
57	0.0	0.0	0.0	0.0	0.0	0.0	0.0	0.0	0.0	0.0	0.1	0.2
58	0.0	0.0	0.0	0.0	0.0	0.0	0.0	0.0	0.0	0.0	0.1	0.1
59	0.0	0.0	0.0	0.0	0.0	0.0	0.0	0.0	0.0	0.0	0.1	0.1
60	0.0	0.0	0.0	0.0	0.0	0.0	0.0	0.0	0.0	0.0	0.0	0.1
61	0.0	0.0	0.0	0.0	0.0	0.0	0.0	0.0	0.0	0.0	0.0	0.1
62	0.0	0.0	0.0	0.0	0.0	0.0	0.0	0.0	0.0	0.0	0.0	0.1
63	0.0	0.0	0.0	0.0	0.0	0.0	0.0	0.0	0.0	0.0	0.0	0.1
64	0.0	0.0	0.0	0.0	0.0	0.0	0.0	0.0	0.0	0.0	0.0	0.1
65	0.0	0.0	0.0	0.0	0.0	0.0	0.0	0.0	0.0	0.0	0.0	0.1
66	0.0	0.0	0.0	0.0	0.0	0.0	0.0	0.0	0.0	0.0	0.0	0.0
67	0.0	0.0	0.0	0.0	0.0	0.0	0.0	0.0	0.0	0.0	0.0	0.0
68	0.0	0.0	0.0	0.0	0.0	0.0	0.0	0.0	0.0	0.0	0.0	0.0
69	0.0	0.0	0.0	0.0	0.0	0.0	0.0	0.0	0.0	0.0	0.0	0.0
70	0.0	0.0	0.0	0.0	0.0	0.0	0.0	0.0	0.0	0.0	0.0	0.0
TOTAL	72.7	63.8	72.7	74.1	78.7	70.6	59.6	65.0	55.5	55.0	58.6	57.1

Table 6.11 Cyclic Stress Occurrences per interval, Gage 2 on MARKET, 1976

STRS. AMPL. (KSI)	S.S. 1	S.S. 2	S.S. 3	S.S. 4	S.S. 5	S.S. 6	S.S. 7	S.S. 8	S.S. 9	S.S. 10	S.S. 11	S.S. 12
1	39.6	29.[illegible]	9.5	27.7	23.1	5.9	1.3	1.0	1.8	0.4	0.1	0.0
2	27.9	20.7	14.1	14.9	10.2	13.6	3.5	2.7	4.9	1.2	0.5	0.1
3	8.0	10.6	13.1	11.1	8.4	14.5	4.8	3.8	7.0	2.0	0.6	0.3
4	2.0	6.4	11.1	8.2	7.0	11.9	5.2	4[illegible]	7.9	2.7	1.0	0.5
5	0.5	3.9	8.2	5.6	5.7	9.0	5.[illegible]	4.1	7.[illegible]	3.3	1.4	0.7
6	0.1	2.4	5.4	3.5	4.4	6.4	4.8	3.6	7.1	3.8	1.8	1.0
7	0.0	1.4	3.4	2.0	3.4	4.4	4.4	3.4	6.[illegible]	4.2	2.1	1.2
8	0.0	0.7	2.1	1.1	2.5	3.0	3.9	2.9	5.2	4.4	2.5	1.5
9	0.0	0.4	1.3	0.6	1.9	2.0	3.5	2.5	4.5	4.5	2.8	1.7
10	0.0	0.2	0.8	0.4	1.5	1.4	3.0	2.1	3.9	4.5	3.1	2.0
11	0.0	0.1	0.6	0.2	1.1	1.0	2.6	1.8	3.5	4.4	3.3	2.2
12	0.0	0.0	0.4	0.1	0.9	0.7	2.2	1.6	3.0	4.1	3.4	2.5
13	0.0	0.0	0.3	0.1	0.7	0.5	1.9	1.4	2.6	3.9	3.5	2.7
14	0.0	0.0	0.2	0.0	0.5	0.3	1.6	1.3	2.3	3.5	3.5	2.8
15	0.0	0.0	0.1	0.0	0.4	0.2	1.3	1.2	1.9	3.2	3.5	3.0
16	0.0	0.0	0.1	0.0	0.3	0.2	1.1	1.1	1.6	2.8	3.4	3.1
17	0.0	0.0	0.1	0.0	0.2	0.1	0.9	1.0	1.3	2.4	3.2	3.1
18	0.0	0.0	0.0	0.0	0.1	0.1	0.7	1.0	1.1	2.1	3.0	3.[illegible]
19	0.0	0.0	0.0	0.0	0.1	0.1	0.6	0.9	0.9	1.8	2.8	3.1
20	0.0	0.0	0.0	0.0	0.1	0.0	0.5	0.8	0.7	1.4	2.5	3.0
21	0.0	0.0	0.0	0.0	0.0	0.0	0.4	0.7	0.6	1.2	2.3	2.8
22	0.0	0.0	0.0	0.0	0.0	0.0	0.3	0.6	0.5	0.9	2.0	2.7
23	0.0	0.0	0.0	0.0	0.0	0.0	0.3	0.6	0.4	0.8	1.7	2.5
24	0.0	0.0	0.0	0.0	0.0	0.0	0.2	0.5	0.3	0.6	1.5	2.3
25	0.0	0.0	0.0	0.0	0.0	0.0	0.2	0.5	0.3	0.4	1.3	2.0
26	0.0	0.0	0.0	0.0	0.0	0.0	0.2	0.4	0.2	0.3	1.0	1.8
27	0.0	0.0	0.0	0.0	0.0	0.0	0.1	0.4	0.2	0.3	0.9	1.6
28	0.0	0.0	0.0	0.0	0.0	0.0	0.1	0.2	0.1	0.2	0.7	1.3
29	0.0	0.0	0.0	0.0	0.0	0.0	0.1	0.3	0.1	0.1	0.6	1.1
30	0.0	0.0	0.0	0.0	0.0	0.0	0.1	0.2	0.1	0.1	0.4	0.9
31	0.0	0.0	0.0	0.0	0.0	0.0	0.1	0.2	0.1	0.1	0.3	0.8
32	0.0	0.0	0.0	0.0	0.0	0.0	0.1	0.2	0.1	0.0	0.3	0.6
33	0.0	0.0	0.0	0.0	0.0	0.0	0.0	0.1	0.0	0.0	0.2	0.5
34	0.0	0.0	0.0	0.0	0.0	0.0	0.0	0.1	0.0	0.0	0.1	0.4
35	0.0	0.0	0.0	0.0	0.0	0.0	0.0	0.1	0.0	0.0	0.1	0.3
36	0.0	0.0	0.0	0.0	0.0	0.0	0.0	0.1	0.0	0.0	0.1	0.2
37	0.0	0.0	0.0	0.0	0.0	0.0	0.0	0.1	0.0	0.0	0.1	0.1
38	0.0	0.0	0.0	0.0	0.0	0.0	0.0	0.1	0.0	0.0	0.0	0.1
39	0.0	0.0	0.0	0.0	0.0	0.0	0.0	0.1	0.0	0.0	0.0	0.1
40	0.0	0.0	0.0	0.0	0.0	0.0	0.0	0.0	0.0	0.0	0.0	0.1
41	0.0	0.0	0.0	0.0	0.0	0.0	0.0	0.0	0.0	0.0	0.0	0.0
42	0.0	0.0	0.0	0.0	0.0	0.0	0.0	0.0	0.0	0.0	0.0	0.0
43	0.0	0.0	0.0	0.0	0.0	0.0	0.0	0.0	0.0	0.0	0.0	0.0
44	0.0	0.0	0.0	0.0	0.0	0.0	0.0	0.0	0.0	0.0	0.0	0.0
45	0.0	0.0	0.0	0.0	0.0	0.0	0.0	0.0	0.0	0.0	0.0	0.0
46	0.0	0.0	0.0	0.0	0.0	0.0	0.0	0.0	0.0	0.0	0.0	0.0
47	0.0	0.0	0.0	0.0	0.0	0.0	0.0	0.0	0.0	0.0	0.0	0.0
48	0.0	0.0	0.0	0.0	0.0	0.0	0.0	0.0	0.0	0.0	0.0	0.0
49	0.0	0.0	0.0	0.0	0.0	0.0	0.0	0.0	0.0	0.0	0.0	0.0
50	0.0	0.0	0.0	0.0	0.0	0.0	0.0	0.0	0.0	0.0	0.0	0.0
51	0.0	0.0	0.0	0.0	0.0	0.0	0.0	0.0	0.0	0.0	0.0	0.0
52	0.0	0.0	0.0	0.0	0.0	0.0	0.0	0.0	0.0	0.0	0.0	0.0
53	0.0	0.0	0.0	0.0	0.0	0.0	0.0	0.0	0.0	0.0	0.0	0.0
54	0.0	0.0	0.0	0.0	0.0	0.0	0.0	0.0	0.0	0.0	0.0	0.0
55	0.0	0.0	0.0	0.0	0.0	0.0	0.0	0.0	0.0	0.0	0.0	0.0
56	0.0	0.0	0.0	0.0	0.0	0.0	0.0	0.0	0.0	0.0	0.0	0.0
57	0.0	0.0	0.0	0.0	0.0	0.0	0.0	0.0	0.0	0.0	0.0	0.0
58	0.0	0.0	0.0	0.0	0.0	0.0	0.0	0.0	0.0	0.0	0.0	0.0
59	0.0	0.0	0.0	0.0	0.0	0.0	0.0	0.0	0.0	0.0	0.0	0.0
60	0.0	0.0	0.0	0.0	0.0	0.0	0.0	0.0	0.0	0.0	0.0	0.0
61	0.0	0.0	0.0	0.0	0.0	0.0	0.0	0.0	0.0	0.0	0.0	0.0
62	0.0	0.0	0.0	0.0	0.0	0.0	0.0	0.0	0.0	0.0	0.0	0.0
63	0.0	0.0	0.0	0.0	0.0	0.0	0.0	0.0	0.0	0.0	0.0	0.0
64	0.0	0.0	0.0	0.0	0.0	0.0	0.0	0.0	0.0	0.0	0.0	0.0
65	0.0	0.0	0.0	0.0	0.0	0.0	0.0	0.0	0.0	0.0	0.0	0.0
66	0.0	0.0	0.0	0.0	0.0	0.0	0.0	0.0	0.0	0.0	0.0	0.0
67	0.0	0.0	0.0	0.0	0.0	0.0	0.0	0.0	0.0	0.0	0.0	0.0
68	0.0	0.0	0.0	0.0	0.0	0.0	0.0	0.0	0.0	0.0	0.0	0.0
69	0.0	0.0	0.0	0.0	0.0	0.0	0.0	0.0	0.0	0.0	0.0	0.0
70	0.0	0.0	0.0	0.0	0.0	0.0	0.0	0.0	0.0	0.0	0.0	0.0
TOTAL	76.2	76.1	70.5	75.5	72.5	75.3	55.1	48.3	78.1	65.7	61.2	59.7

Table 6.12 Cyclic Stress Occurences per Interval, Gauge 8 on MARKET, 1976

STRS. AMPL. (KSI)	S.S. 1	S.S. 2	S.S. 3	S.S. 4	S.S. 5	S.S. 6	S.S. 7	S.S. 8	S.S. 9	S.S. 10	S.S. 11	S.S. 12
1	55.1	33.0	12.0	29.2	23.9	7.4	1.8	1.5	2.2	0.5	0.6	0.3
2	20.6	20.2	16.8	14.3	11.0	16.3	4.6	3.7	6.0	1.4	1.3	0.8
3	3.4	10.1	15.0	11.5	9.0	16.3	5.9	4.8	8.4	2.2	1.8	1.1
4	0.6	5.8	11.4	8.0	7.4	12.5	6.2	5.0	9.0	3.0	2.3	1.4
5	0.1	3.5	7.3	5.2	5.7	8.7	5.9	4.7	8.4	3.6	2.6	1.7
6	0.0	2.1	4.2	3.1	4.1	5.8	5.4	4.1	7.2	4.1	2.9	1.9
7	0.0	1.1	2.4	1.8	2.9	3.8	4.8	3.5	6.1	4.4	3.0	2.1
8	0.0	0.6	1.4	1.0	2.1	2.4	4.1	2.9	5.1	4.6	3.2	2.2
9	0.0	0.2	0.8	0.5	1.5	1.5	3.4	2.4	4.4	4.7	3.2	2.4
10	0.0	0.1	0.5	0.3	1.1	0.9	2.8	2.0	3.8	4.6	3.3	2.5
11	0.0	0.0	0.3	0.1	0.8	0.6	2.3	1.8	3.3	4.4	3.2	2.5
12	0.0	0.0	0.2	0.1	0.6	0.4	1.8	1.6	2.8	4.1	3.2	2.6
13	0.0	0.0	0.1	0.0	0.4	0.2	1.5	1.4	2.4	3.8	3.0	2.6
14	0.0	0.0	0.1	0.0	0.3	0.1	1.2	1.3	2.0	3.4	2.9	2.6
15	0.0	0.0	0.0	0.0	0.2	0.1	0.9	1.2	1.6	3.0	2.7	2.6
16	0.0	0.0	0.0	0.0	0.1	0.1	0.7	1.0	1.3	2.6	2.6	2.5
17	0.0	0.0	0.0	0.0	0.1	0.0	0.6	0.9	1.1	2.3	2.4	2.5
18	0.0	0.0	0.0	0.0	0.0	0.0	0.5	0.8	0.9	1.9	2.2	2.4
19	0.0	0.0	0.0	0.0	0.0	0.0	0.4	0.7	0.7	1.6	2.0	2.3
20	0.0	0.0	0.0	0.0	0.0	0.0	0.3	0.6	0.6	1.3	1.8	2.2
21	0.0	0.0	0.0	0.0	0.0	0.0	0.2	0.5	0.5	1.1	1.6	2.1
22	0.0	0.0	0.0	0.0	0.0	0.0	0.2	0.5	0.4	0.9	1.4	1.9
23	0.0	0.0	0.0	0.0	0.0	0.0	0.1	0.4	0.3	0.7	1.3	1.8
24	0.0	0.0	0.0	0.0	0.0	0.0	0.1	0.3	0.3	0.6	1.1	1.7
25	0.0	0.0	0.0	0.0	0.0	0.0	0.1	0.3	0.2	0.5	0.9	1.5
26	0.0	0.0	0.0	0.0	0.0	0.0	0.1	0.2	0.2	0.4	0.8	1.4
27	0.0	0.0	0.0	0.0	0.0	0.0	0.1	0.2	0.2	0.3	0.7	1.2
28	0.0	0.0	0.0	0.0	0.0	0.0	0.0	0.2	0.1	0.2	0.6	1.1
29	0.0	0.0	0.0	0.0	0.0	0.0	0.0	0.1	0.1	0.2	0.5	1.0
30	0.0	0.0	0.0	0.0	0.0	0.0	0.0	0.1	0.1	0.1	0.4	0.9
31	0.0	0.0	0.0	0.0	0.0	0.0	0.0	0.1	0.1	0.1	0.3	0.8
32	0.0	0.0	0.0	0.0	0.0	0.0	0.0	0.1	0.1	0.1	0.3	0.7
33	0.0	0.0	0.0	0.0	0.0	0.0	0.0	0.1	0.1	0.1	0.2	0.6
34	0.0	0.0	0.0	0.0	0.0	0.0	0.0	0.0	0.0	0.0	0.2	0.5
35	0.0	0.0	0.0	0.0	0.0	0.0	0.0	0.0	0.0	0.0	0.2	0.4
36	0.0	0.0	0.0	0.0	0.0	0.0	0.0	0.0	0.0	0.0	0.1	0.4
37	0.0	0.0	0.0	0.0	0.0	0.0	0.0	0.0	0.0	0.0	0.1	0.3
38	0.0	0.0	0.0	0.0	0.0	0.0	0.0	0.0	0.0	0.0	0.1	0.3
39	0.0	0.0	0.0	0.0	0.0	0.0	0.0	0.0	0.0	0.0	0.1	0.2
40	0.0	0.0	0.0	0.0	0.0	0.0	0.0	0.0	0.0	0.0	0.0	0.2
41	0.0	0.0	0.0	0.0	0.0	0.0	0.0	0.0	0.0	0.0	0.0	0.1
42	0.0	0.0	0.0	0.0	0.0	0.0	0.0	0.0	0.0	0.0	0.0	0.1
43	0.0	0.0	0.0	0.0	0.0	0.0	0.0	0.0	0.0	0.0	0.0	0.1
44	0.0	0.0	0.0	0.0	0.0	0.0	0.0	0.0	0.0	0.0	0.0	0.1
45	0.0	0.0	0.0	0.0	0.0	0.0	0.0	0.0	0.0	0.0	0.0	0.1
46	0.0	0.0	0.0	0.0	0.0	0.0	0.0	0.0	0.0	0.0	0.0	0.0
47	0.0	0.0	0.0	0.0	0.0	0.0	0.0	0.0	0.0	0.0	0.0	0.0
48	0.0	0.0	0.0	0.0	0.0	0.0	0.0	0.0	0.0	0.0	0.0	0.0
49	0.0	0.0	0.0	0.0	0.0	0.0	0.0	0.0	0.0	0.0	0.0	0.0
50	0.0	0.0	0.0	0.0	0.0	0.0	0.0	0.0	0.0	0.0	0.0	0.0
51	0.0	0.0	0.0	0.0	0.0	0.0	0.0	0.0	0.0	0.0	0.0	0.0
52	0.0	0.0	0.0	0.0	0.0	0.0	0.0	0.0	0.0	0.0	0.0	0.0
53	0.0	0.0	0.0	0.0	0.0	0.0	0.0	0.0	0.0	0.0	0.0	0.0
54	0.0	0.0	0.0	0.0	0.0	0.0	0.0	0.0	0.0	0.0	0.0	0.0
55	0.0	0.0	0.0	0.0	0.0	0.0	0.0	0.0	0.0	0.0	0.0	0.0
56	0.0	0.0	0.0	0.0	0.0	0.0	0.0	0.0	0.0	0.0	0.0	0.0
57	0.0	0.0	0.0	0.0	0.0	0.0	0.0	0.0	0.0	0.0	0.0	0.0
58	0.0	0.0	0.0	0.0	0.0	0.0	0.0	0.0	0.0	0.0	0.0	0.0
59	0.0	0.0	0.0	0.0	0.0	0.0	0.0	0.0	0.0	0.0	0.0	0.0
60	0.0	0.0	0.0	0.0	0.0	0.0	0.0	0.0	0.0	0.0	0.0	0.0
61	0.0	0.0	0.0	0.0	0.0	0.0	0.0	0.0	0.0	0.0	0.0	0.0
62	0.0	0.0	0.0	0.0	0.0	0.0	0.0	0.0	0.0	0.0	0.0	0.0
63	0.0	0.0	0.0	0.0	0.0	0.0	0.0	0.0	0.0	0.0	0.0	0.0
64	0.0	0.0	0.0	0.0	0.0	0.0	0.0	0.0	0.0	0.0	0.0	0.0
65	0.0	0.0	0.0	0.0	0.0	0.0	0.0	0.0	0.0	0.0	0.0	0.0
66	0.0	0.0	0.0	0.0	0.0	0.0	0.0	0.0	0.0	0.0	0.0	0.0
67	0.0	0.0	0.0	0.0	0.0	0.0	0.0	0.0	0.0	0.0	0.0	0.0
68	0.0	0.0	0.0	0.0	0.0	0.0	0.0	0.0	0.0	0.0	0.0	0.0
69	0.0	0.0	0.0	0.0	0.0	0.0	0.0	0.0	0.0	0.0	0.0	0.0
70	0.0	0.0	0.0	0.0	0.0	0.0	0.0	0.0	0.0	0.0	0.0	0.0
TOTAL	76.5	76.7	72.6	75.2	71.0	77.1	55.7	48.9	79.8	66.8	61.2	60.7

Table 6.13 Probability of Occurrence p_j for Atlantic Route

Beaufort No.	Significant Wave height (ft)	Probability of Occurrence (p_j)
1	0.01	
2	0.5	
3	1.3-1.8	0.31836
4	2.6-4.7	
5	5.9-7.3	0.18585
6	9 -12	0.37176
7	14-19	0.09858
8	21-29	0.92221
9	32-39	0.0031403
10	42-53	0.0000747
11	57-64	0.00002613
12	75	0.00000187

Note: Significant wave heights, generally for fully developed seas, are shown for visualization purposes only.

Table 6.14 Long-term Composite Stress Histograms for Sealand McLean, Based on Linear Stress-Strain Relationship

Strs. Ampl. (ksi)	No. of Occurrences in 20 Years		
	Gage FvB 1975	Gage 2 1977 Gage 3 1978	Gage 8 1977 Gage 8 1978
1	5183369.	8846192.	9612198.
2	5624119.	10338407.	8823468.
3	4908472.	7299186.	6108445.
4	4047811.	5098375.	4367842.
5	3287474.	3561304.	3166540.
6	2685228.	2438684.	2296699.
7	2246169.	1652590.	1666941.
8	1926758.	1121016.	1218520.
9	1681983.	768727.	903223.
10	1481836.	542710.	680285.
11	1309542.	396926.	522036.
12	1157091.	302019.	408674.
13	1020770.	238428.	326202.
14	898568.	191777.	265057.
15	789343.	156144.	214972.
16	692137.	132264.	179781.
17	606008.	112280.	151578.
18	529870.	95969.	128476.
19	462764.	76660.	107662.
20	403908.	65932.	92028.
21	352328.	56299.	78726.
22	307413.	47878.	67383.
23	268280.	40588.	57573.
24	234284.	34195.	44591.
25	204807.	28622.	38240.
26	179174.	23944.	32802.
27	157000.	10254.	28105.
28	137741.	8399.	24048.
29	121028.	6777.	20557.
30	106466.	5502.	8045.
31	93318.	4344.	6740.
32	82400.	3417.	4991.
33	72833.		4203.
34	64452.		614.
35	57173.		551.
36	48432.		494.
37	43245.		442.
38	38580.		395.
39	34520.		353.
40	15945.		316.
41	12195.		282.
42	8226.		251.
43	7461.		223.
44	6770.		198.
45	6151.		177.
46	5569.		157.
47			139.
48			123.
49			108.
50			7.
51			6.
52			6.
53			5.
54			4.
55			2.
56			1.
57			1.
58			1.
59			1.
TOTAL	43609009.	43705808.	41661490.

Table 6.15 Long-term Composite Stress Histograms for Sealand Market, Based on Linear Stress-Strain Relationship

Strs. Ampl. (ksi)	No. of Occurrences in 20 Years	
	Gage 2 1976	Gage 8 1976
1	8852827.	10394047.
2	7976351.	8452890.
3	6438592.	6828799.
4	5040528.	5177707.
5	3789665.	3695569.
6	2755503.	2544937.
7	1960722.	1725809.
8	1395757.	1171621.
9	1007788.	805197.
10	742082.	562209.
11	555950.	396807.
12	420353.	285208.
13	322265.	205347.
14	246068.	150530.
15	190760.	108979.
16	148333.	81547.
17	115615.	53695.
18	88672.	38641.
19	70053.	31540.
20	47663.	25720.
21	35056.	20958.
22	29681.	17083.
23	25121.	13895.
24	21232.	11314.
25	17953.	9187.
26	15182.	7448.
27	12810.	6036.
28	10816.	2276.
29	9136.	1867.
30	7713.	1512.
31	6498.	1227.
32	5461.	986.
33	1928.	787.
34	1645.	3.
35	1405.	3.
36	1187.	2.
37	1012.	2.
38	848.	1.
39	718.	1.
TOTAL	42370950.	42831388.

Table 6.16 Long-term Composite Stress Histograms for Sealand McLean, Based on Nonlinear Stress-Strain Relationship

Strs. Ampl. (ksi)	No. of Occurrences in 20 Years		
	Gage F_yB 1975	Gage 2 1977 Gage 3 1978	Gage 8 1977 Gage 8 1978
1	5183369.	8846192.	9612198.
2	5624119.	10338407.	8823468.
3	4908472.	7299186.	6108445.
4	4047811.	5098375.	4367842.
5	3287474.	3561304.	3166540.
6	2685228.	2438684.	2296699.
7	2246169.	1652590.	1666941.
8	1926758.	1121016.	1218520.
9	1681983.	768727.	903223.
10	1481836.	542710.	680285.
11	1309542.	396926.	522036.
12	1157091.	302019.	408674.
13	1020770.	238428.	326202.
14	898568.	191777.	265057.
15	789343.	156144.	214972.
16	692137.	132264.	179781.
17	606008.	112280.	151578.
18	529870.	95969.	128476.
19	462764.	76660.	107662.
20	403908.	65932.	92028.
21	352328.	56299.	78726.
22	307413.	47878.	67383.
23	268280.	40588.	57573.
24	234284.	34195.	44591.
25	204807.	28622.	38240.
26	179174.	23944.	32802.
27	157000.	10254.	28105.
28	137741.	8399.	24048.
29	121028.	6777.	20557.
30	199784.	9846.	14785.
31	219684.	3417.	9808.
32	148849.		1488.
33	89045.		1065.
34	27882.		755.
35	18490.		532.
36			370.
37			24.
38			7.
39			3.
40			0.
41			0.
TOTAL	43609009.	43705808.	41661490.

Table 6.17 Long-term Composite Stress Histograms for Sealand Market, Based on Nonlinear Stress-Strain Relationship

Strs. Ampl. (ksi)	No. of Occurrences in 20 Years	
	Gage 2 1976	Gage 8 1976
1	8252827.	10394047.
2	7976351.	8452890.
3	6438592.	6828799.
4	5040528.	5177707.
5	3789665.	3695569.
6	2755503.	2544937.
7	1960722.	1725809.
8	1395757.	1171621.
9	1007788.	805197.
10	742082.	562209.
11	555950.	396807.
12	420353.	285208.
13	322265.	205347.
14	246068.	150530.
15	190760.	108979.
16	148333.	81547.
17	115615.	53695.
18	88672.	38641.
19	70053.	31540.
20	47663.	25720.
21	35056.	20958.
22	29681.	17083.
23	25121.	13895.
24	21232.	11314.
25	17953.	9187.
26	15182.	7448.
27	12810.	6036.
28	10816.	2276.
29	9136.	1867.
30	14211.	2738.
31	9034.	1776.
32	3604.	7.
33	1566.	3.
34		0.
35		0.
TOTAL	42370950.	42831388.

Table 6.18 Comparison of Linear and Nonlinear Long-term Stress Histograms, Sealand Market

Stress Amplitude (ksi)	Number of Occurrences in 20 Years			
	Gage 2 (Unmodified)		Gage 8 (Modified)	
	Linear	Nonlinear	Linear	Nonlinear
1	8852827.	8852827.	10394047.	10394047.
2	7976351.	7976351.	8452890.	8452890.
3	6438592.	6438592.	6828799.	6828799.
4	5040528.	5040528.	5177707.	5177707.
5	3789665.	3789665.	3695569.	3695569.
6	2755503.	2755503.	2544937.	2544937.
7	1960722.	1960722.	1725809.	1725809.
8	1395757.	1395757.	1171621.	1171621.
9	1007788.	1007788.	805197.	805197.
10	742082.	742082.	562209.	562209.
11	555950.	555950.	396807.	396807.
12	420353.	420353.	285208.	285208.
13	322265.	322265.	205347.	205347.
14	246068.	246068.	150530.	150530.
15	190760.	190760.	108979.	108979.
16	148333.	148333.	81547.	81547.
17	115615.	115615.	53695.	53695.
18	88672.	88672.	38641.	38641.
19	70053.	70053.	31540.	31540.
20	47663.	47663.	25720.	25720.
21	35056.	35056.	20958.	20958.
22	29681.	29681.	17083.	17083.
23	25121.	25121.	13895.	13895.
24	21232.	21232.	11314.	11314.
25	17953.	17953.	9187.	9187.
26	15182.	15182.	7448.	7448.
27	12810.	12810.	6036.	6036.
28	10816.	10816.	2276.	2276.
29	9136.	9136.	1867.	1867.
30	7713.	14211.	1512.	2738.
31	6498.	9034.	1227.	1776.
32	5461.	3604.	986.	7.
33	1928.	1566.	787.	3.
34	1645.		3.	0.
35	1405.		3.	0.
36	1187.		2.	
37	1012.		2.	
38	848.		1.	
39	718.		1.	
Total	42370950.	42370950.	42831388.	42831388.

Note: (1) Linear indicates that stresses are based on linear stress-strain relationship

(2) Nonlinear values correspond to stresses that account for nonlinear cyclic stress strain behavior.

Table 7.1 Results for Fatigue Life Using AWS & ASME S-N Curves

Ship	Measurement Period	Gauge	Fatigue Life (yrs) S-N Curve AWS	ASME
SEALAND McLEAN	Jan-Mar 1975	F_yB *	.09	.21
	May-July 1977	2 **	.89	2.43
	Sept-Jan 1978	3		
	May-July 1977	8 **	.58	1.53
	Sept-Jan 1978	8		
SEALAND MARKET	Oct-Dec 1978	2 *	.86	2.46
		8 **	1.7	5.5

* Original Hatch Corner
** Modified Hatch Corner

Table 7.2 - Design factors in Wirsching's Method

	Design Factor	Value	Comments
Munse's	m	4.805	see Ref. 7.5
"Detail 1F"	K	$10^{13.78}$	
S-N Curve	C_k	0.6	equivalent to the quantity denoted as δF in Ref. 7.5
Stress	B	1.0	suggested by Wirsching for deckstructure of TLP in Ref. 7.9
Analysis	C_B	.25	value is reasonable since stress obtained through instrumental measurement
Miner's	$\tilde{\Delta}$	1.0	suggested by Wirsching in Ref. 6.1 .
Rule	C_Δ	0.3	Value of C_Δ is reasonable, and has a little influence.

Table 7.3 Results for Fatigue Life in a Probability Context using Wirshing's method.

Ship	Measurement Period	Gauge	Median Life (yrs)	Notional P_f	Safety Index
	Jan-Mar 1975	F_yB *	2.4	0.94	-1.58
SEA-LAND McLEAN	May-July 1977 Sept-Jan 1978	2 ** 3	29.6	0.39	0.29
	May-July 1977 Sept-Jan 1978	8 ** 8	18.5	0.52	-0.06
SEA-LAND MARKET	Oct-Dec 1976	2 *	29.3	0.39	0.29
		8 **	63.9	0.19	0.87

* Original Hatch Corner
** Modified Hatch Corner

Table 7.4 Results for Fatigue Life in a Probabilistic Context, on the basis of Munse's method.

Ship	Measurement Period	Gauge		Mean Life (yrs)	Notional P_f
	Jan-Mar 1975	F_yB	*	1.6	0.99
SEA-LAND McLEAN	May-July 1977 Sept-Jan 1978	2 3	**	38.3	0.36
	May-July 1977 Sept-Jan 1978	8 8	**	17.5	0.67
SEA-LAND MARKET	Oct-Dec 1976	2	*	35.5	0.39
		8	**	81.9	0.17

* Original Hatch Corner
** Modified Hatch Corner

Table 7.5 Fatigue Crack Growth Lives Using Fracture Mechanics Model

Data Set				Crack Growth Analysis		
Ship	Sea Trail Period	Gage	Total Interval	Initial Crack Size(in)	Life(yrs) @ $K_{th} = 2ksi\sqrt{in}$	Life(yrs) @ $K_{th} = 5ksi\sqrt{in}$
Sealand McLean	Jan-Mar 1975	FyB	214	0.00394	0.22	0.36
				0.01	0.16	0.18
				0.1	0.07	0.07
	May-Jul 1977 Sep-Jan 1978	2 3	265	0.00394	1.9	7.6
				0.01	1.2	2.3
				0.1	0.5	0.51
	May-Jul 1977 Sep-Jan 1978	8 8	560	0.00394	1.4	4.5
				0.01	0.9	1.5
				0.1	0.38	0.39
Sealand Market	Oct-Dec 1976	2	144	0.00394	1.3	5.0
				0.01	0.83	1.4
				0.1	0.34	0.35
		8	144	0.00394	3	22
				0.01	1.7	5.0
				0.1	0.7	0.7

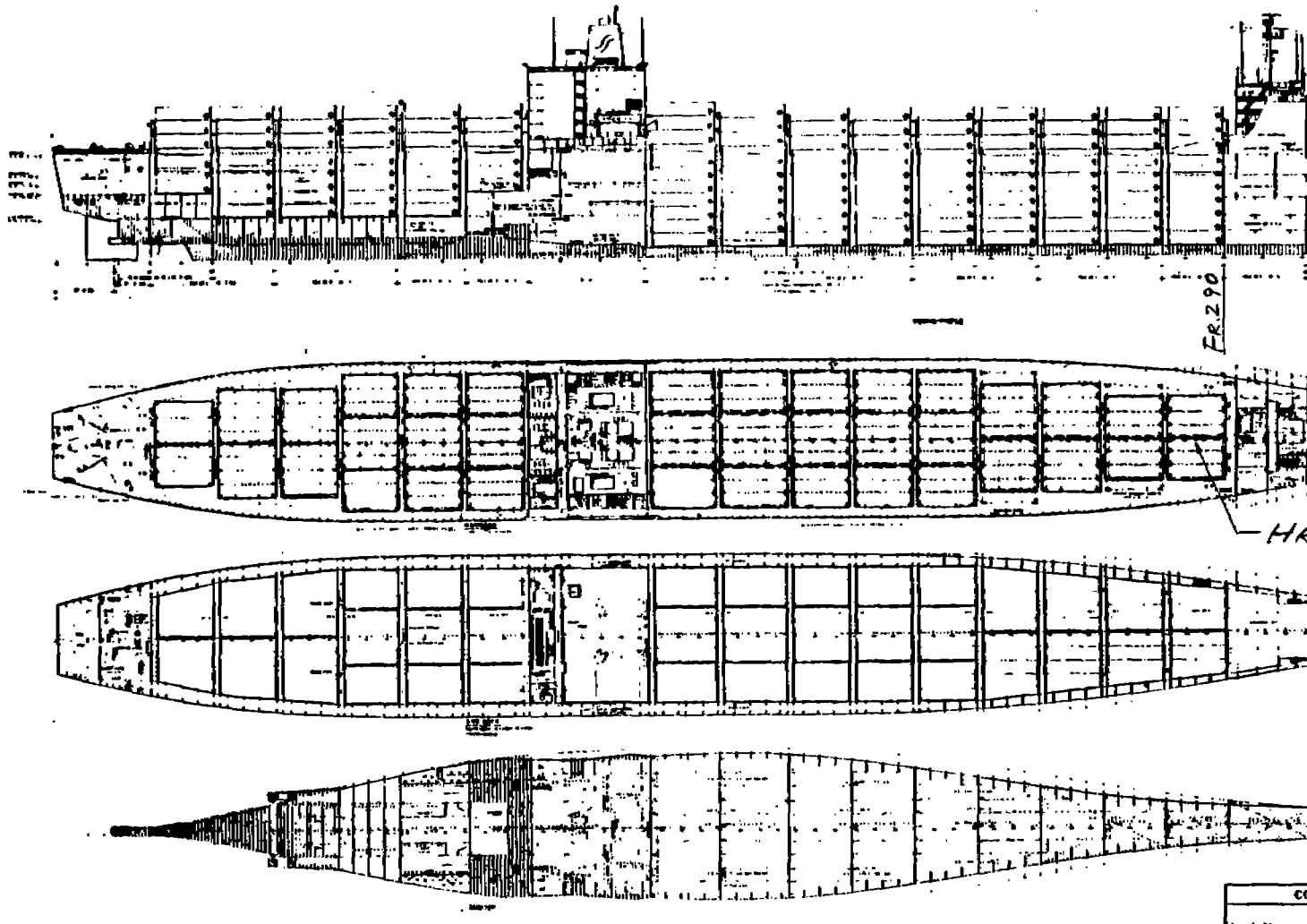

Figure 1.1 General Arrangement

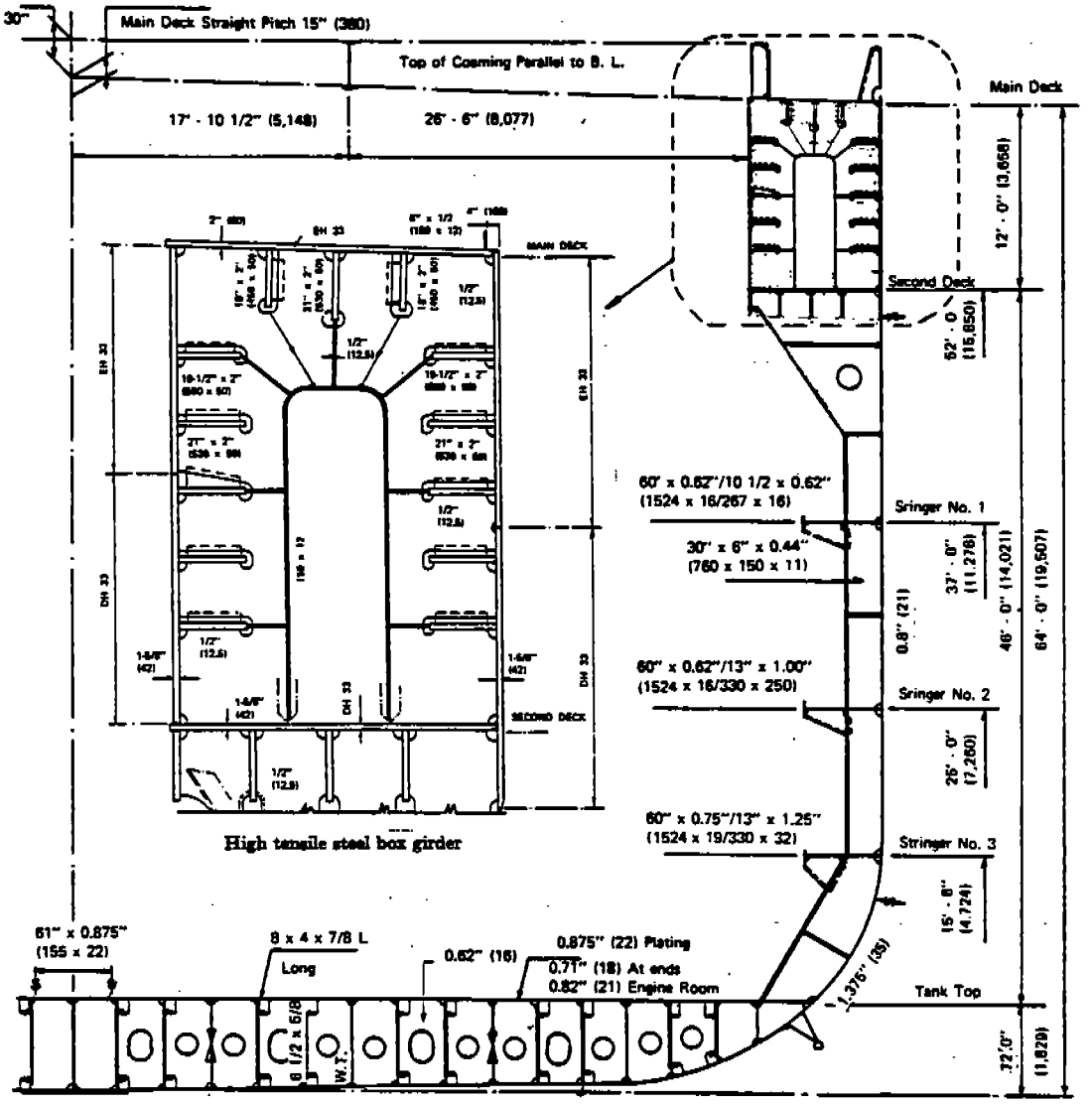

Figure 1.2 Midship Section

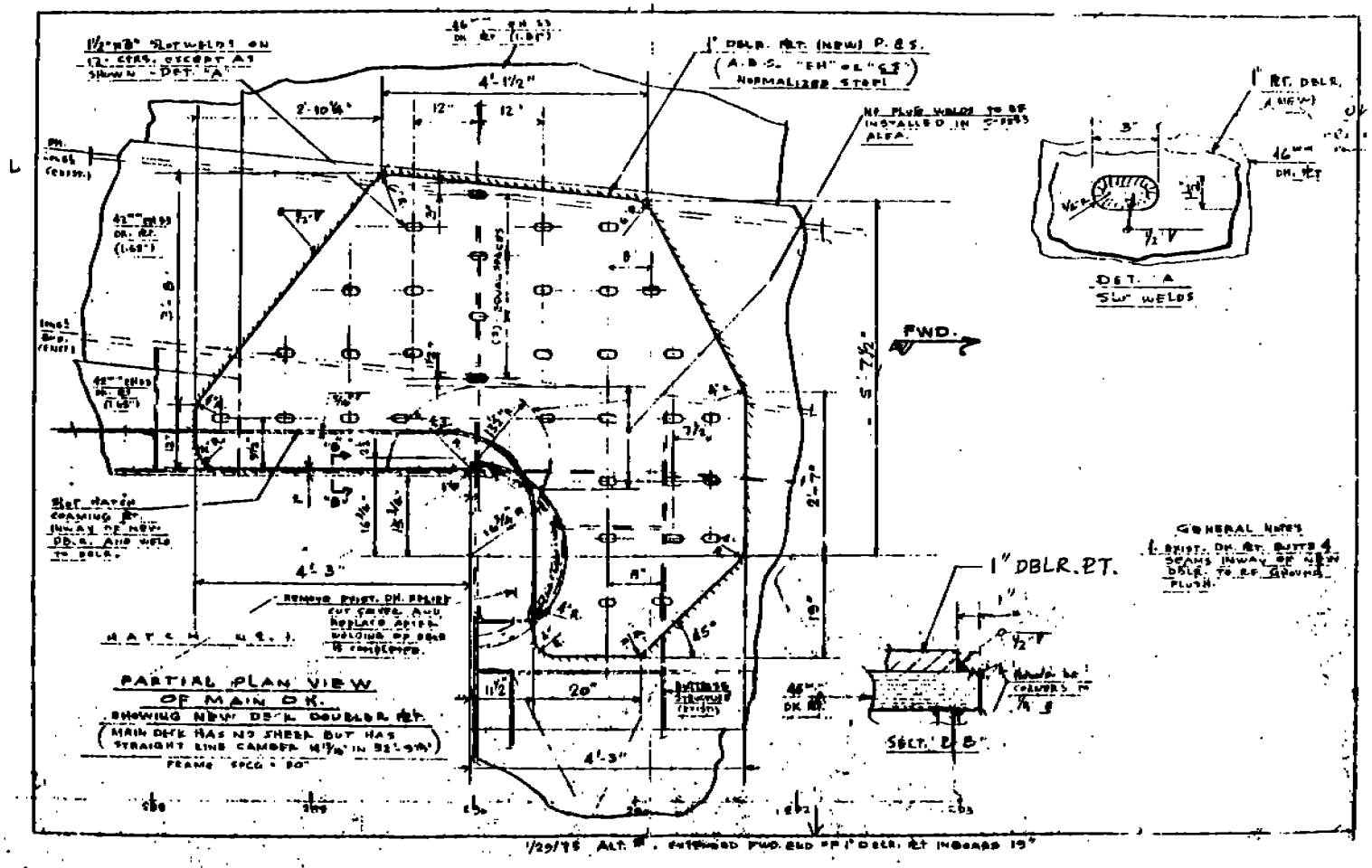

Figure 2.1 Reinforcement, with Doubler Plates, for No.1 Hatch Forward Corners

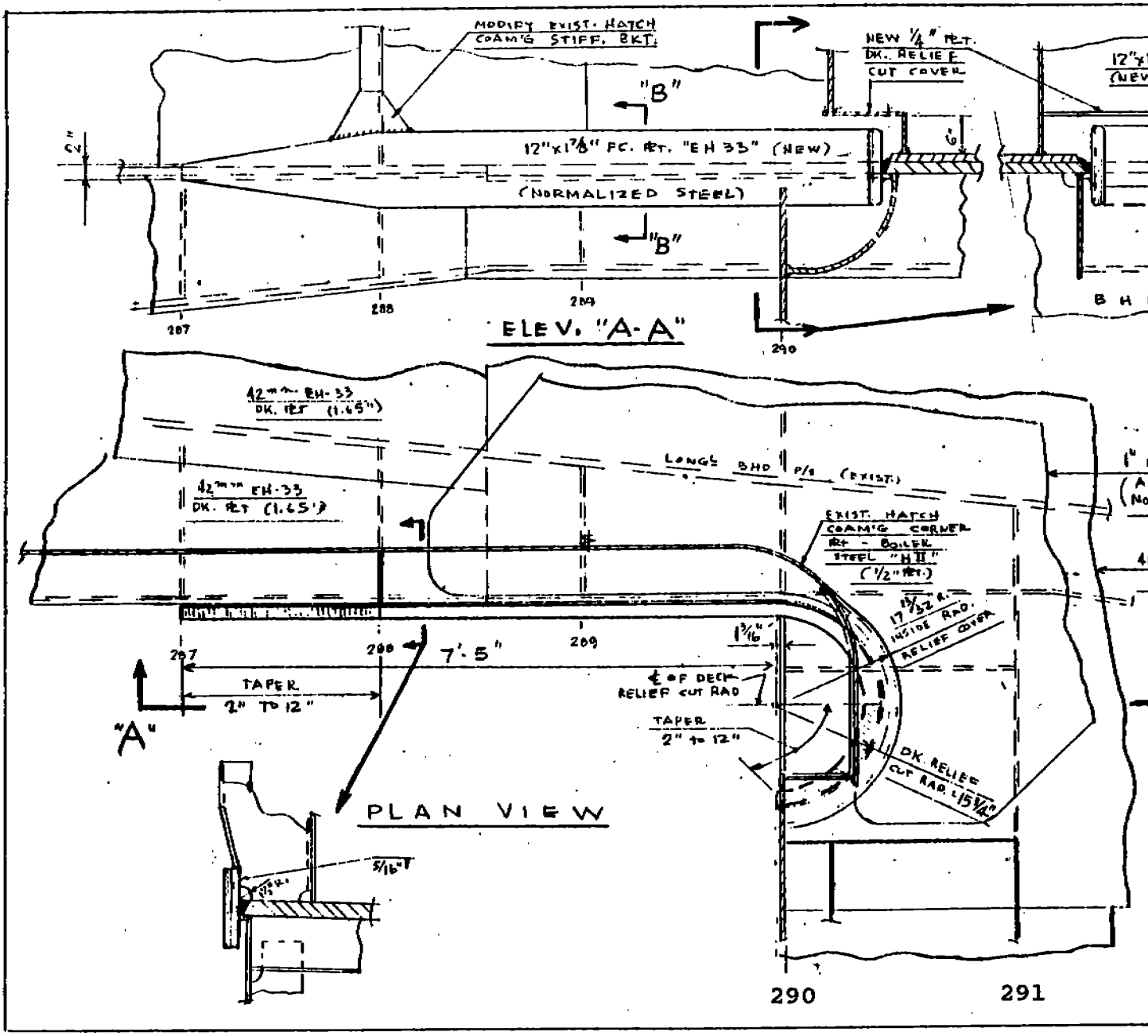

Figure 2.2 Reinforcement, with Face Plates, for No.1 Hatch Forward Corne

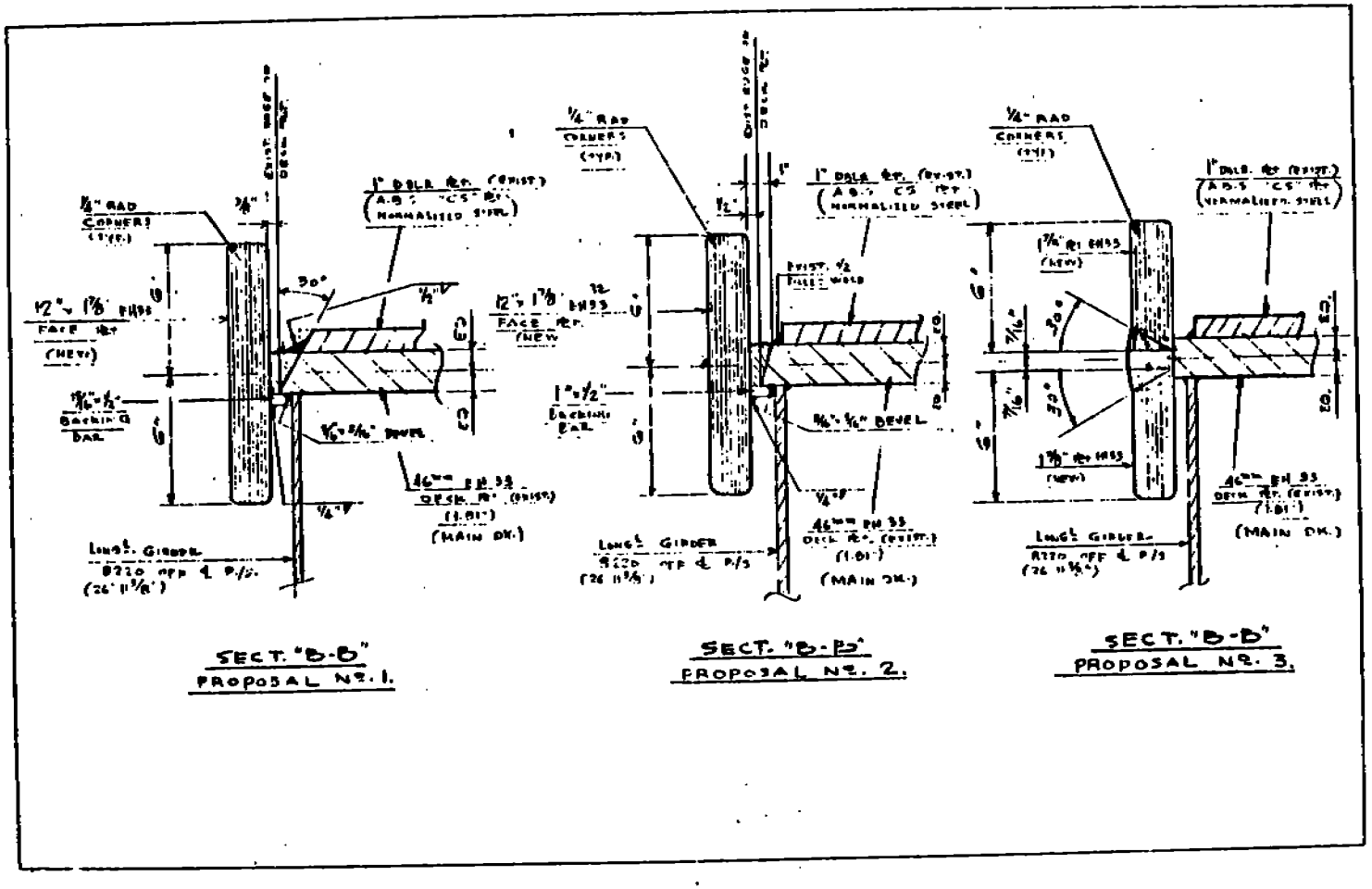

Figure 2.2 (Continued)

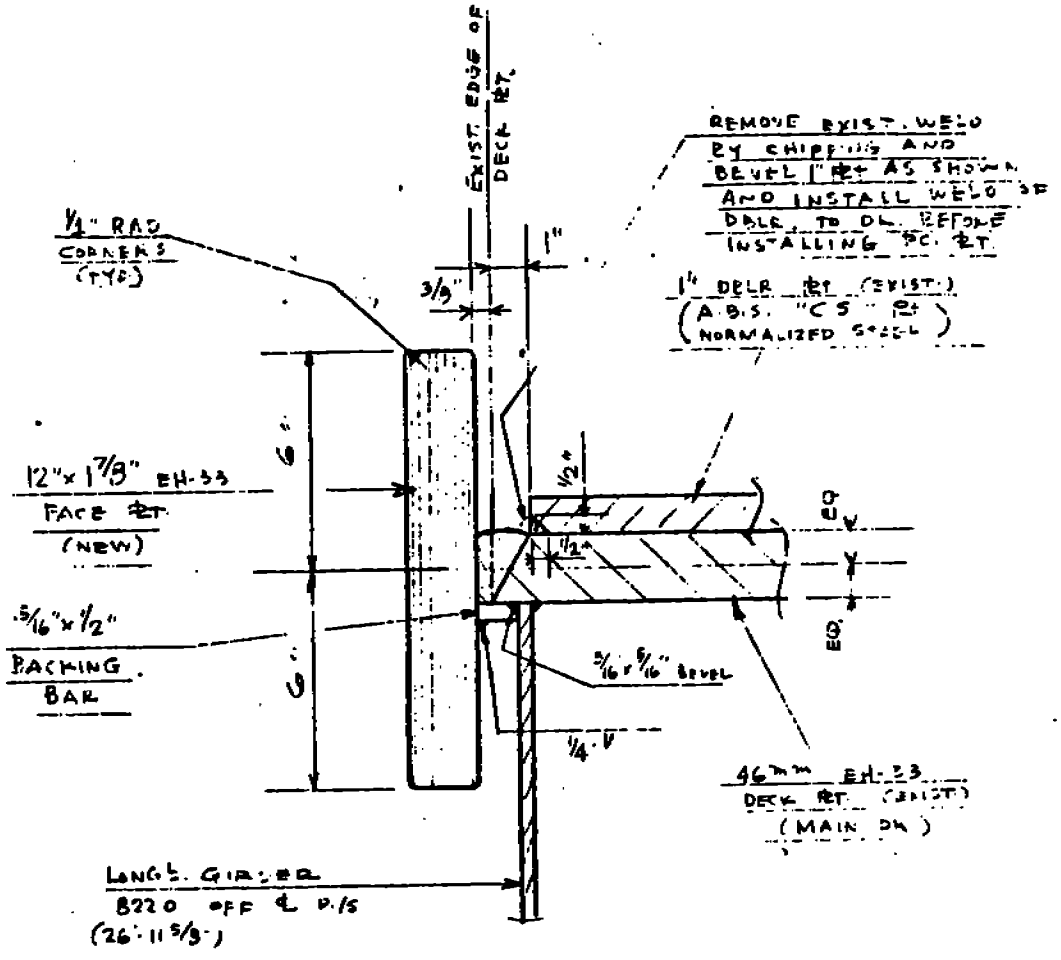

SECT. "B-B"
PROPOSAL NO. 4.

Figure 2.2 (Continued)

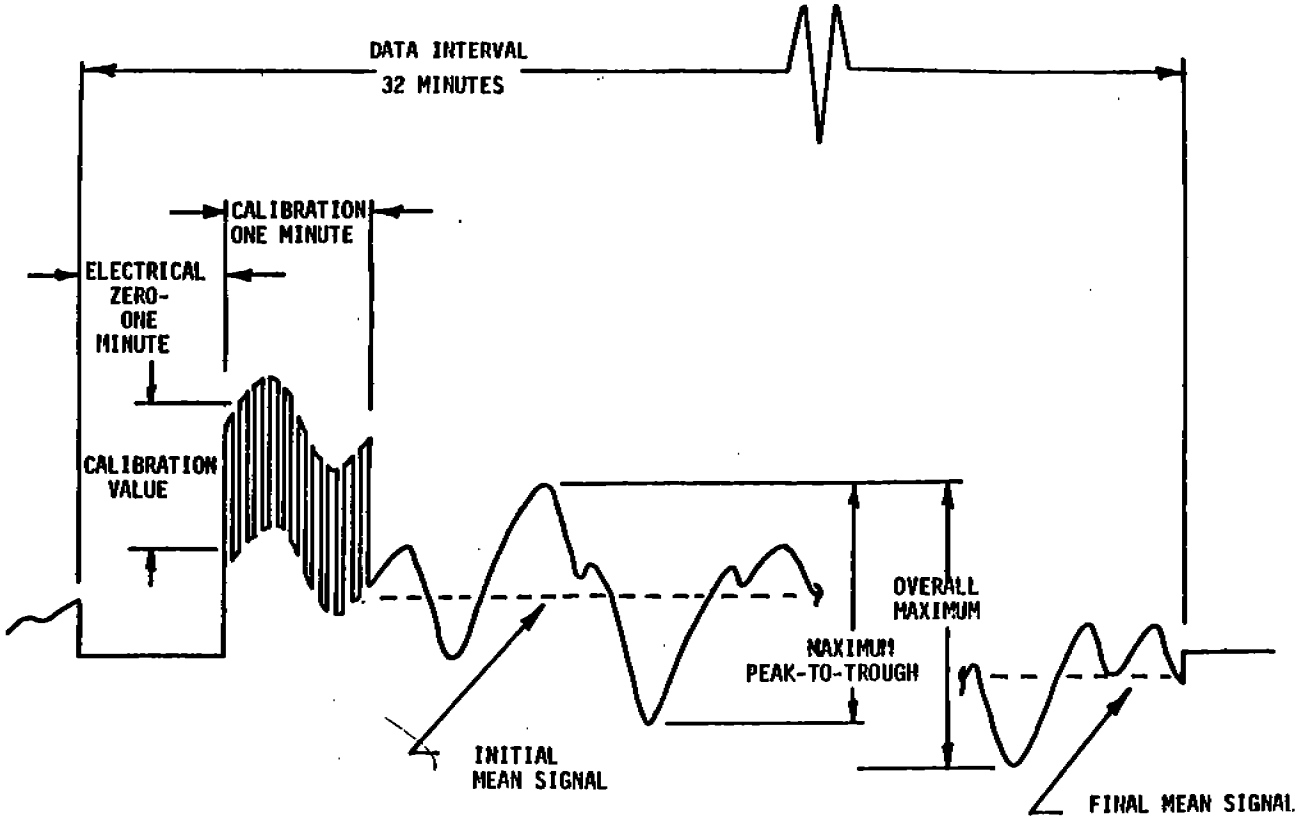

Figure 3.1 Typical Analog Data Interval Record

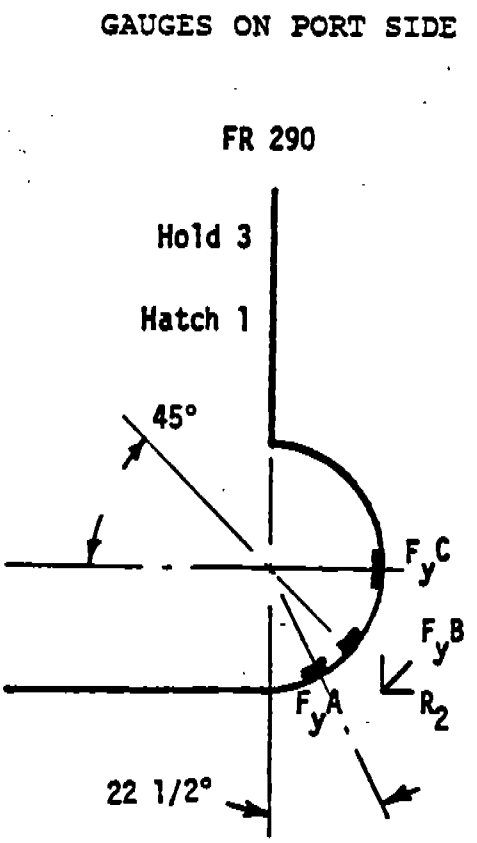

Figure 3.2 Hatch Corner Strain Gauges, S.S. SEALAND McLEAN

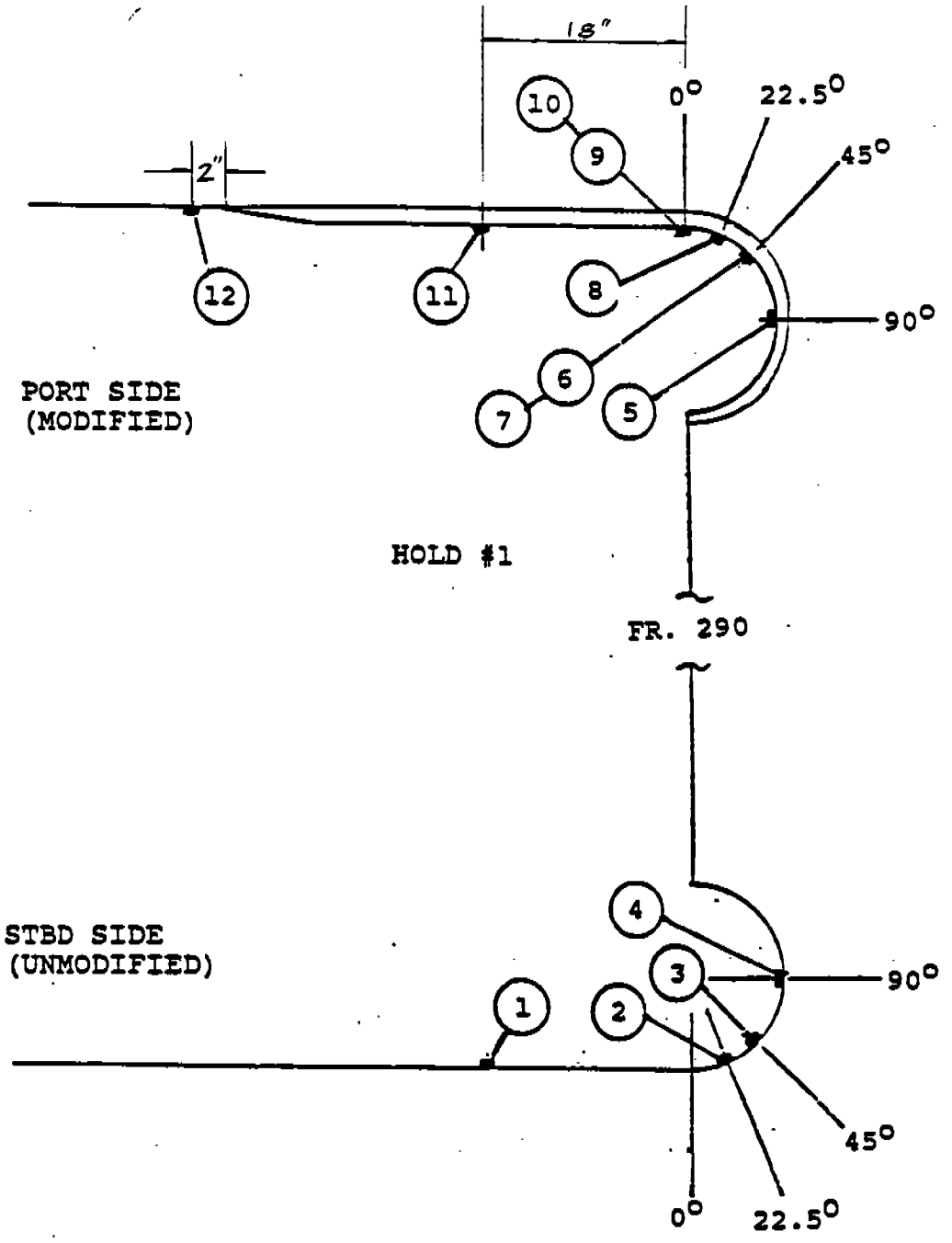

Figure 3.3 Strain Gauges, SEA-LAND MARKET, Port Modified/Stbd Unmodified. Oct-Dec 1976

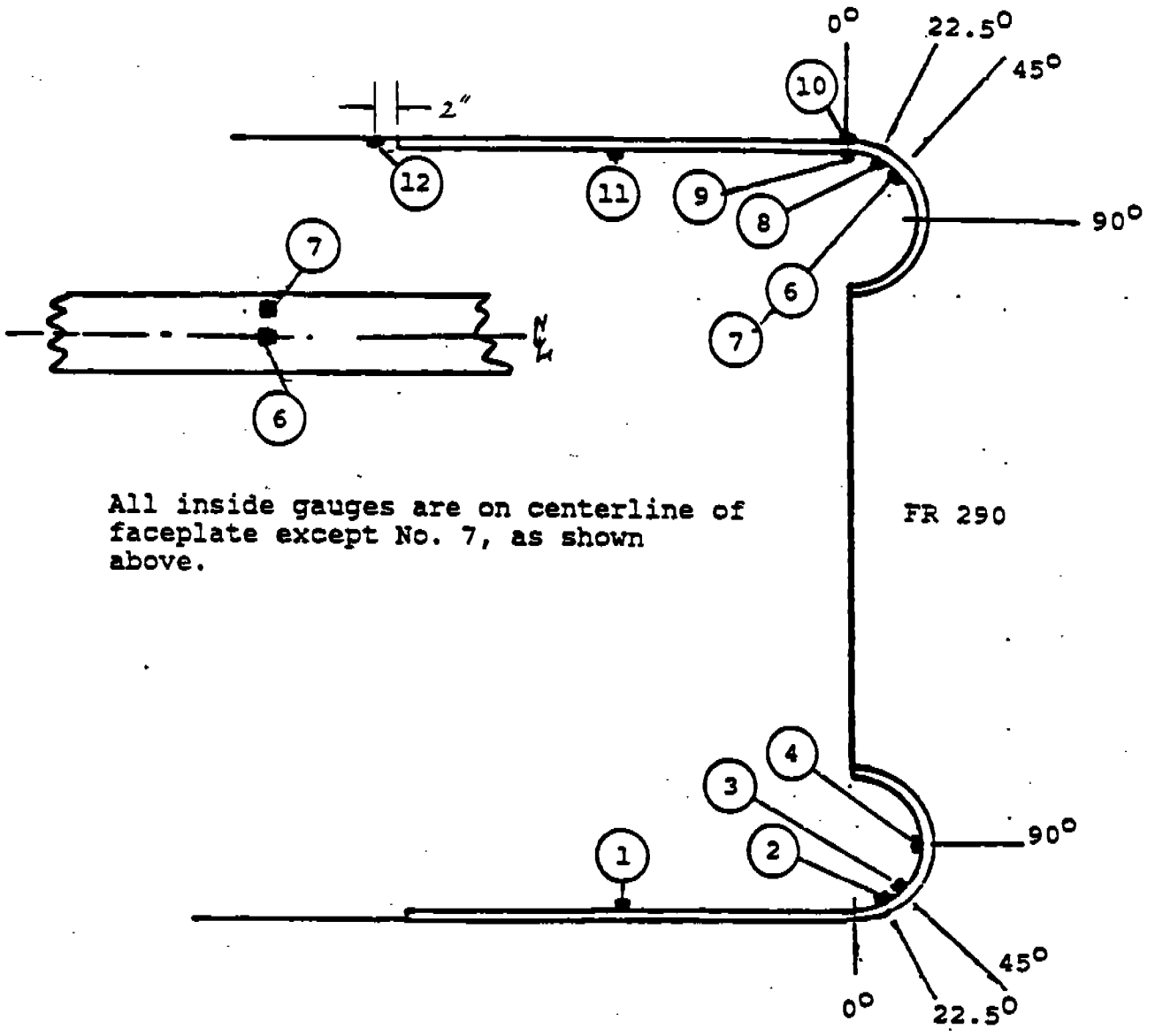

Figure 3.4 Strain Gauges, SEA-LAND McLEAN Modified, May-July 77

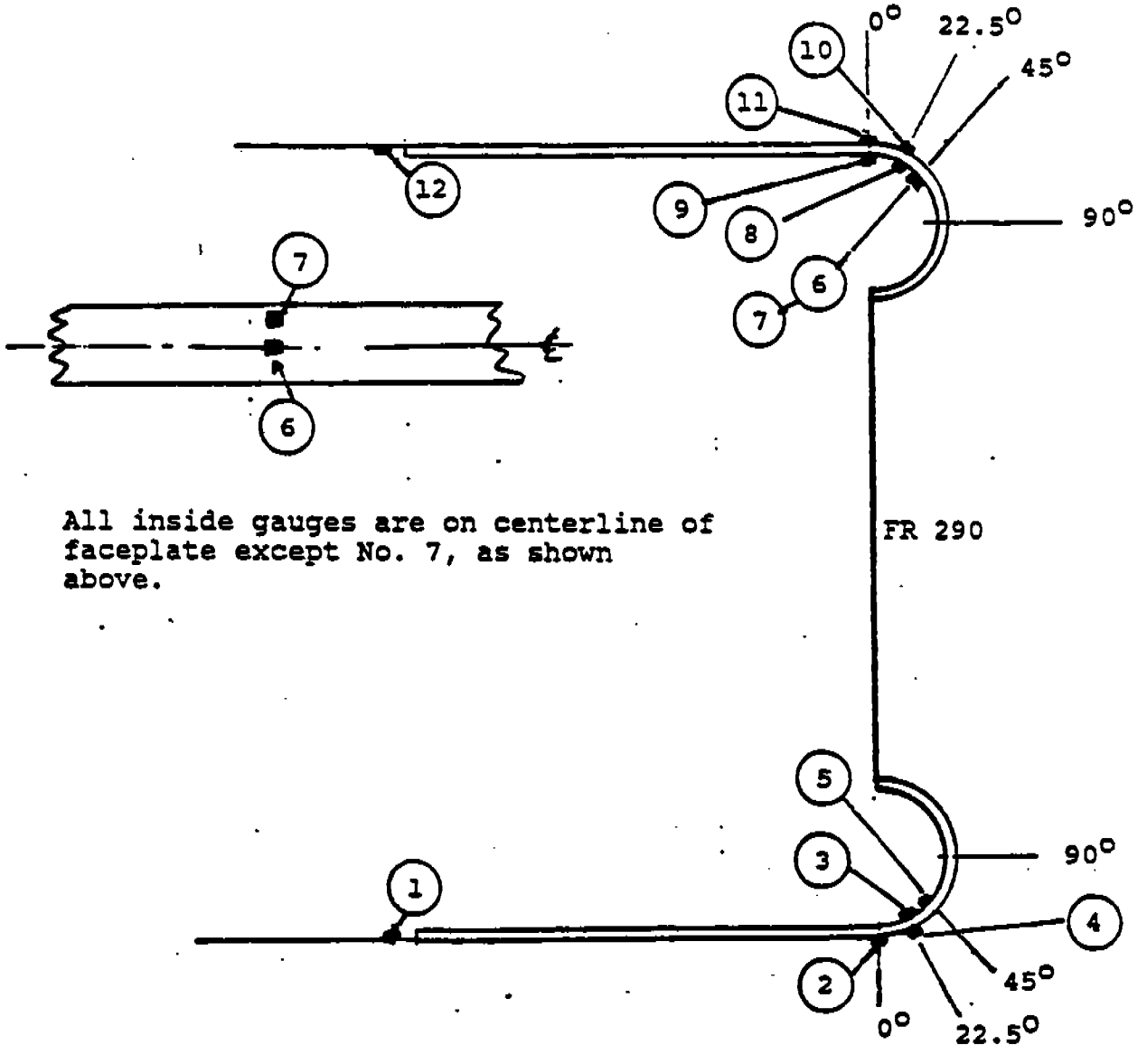

Figure 3.5 Strain Gauges, SEA-LAND McLEAN Modified, Sept 77-Jan 78

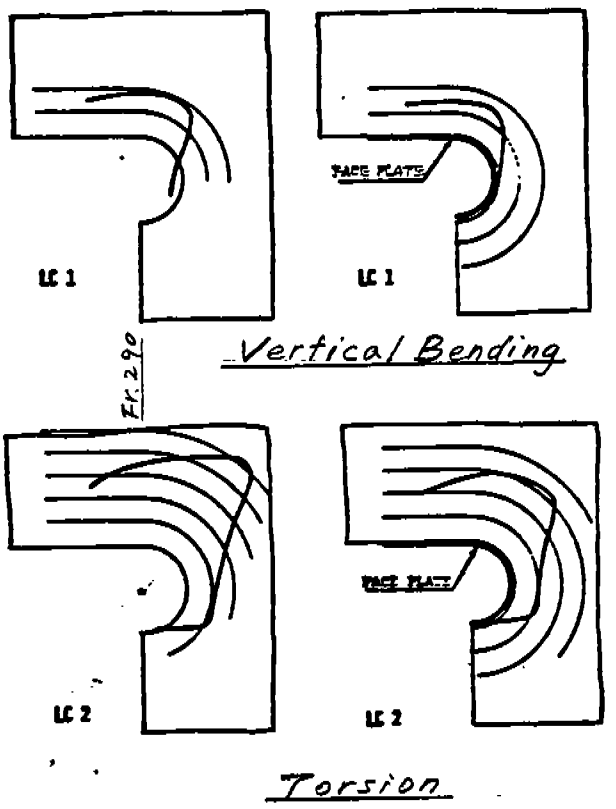

Figure 4.1 Hatch Corner Stresses at Frame 290

Stresses in kg/cm^2, + Tensile

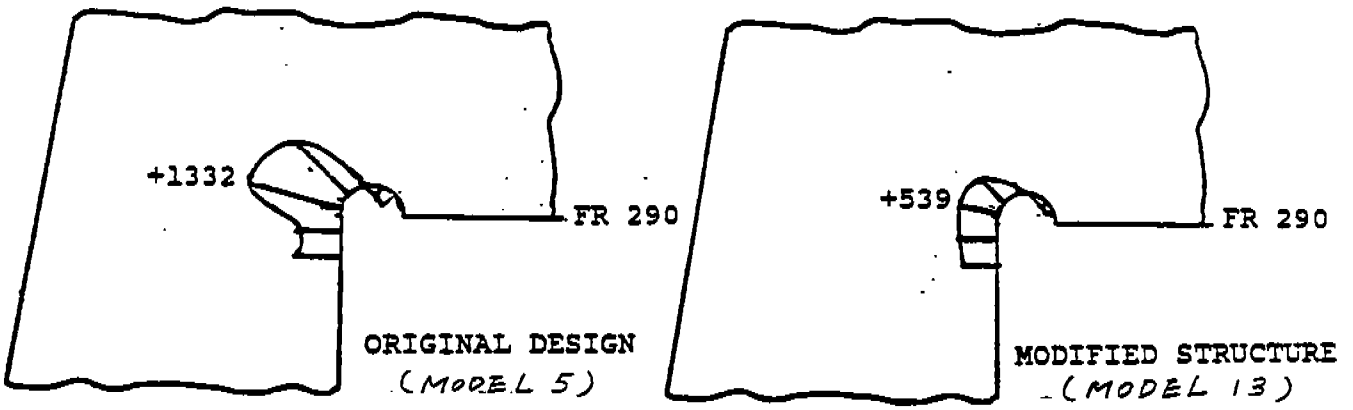

VERTICAL BENDING

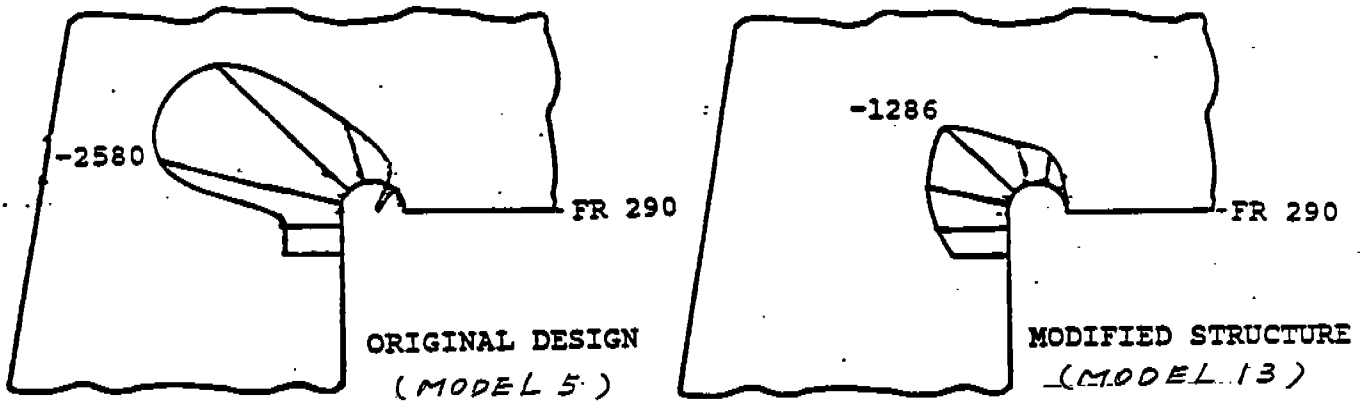

TORSION

Figure 4.2 Hatch Corner Stresses From Finite Element Analysis

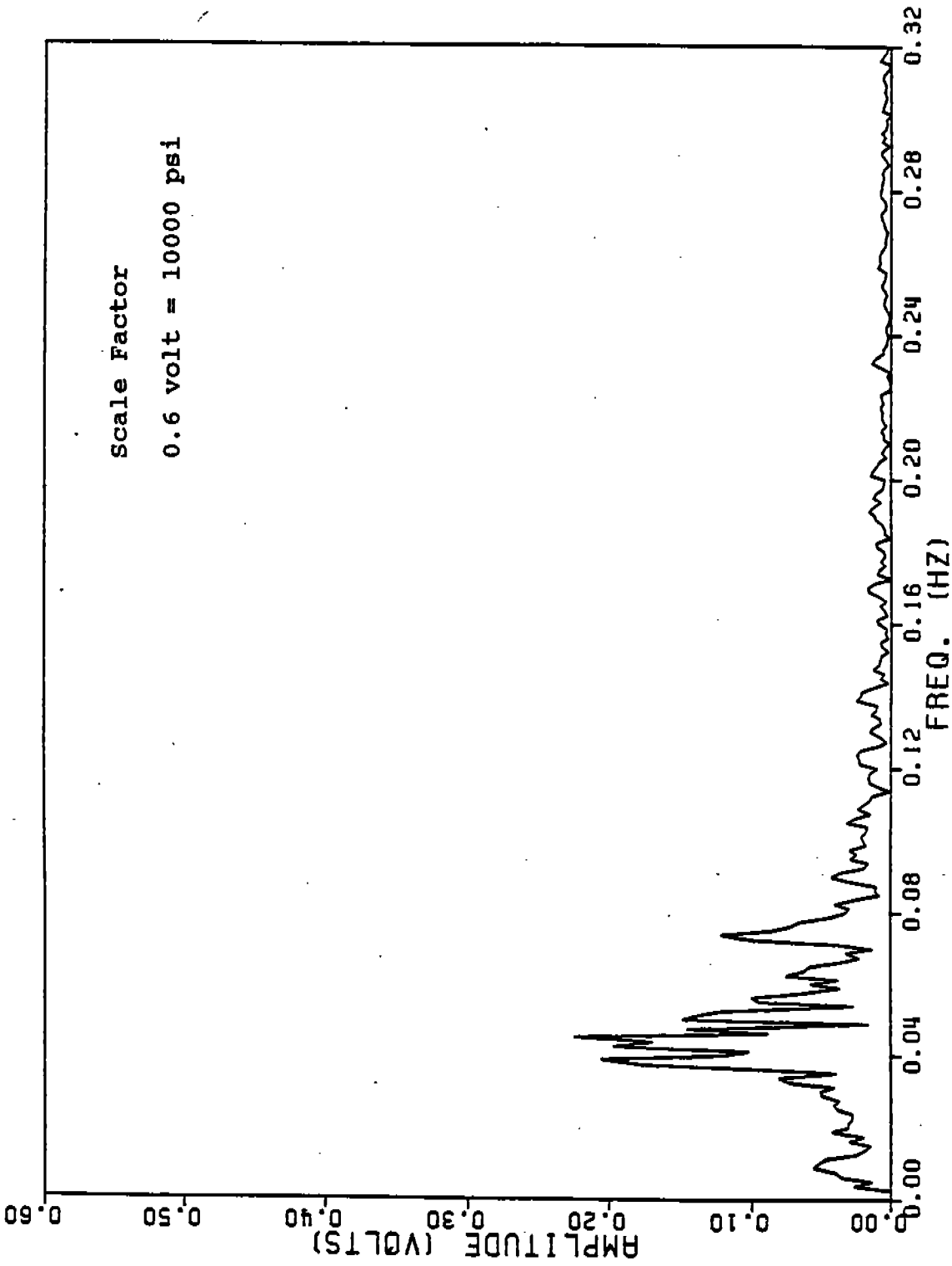

Fig. 5.1 Amplitude Spectrum-FYB-15, file 9

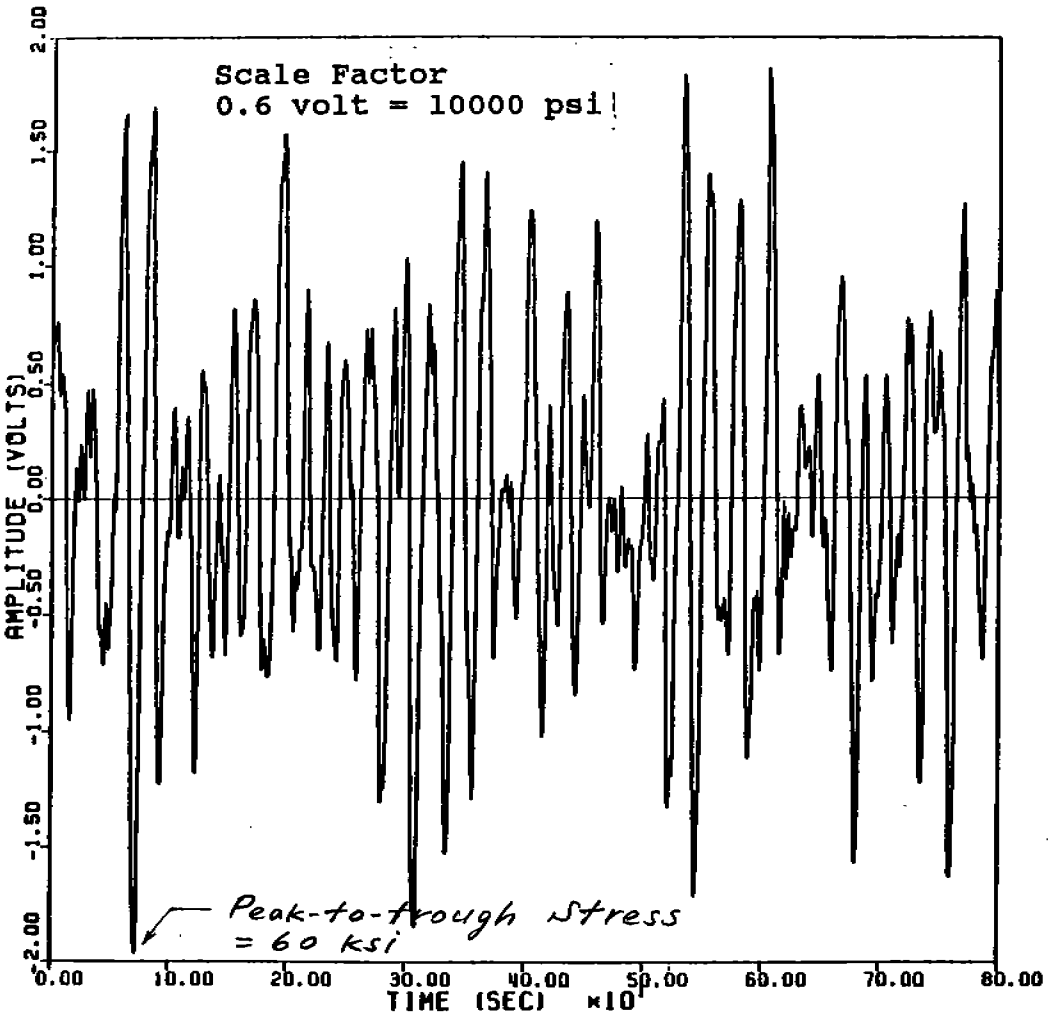

Fig. 5.2 Simulated Time History - FYB-15, File 9

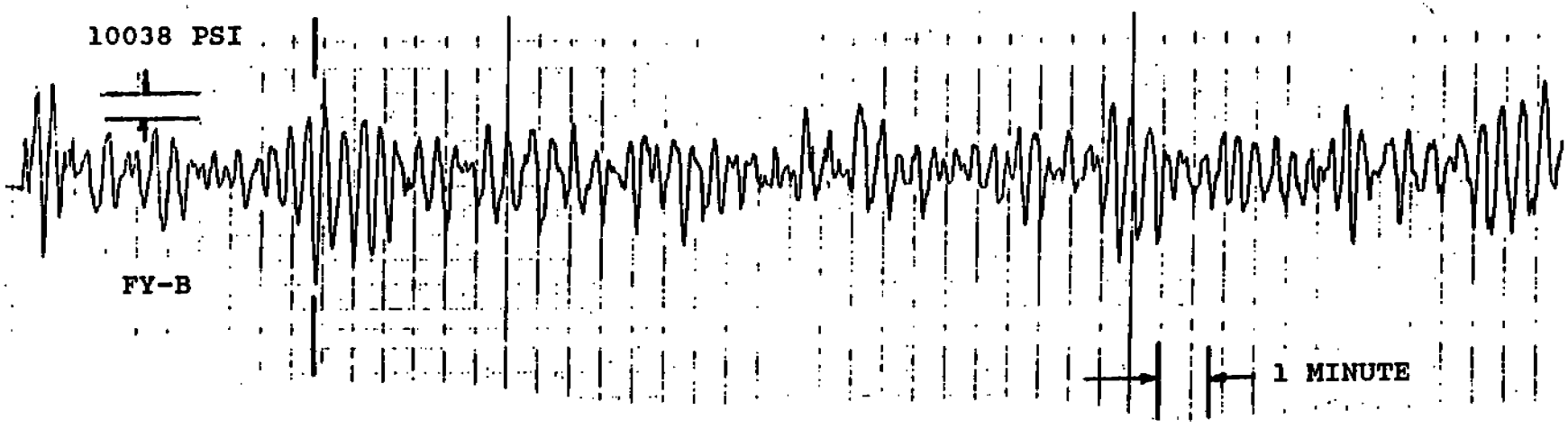

Fig. 5.3 Time History, Voyage 61E Tape 224 Index 12D

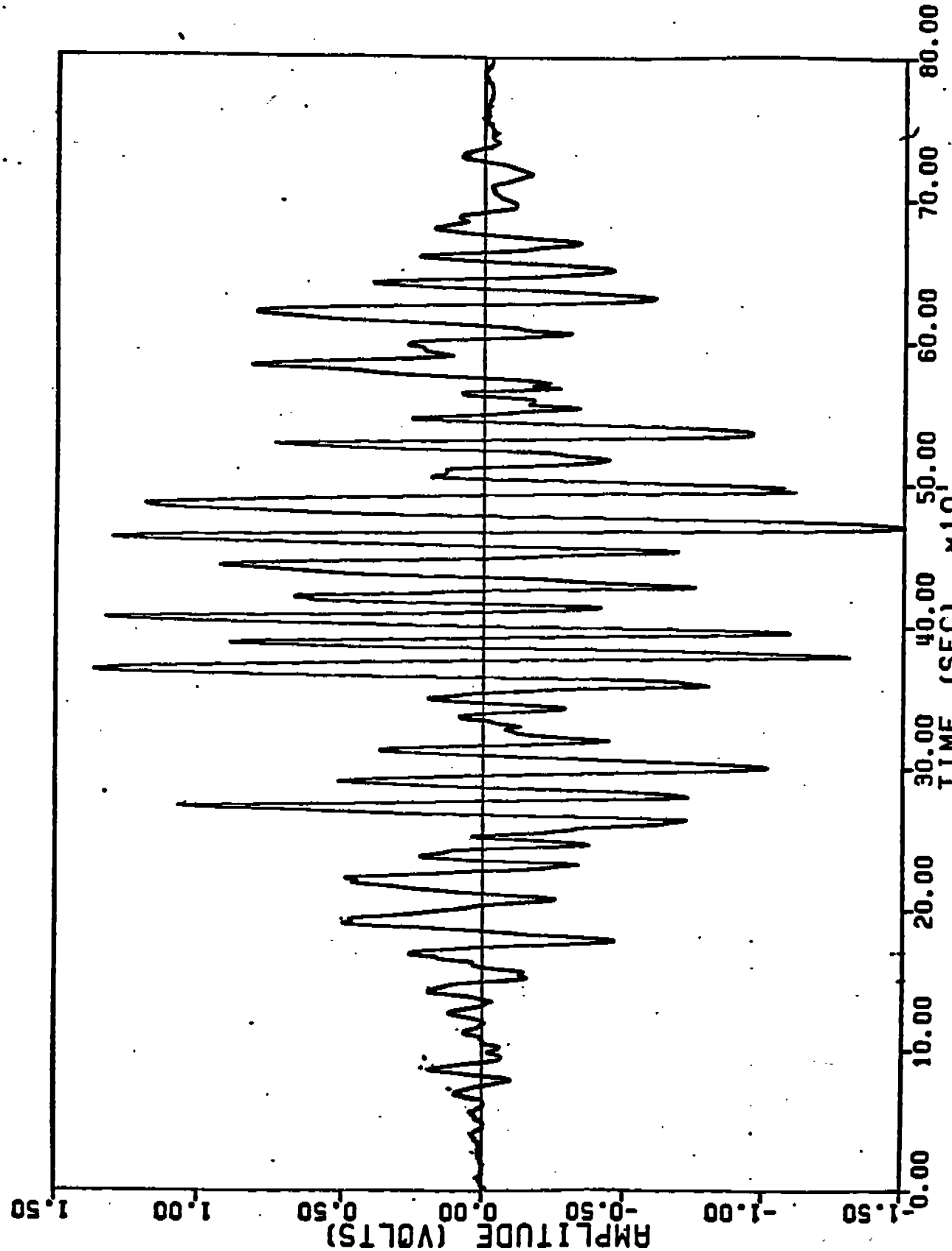

Fig. 5.4 Reconstructed Time History with Beating Phenomenon

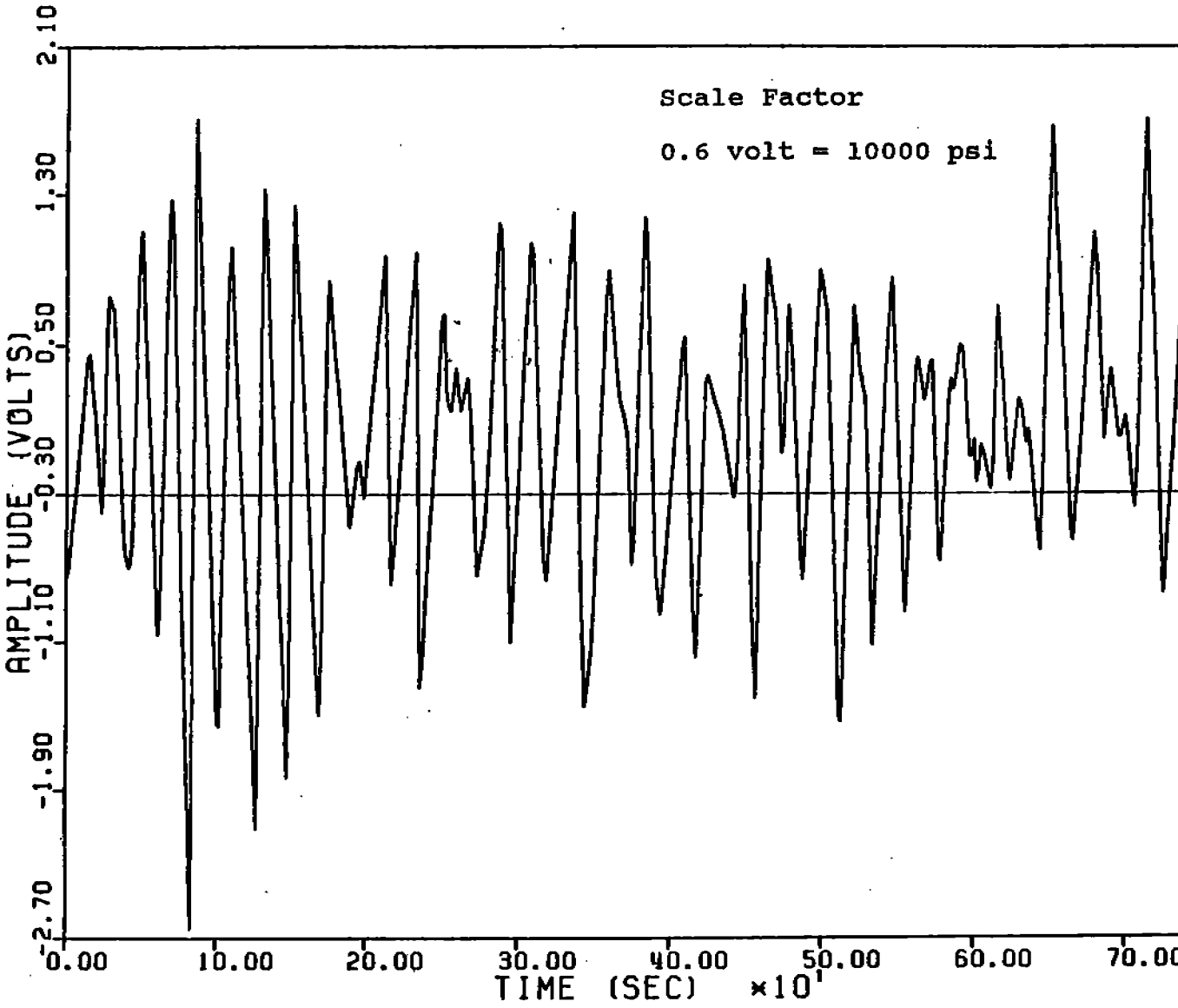

Fig. 5.5 Select Segment of Time History - TAPE 224 Index 12

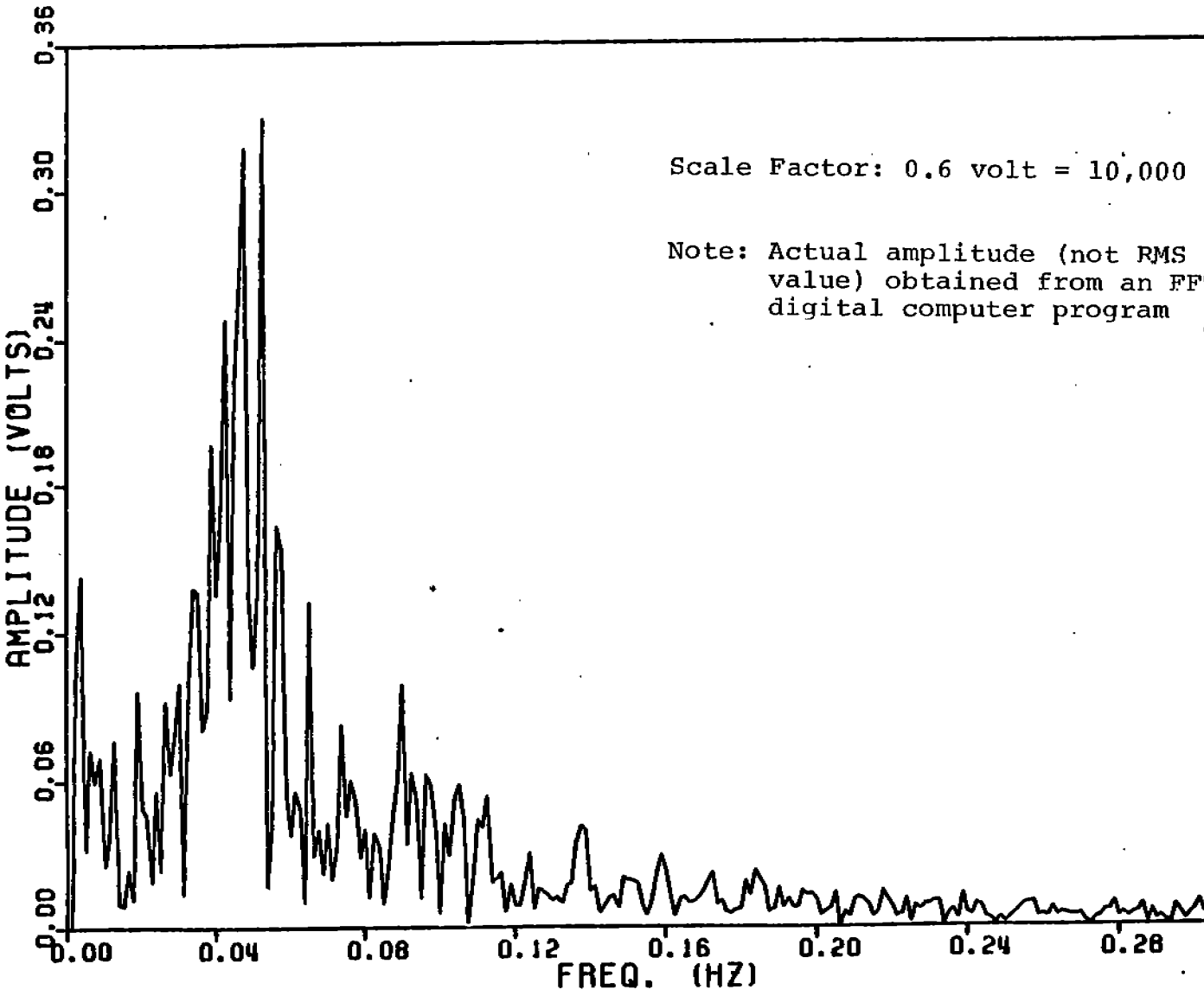

Fig. 5.6 Reconstructed Amplitude Spectrum (for Fig. 5.4 Time

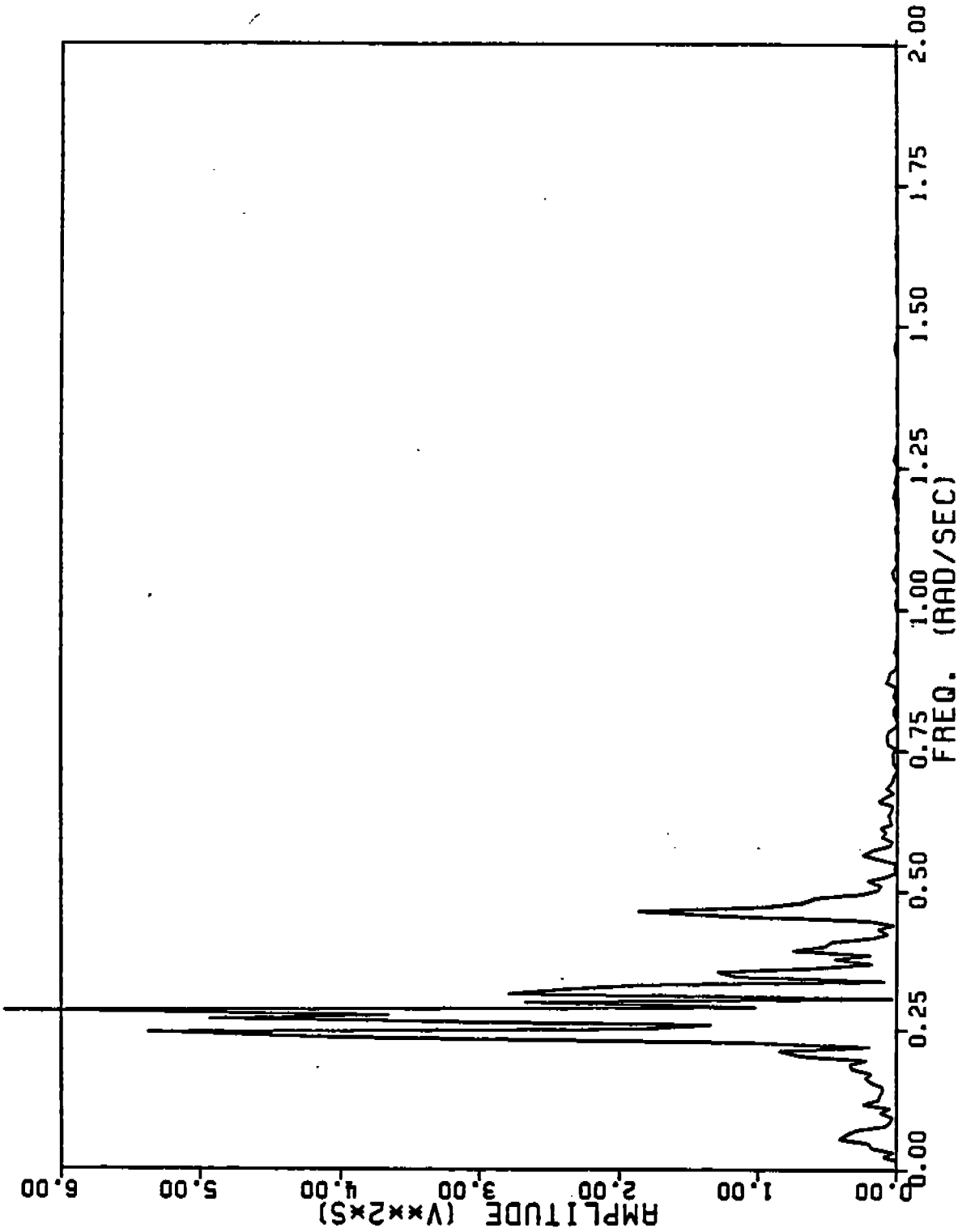

Fig. 6.1 Energy Spectrum Corresponding to the Amplitude Spectrum in Fig.5.1

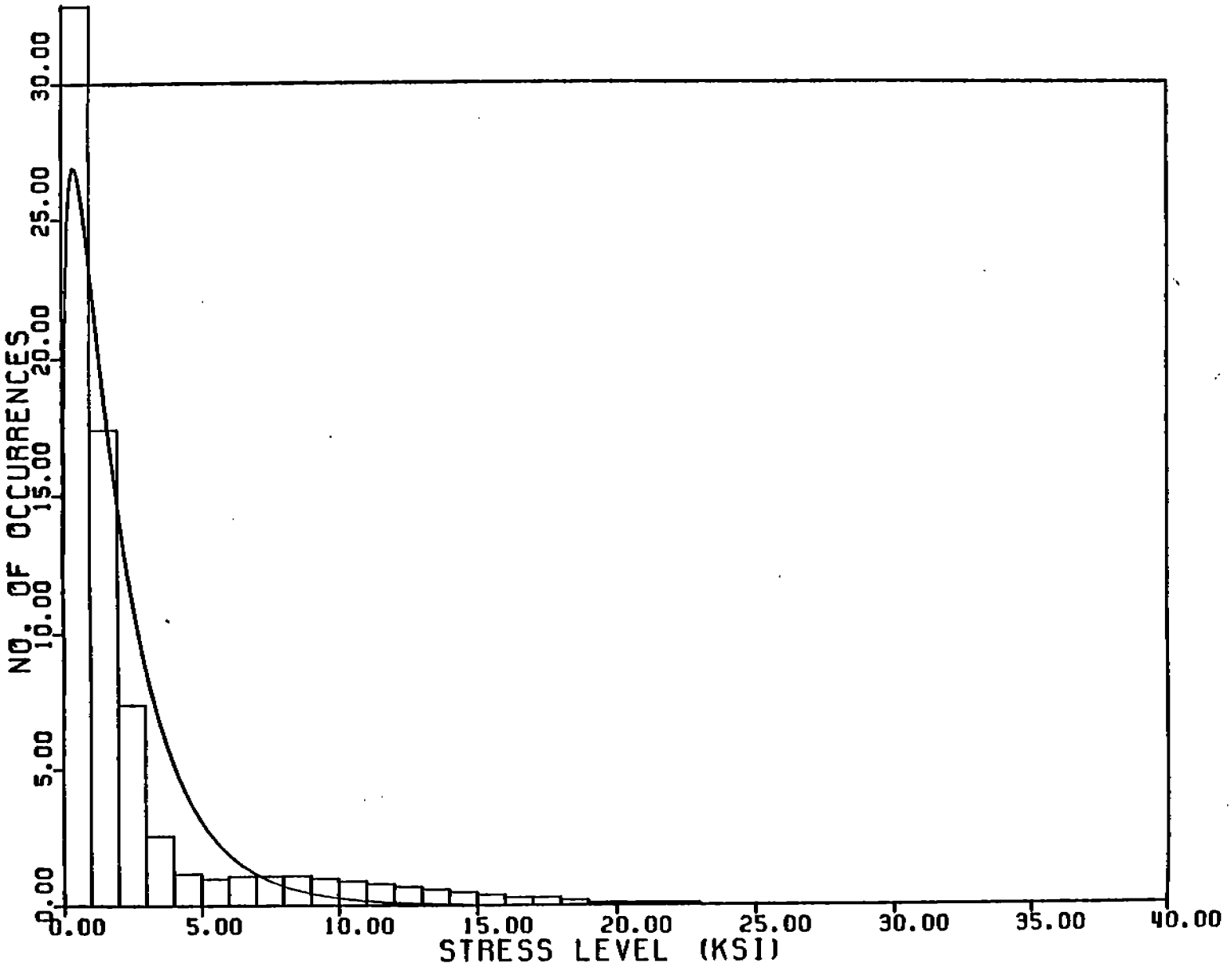

Fig. 6.2(a) Generalized Gamma Distribution, Curve Fitting
Cyclic Stress Histogram - Beaufort No. 1, Gage F_{yb}

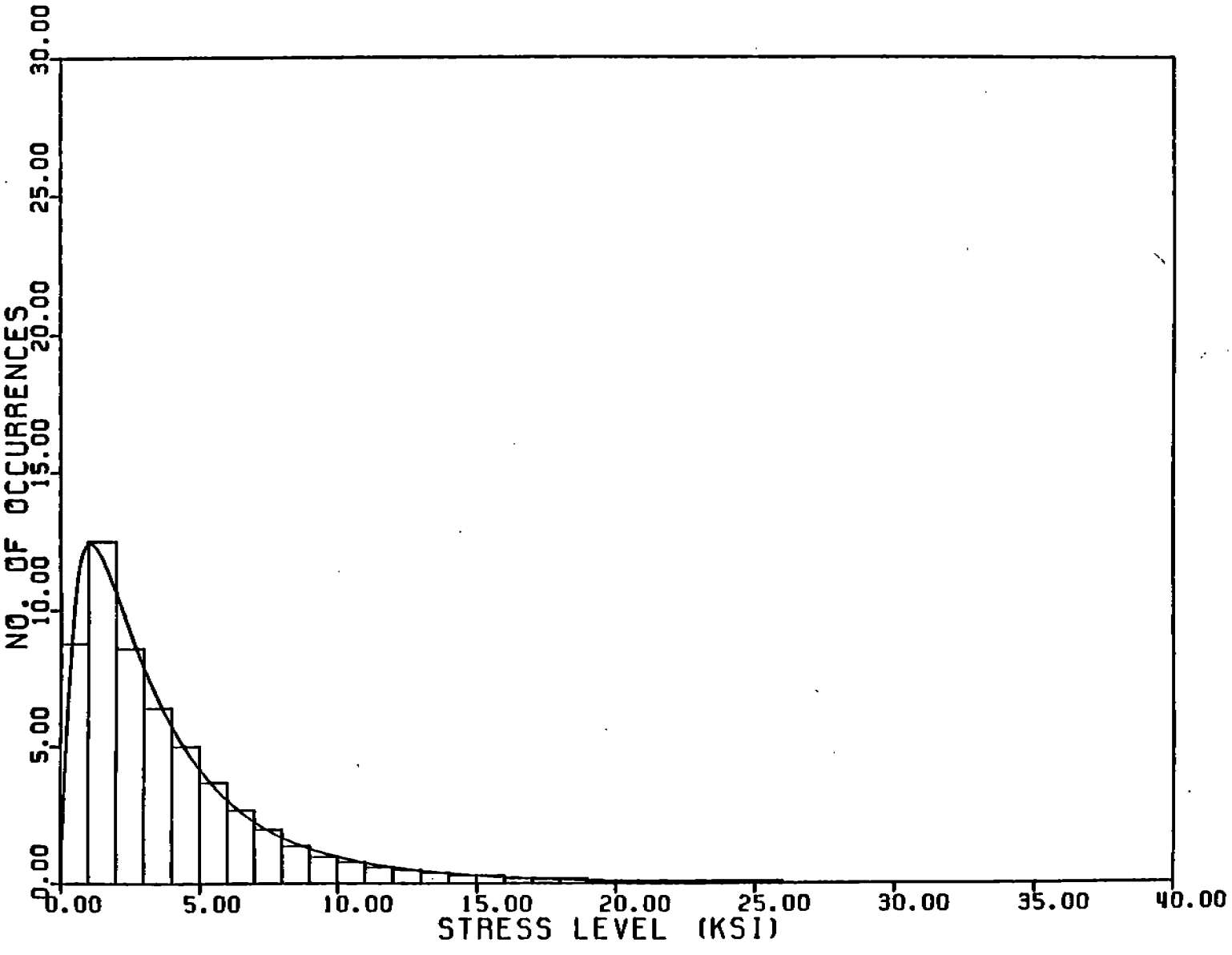

Fig. 6.2(b) Generalized Gamma Distribution, Curve Fitting
Cyclic Stress Histogram - Beaufort No. 4, Gage F_{yb}

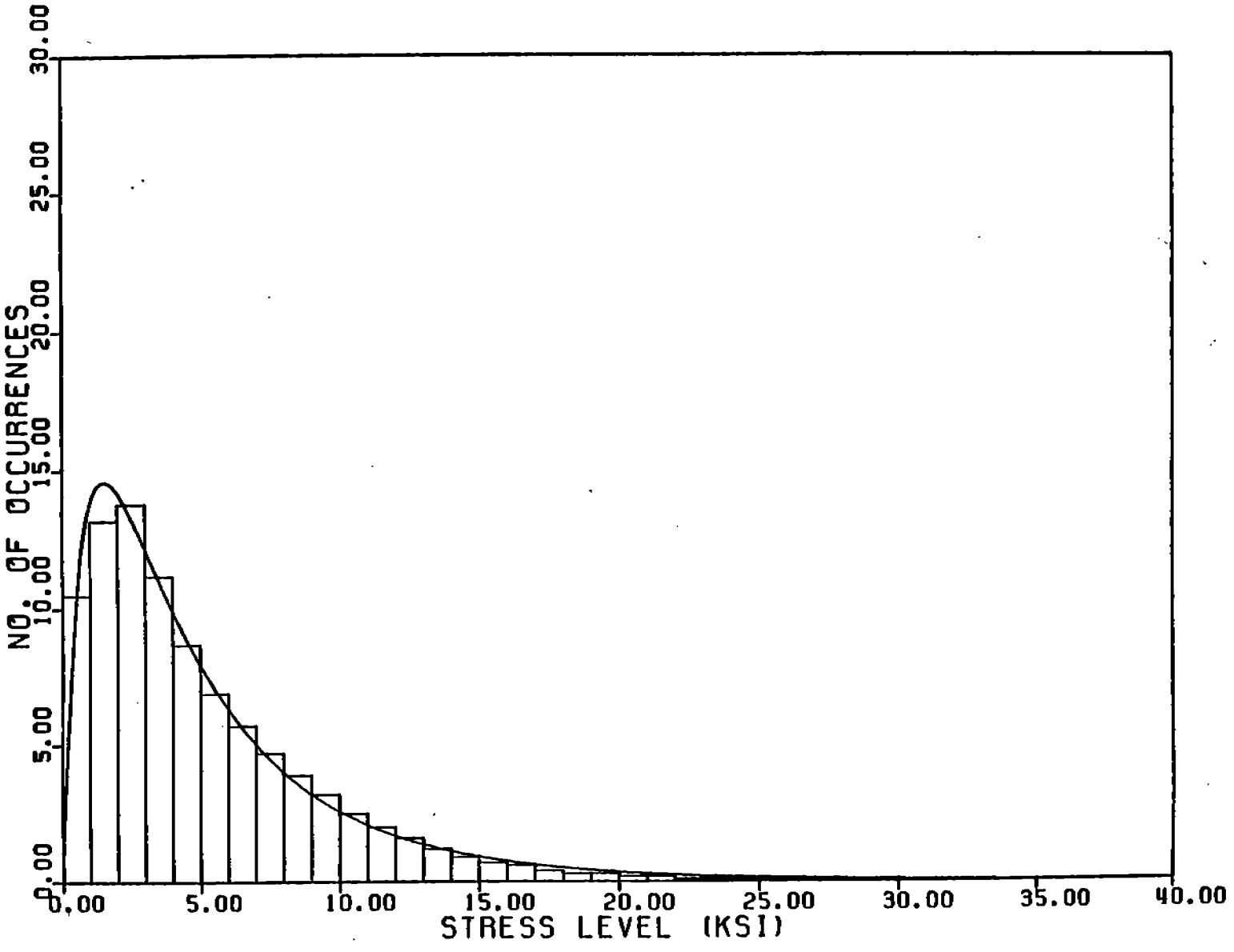

Fig. 6.2(c) Generalized Gamma Distribution, Curve Fitting
Cyclic Stress Histogram - Beaufort No. 7, Gage F_{yb}

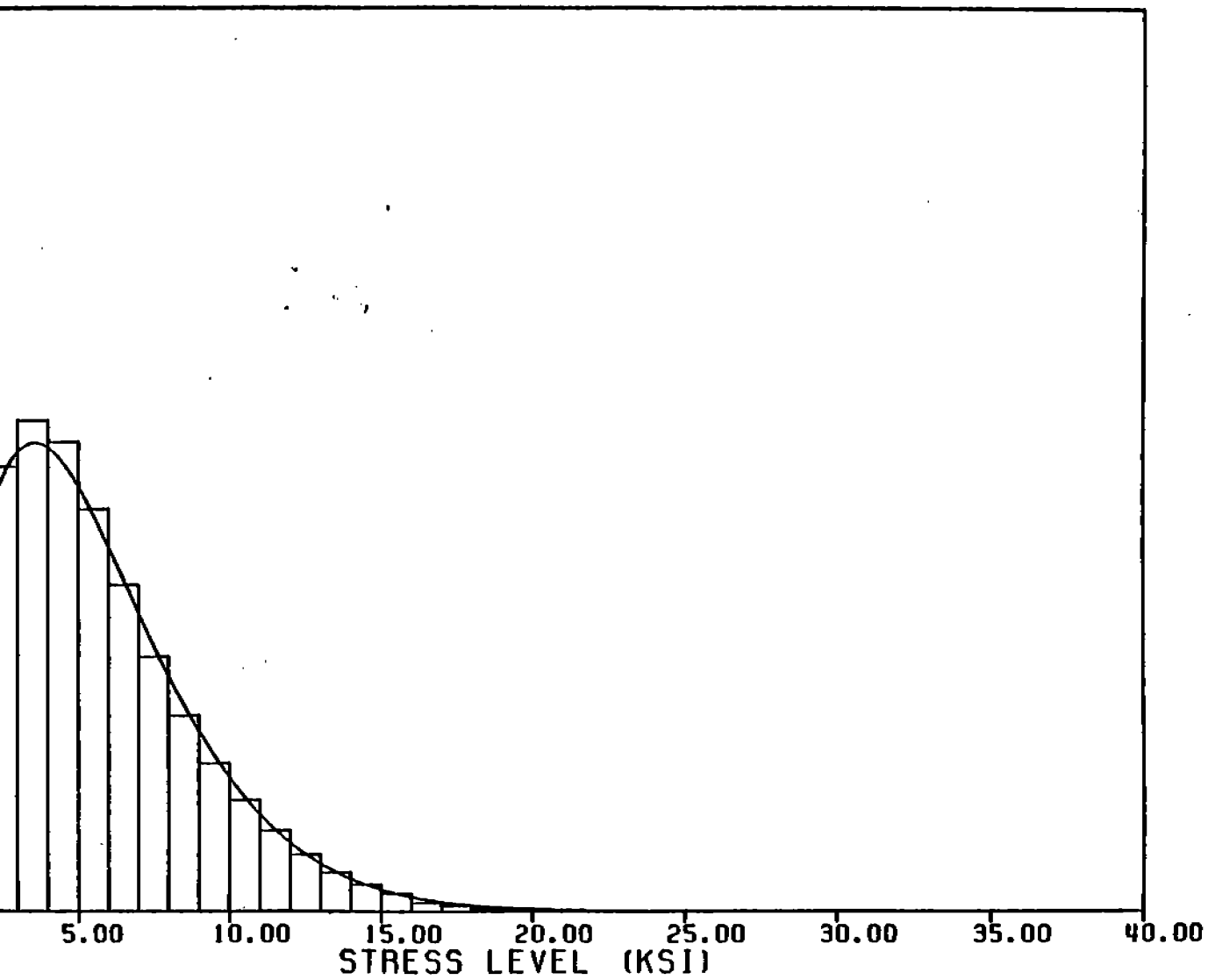

g. 6.2(d) Generalized Gamma Distribution, Curve Fitting
Cyclic Stress Histogram - Beaufort No. 9, Gage Fyb

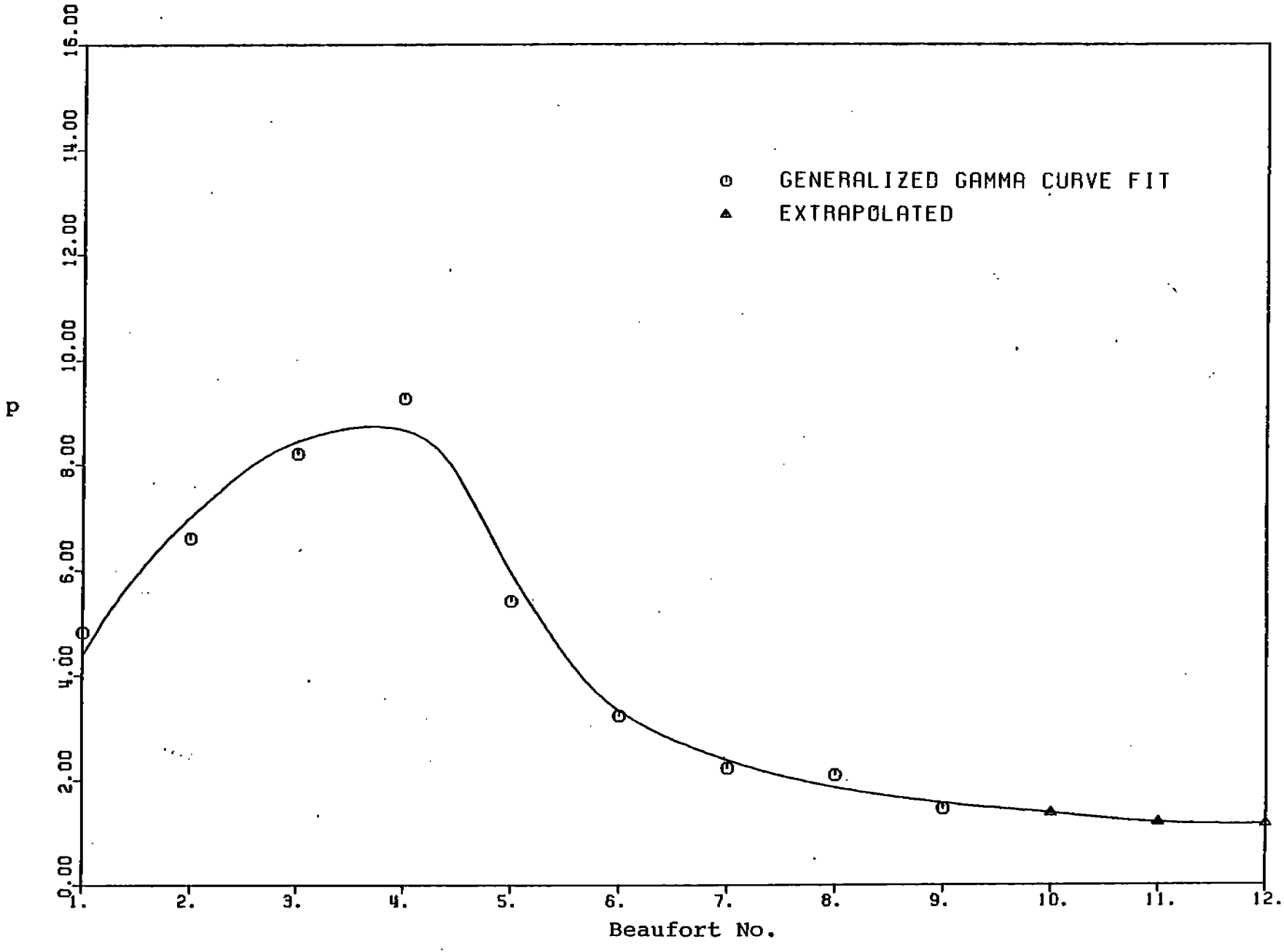

Fig. 6.3(a) Generalized Gamma Parameter p vs. Seastate, Gage F_yB, 1975

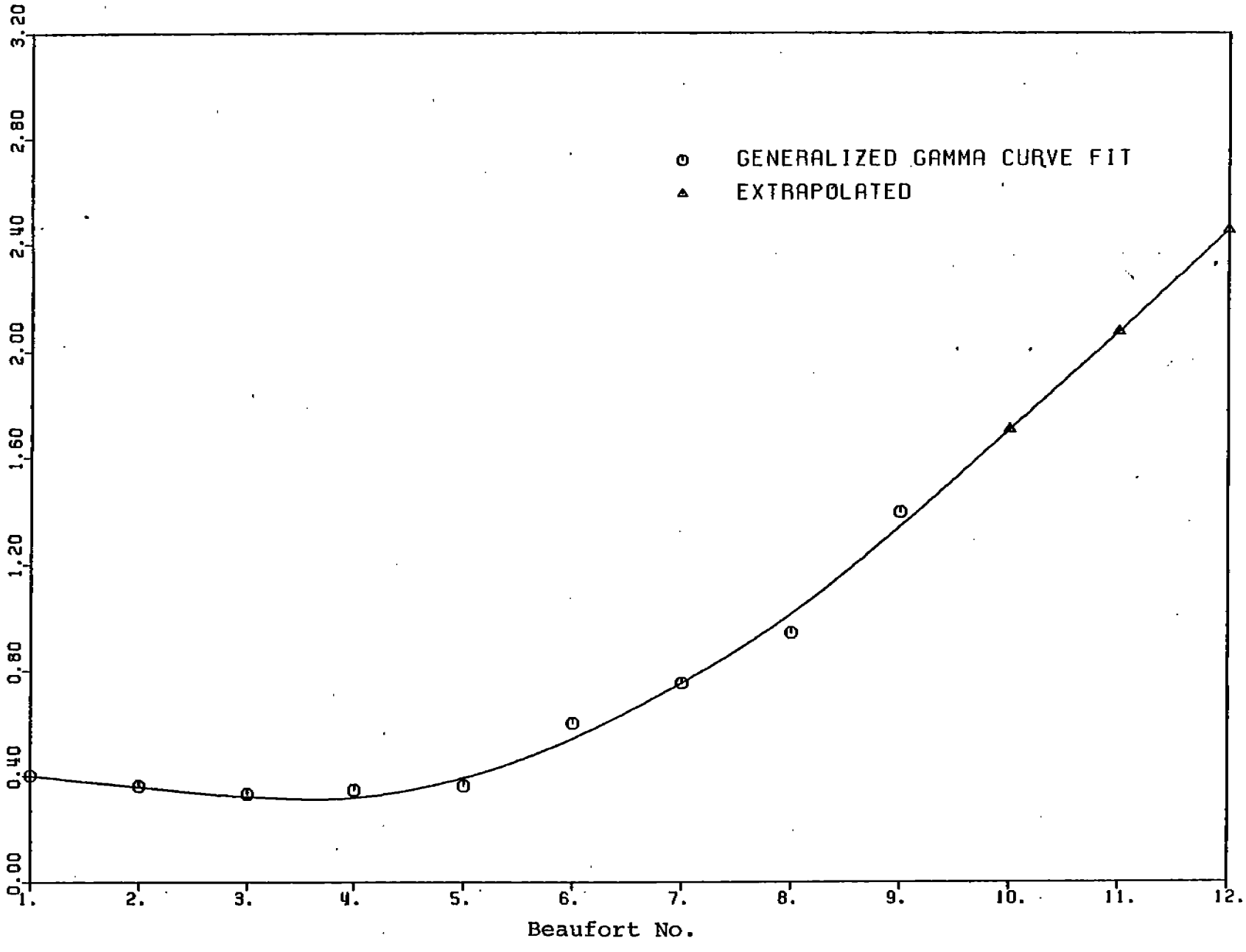

Fig. 6.3(b) Generalized Gamma Parameter q vs. Seastate, Gage $F_y B$, 1975

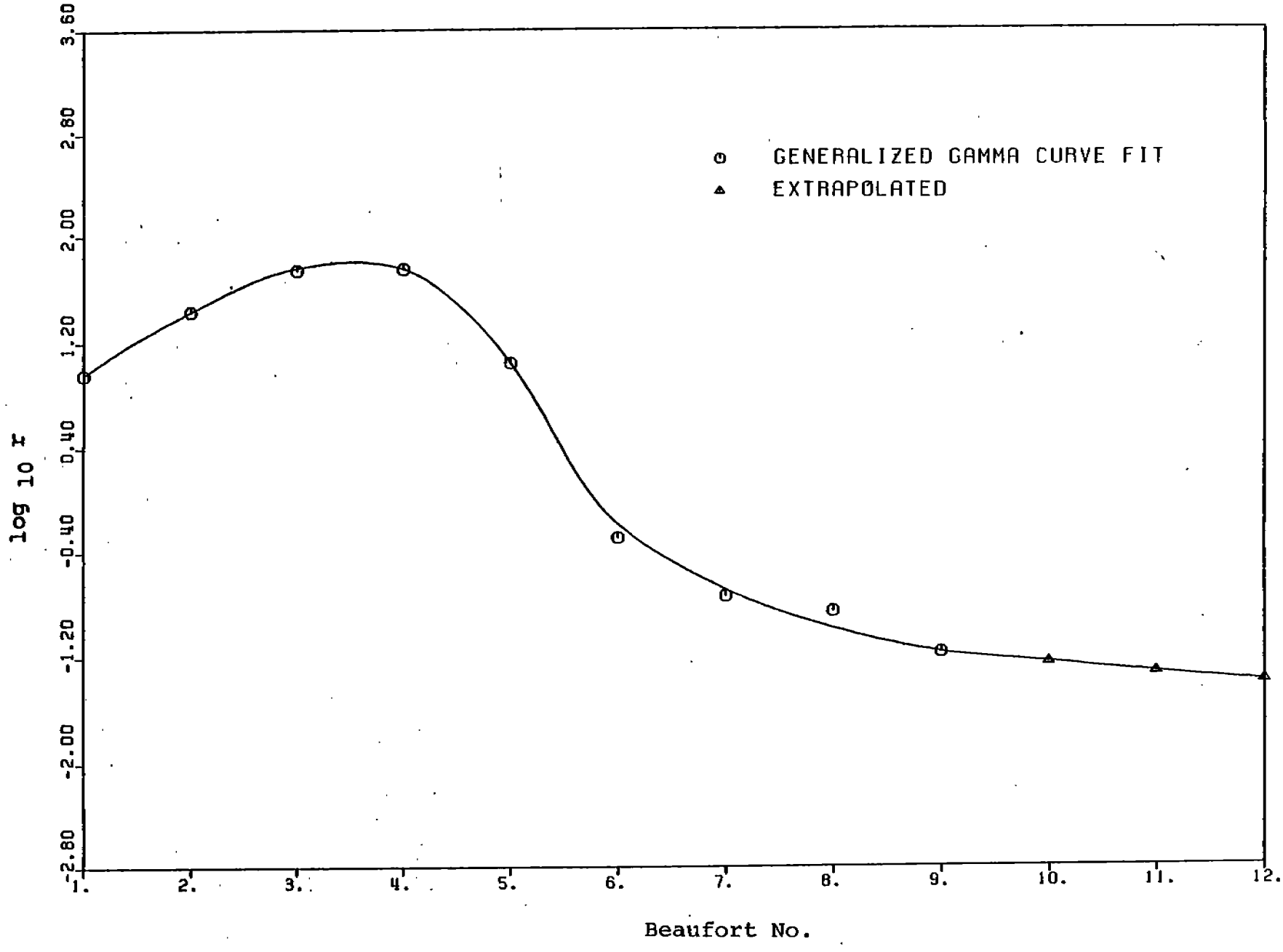

Fig. 6.3(c) Generalized Gamma Parameter r vs. Seastate, Gage F_yB, 1975

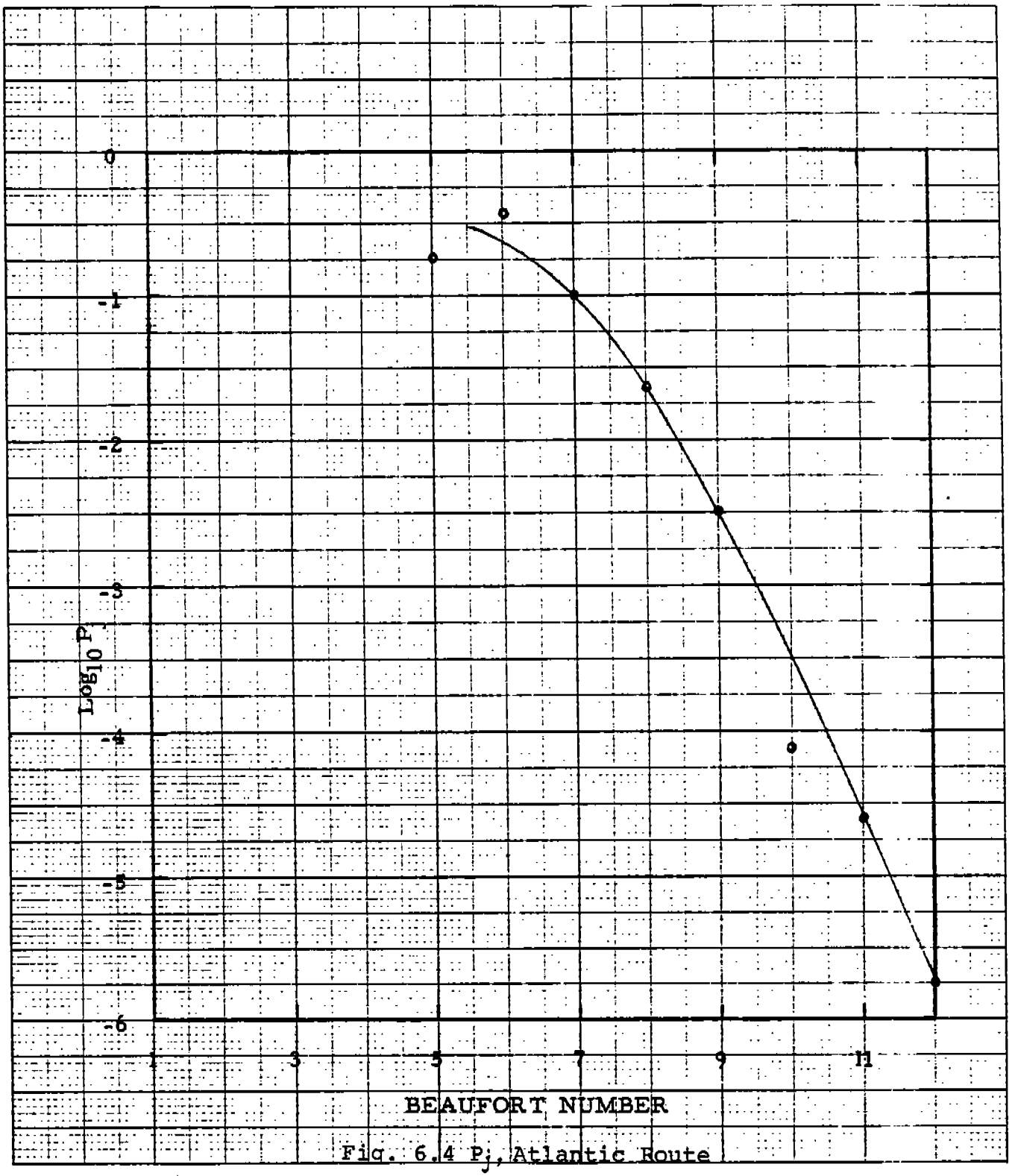

Fig. 6.4 P_j, Atlantic Route

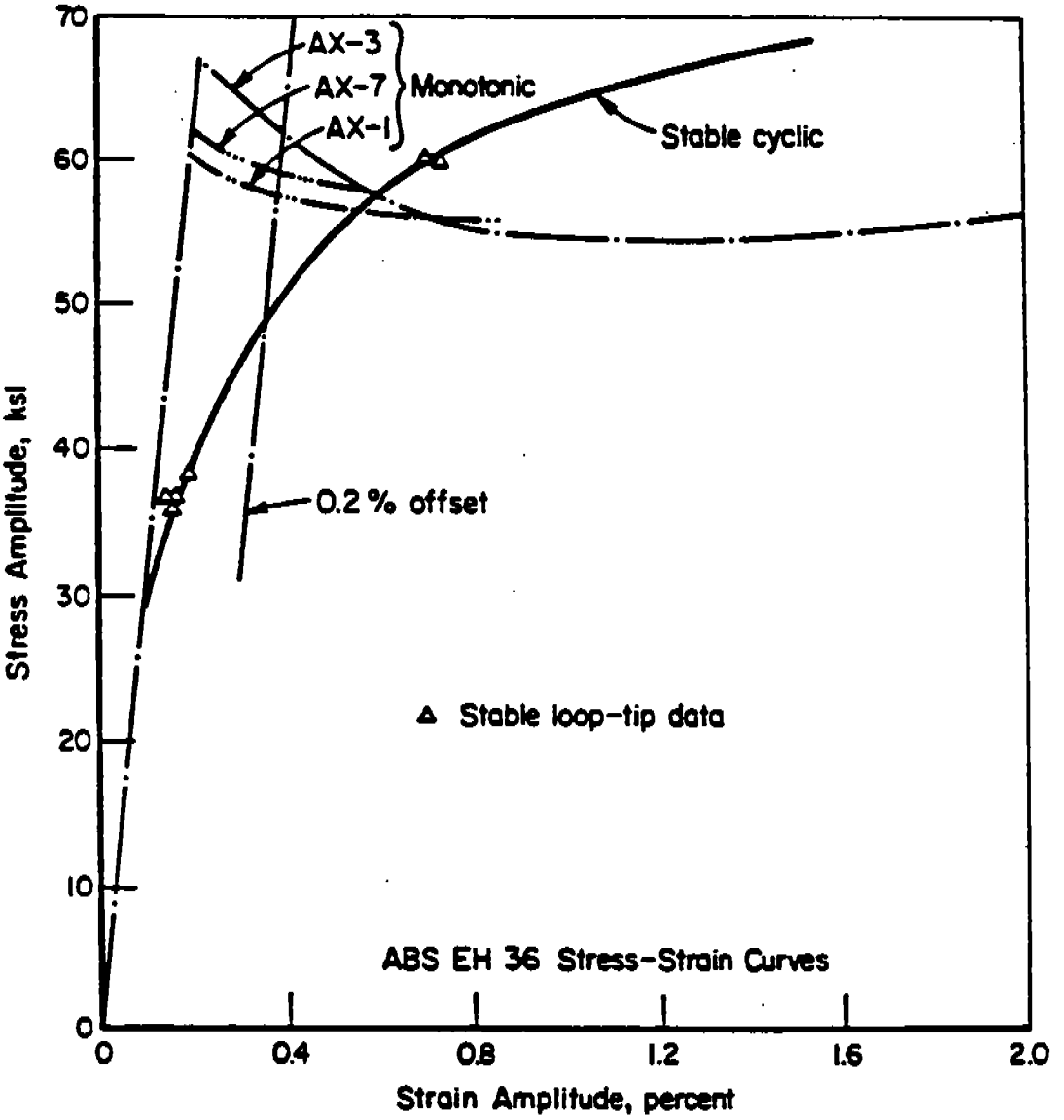

FIGURE 6.5 Cyclic Stress-Strain Relationship

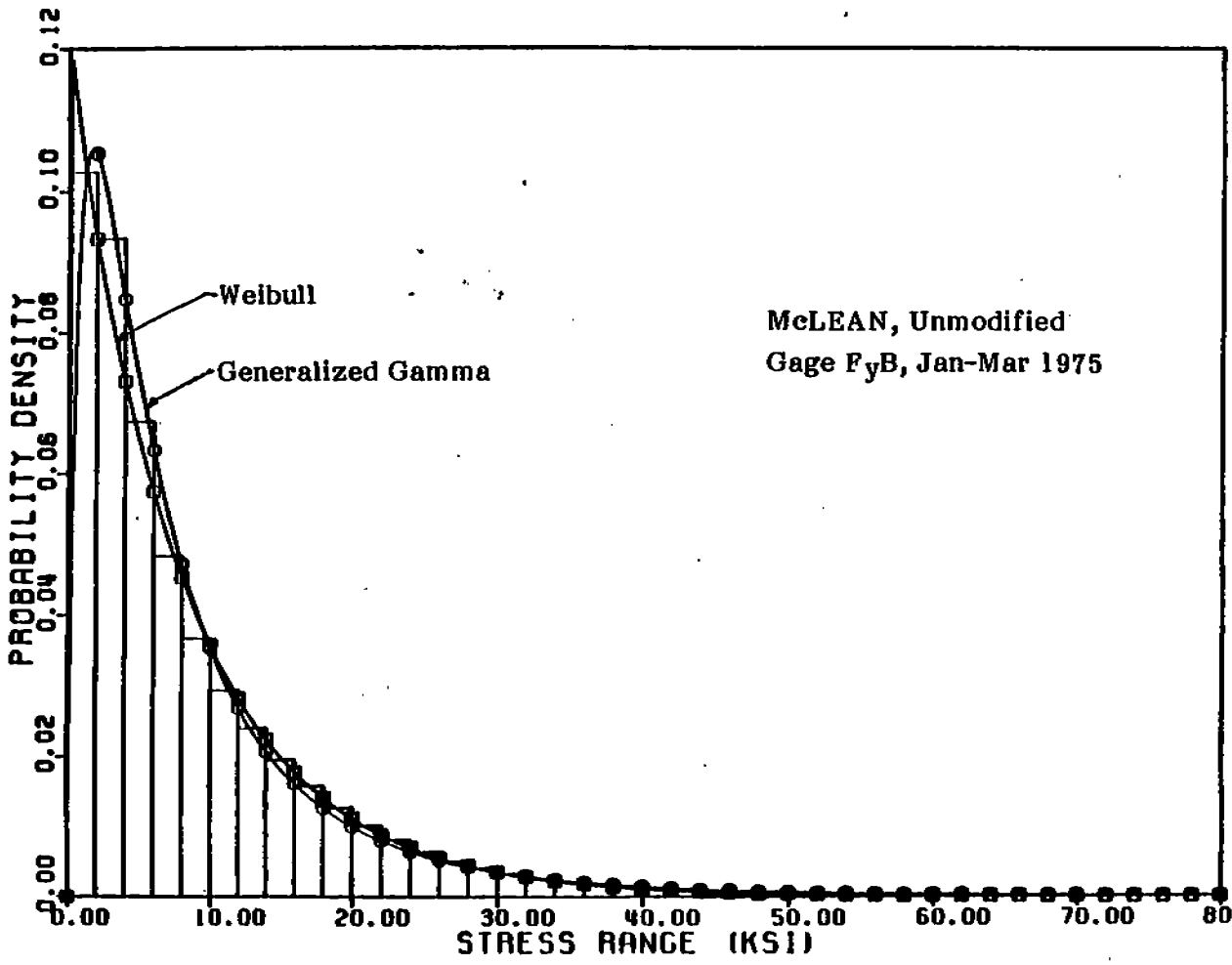

Fig. 6.6 Curve Fitting of Long-Term Stress Histogram, Gage F_{yb} o

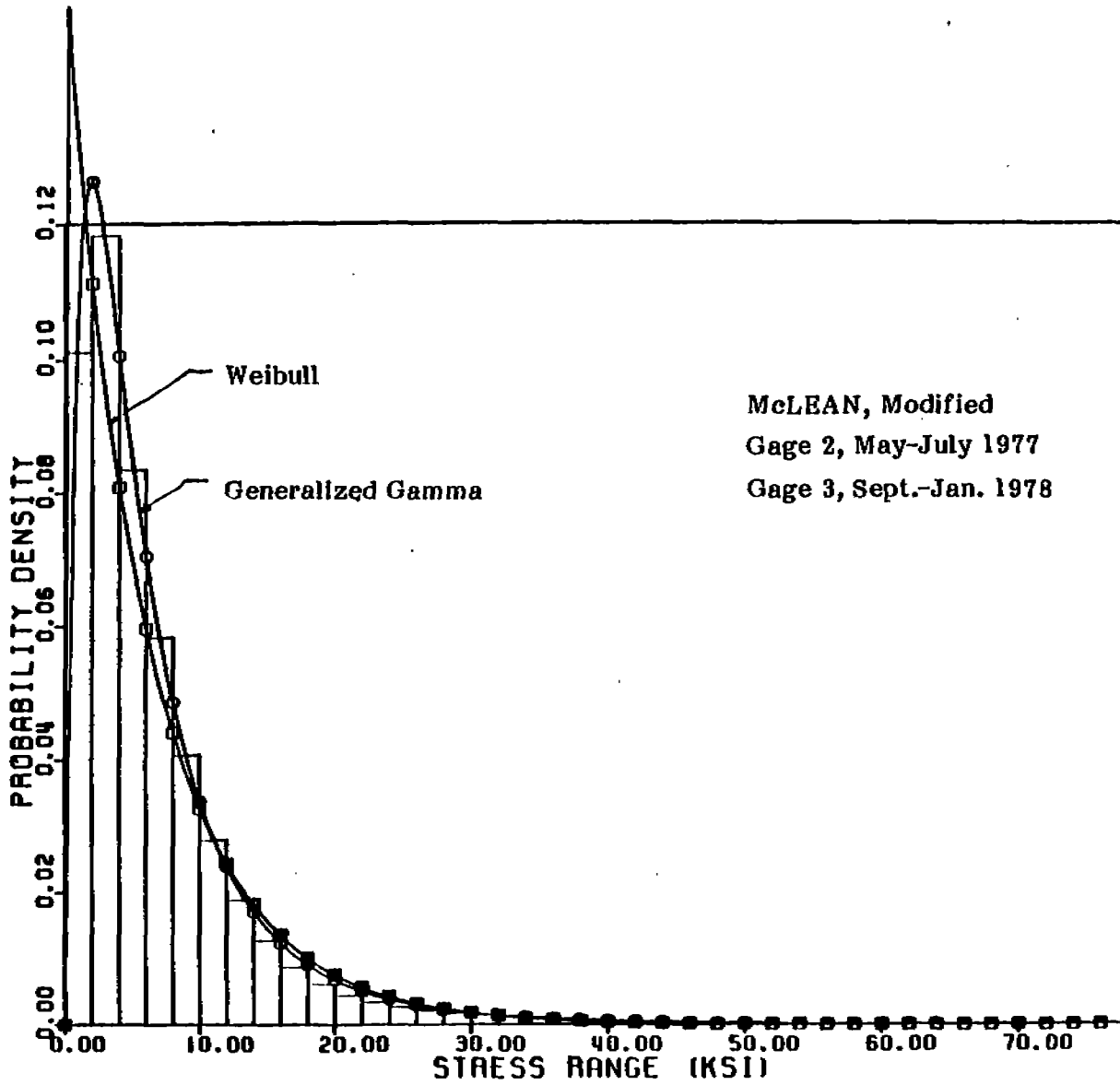

Fig. 6.7 Curve Fitting of Long-Term Stress Histogram,
Gage 2 in May-July 1977 & Gage 3 in Sep-Jan 1978 on McL

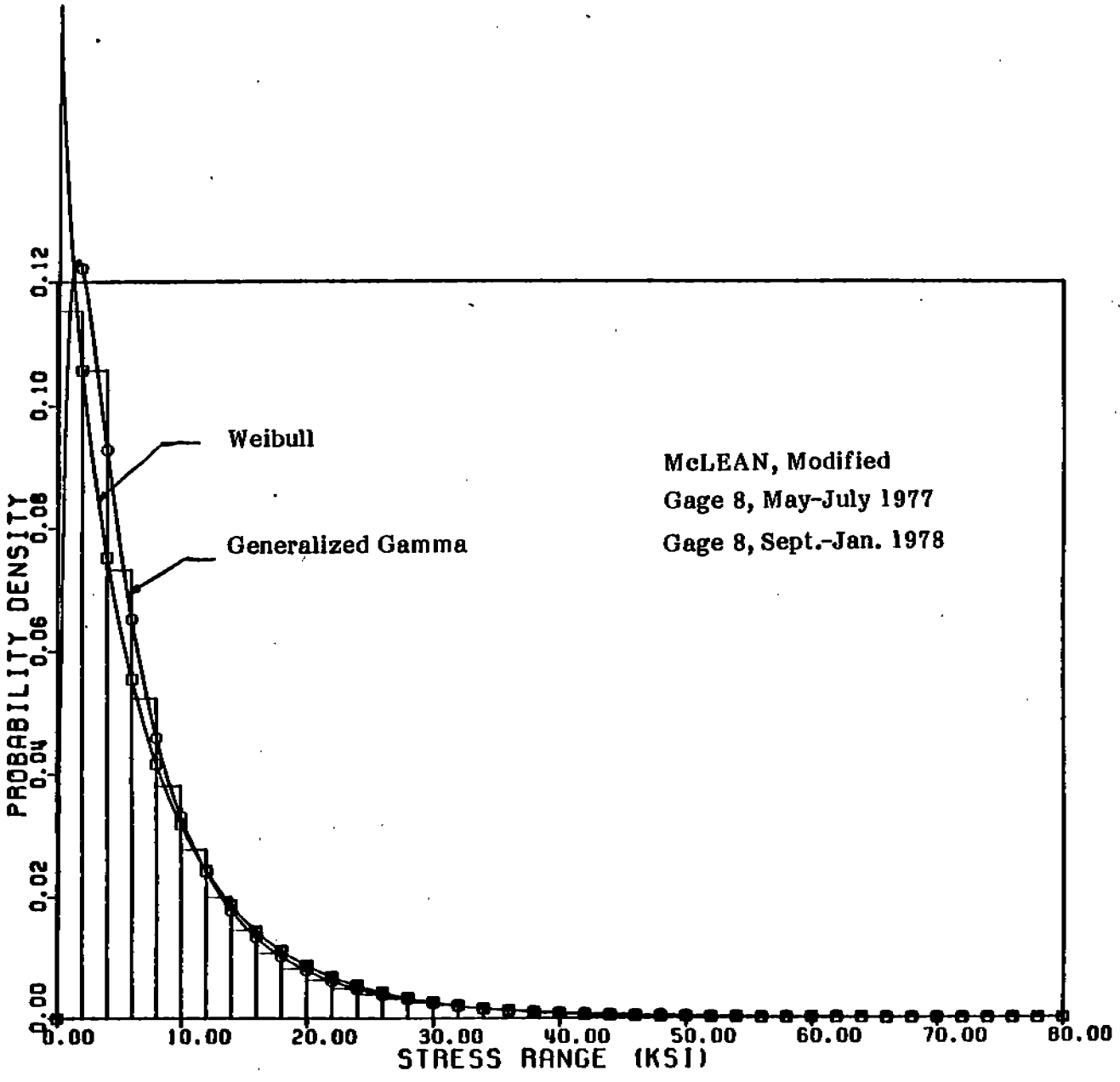

Fig. 6.8 Curve Fitting of Long-Term Stress Histogram, Gage 8 on McLean During Two Seasonal Operations between May 1977 & Jan 1978

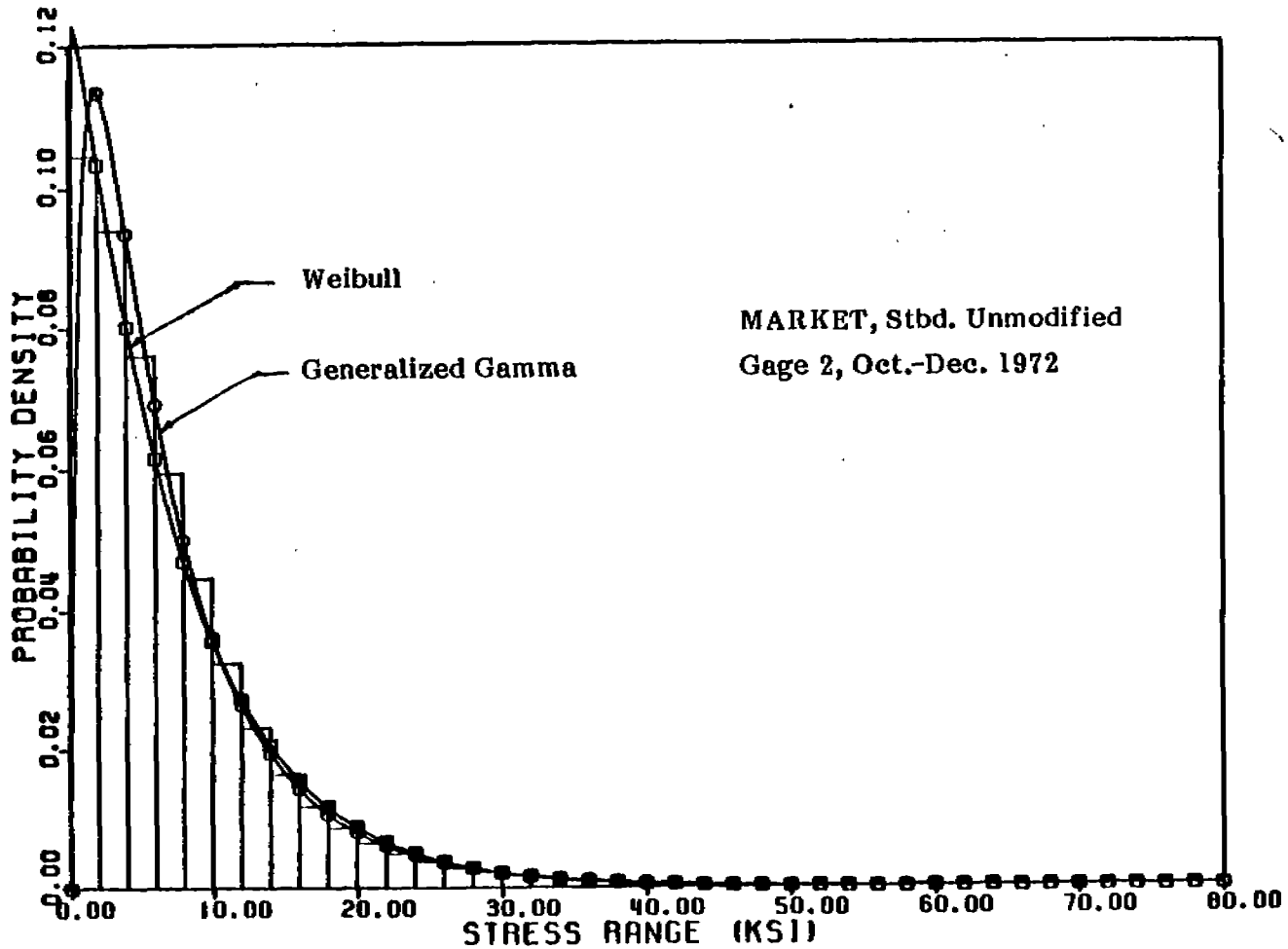

Fig. 6.9 Curve Fitting of Long-Term Stress Histogram, Gage 2 on Market, 1976

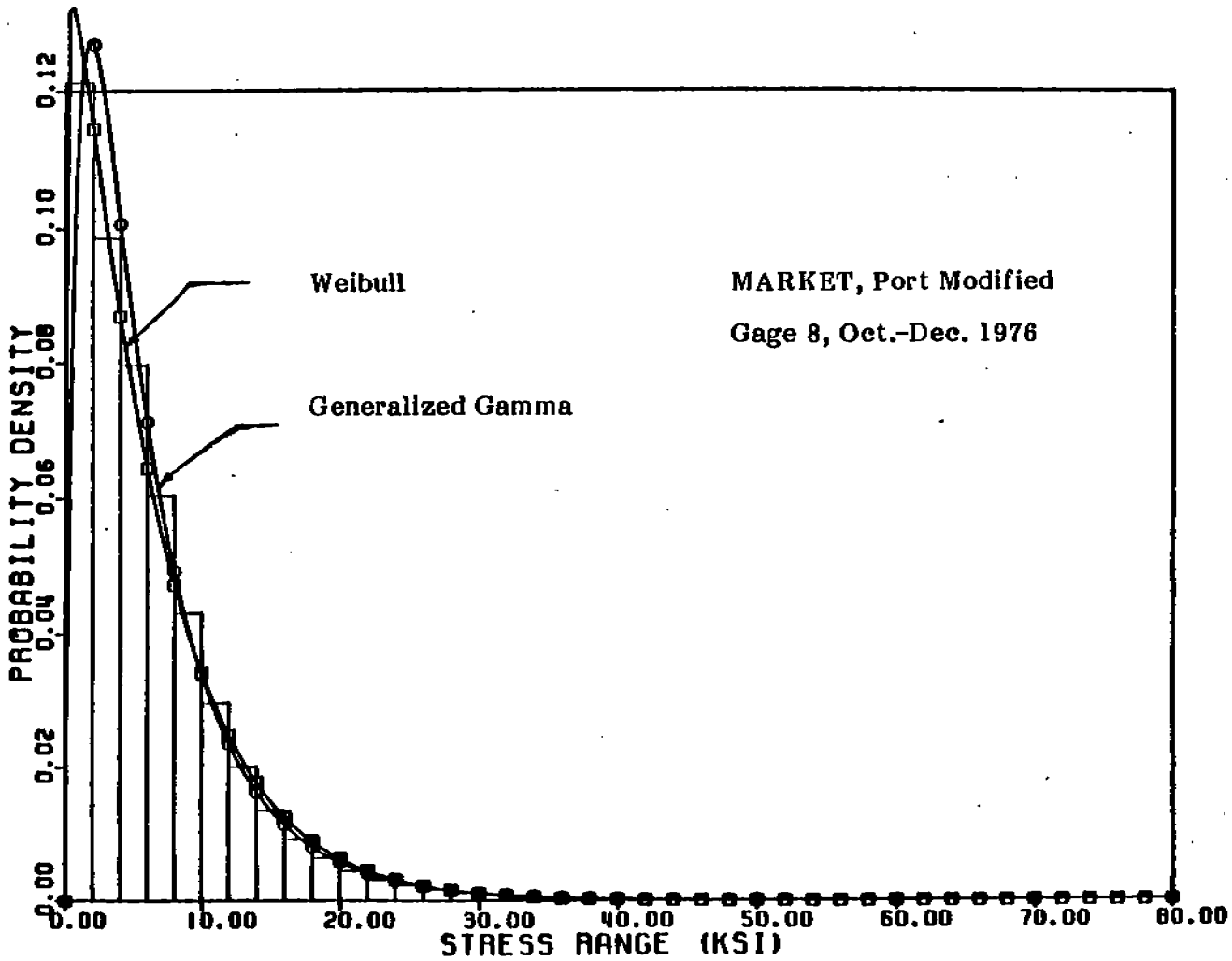

Fig. 6.10 Curve Fitting of Long-Term Stress Histogram, Gage 8 on Market, 1976

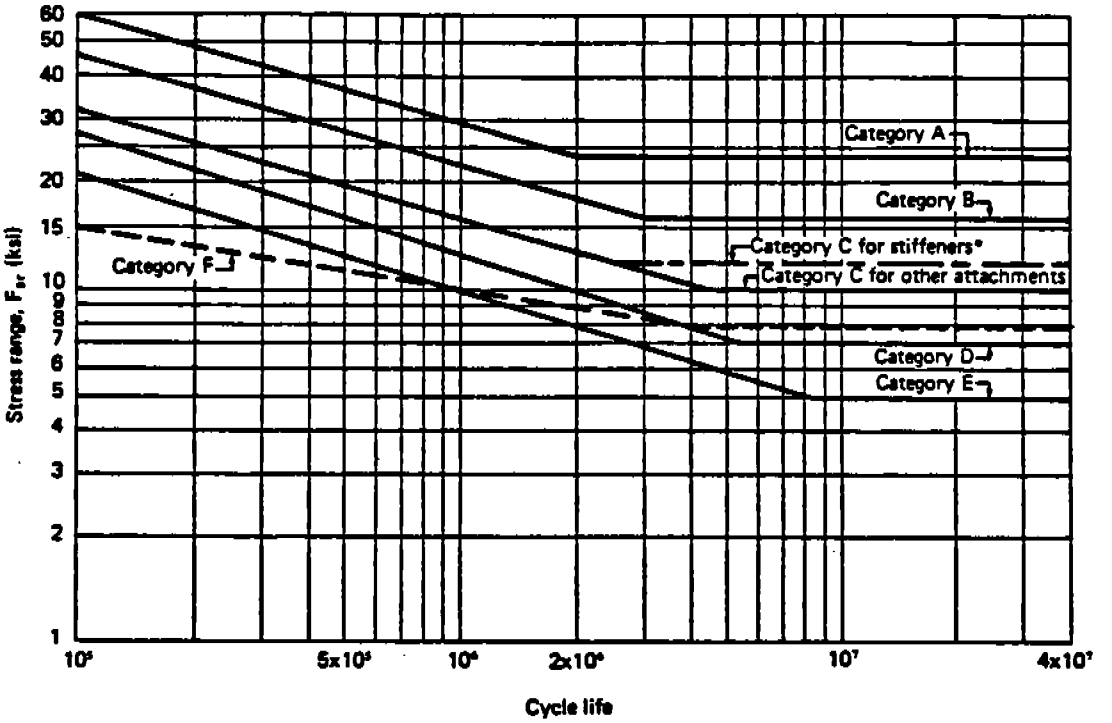

*Transverse stiffener welds on girder webs or flanges

Fig. 7.1(a) Design stress range curves for categories A to F—redundant structures

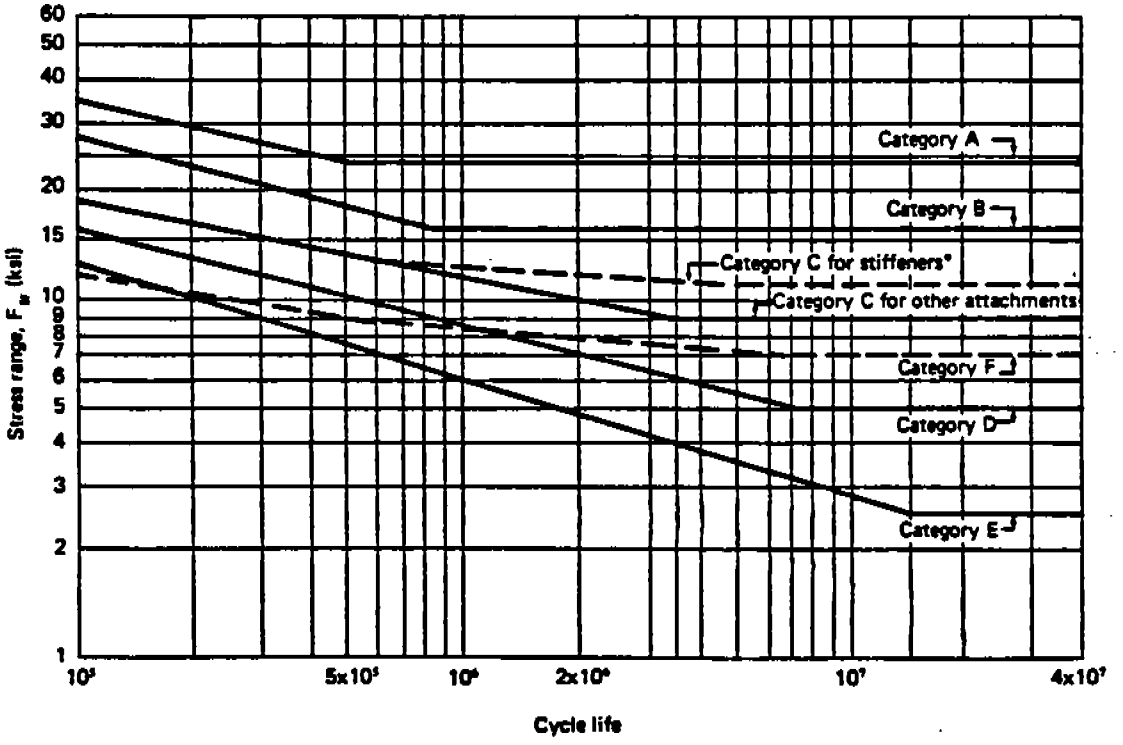

*Transverse stiffener welds on girder webs or flanges

Figure 7.1(b) Design Stress Range Curves for Categories A to F - Nonredundant Structures

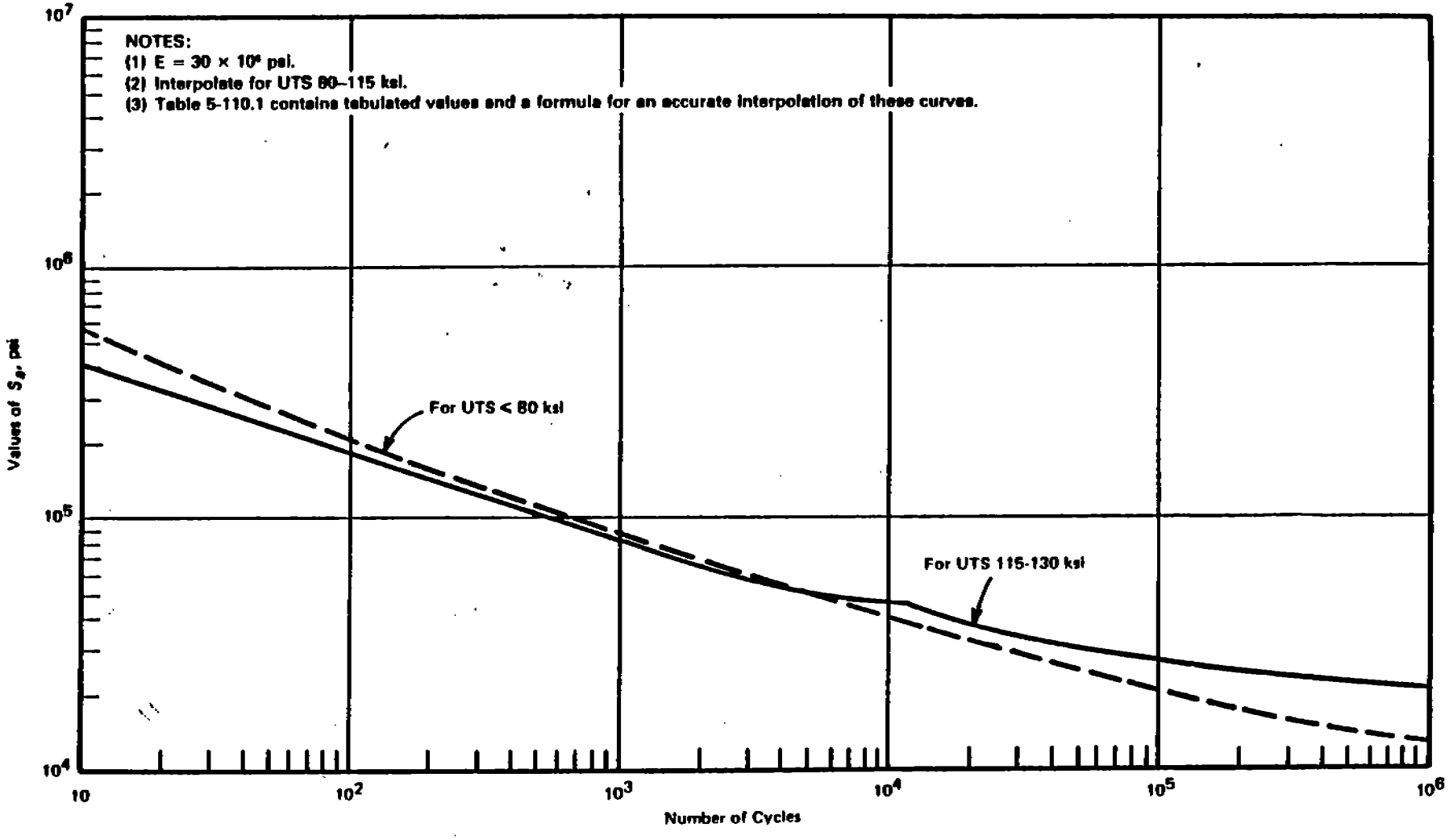

Fig. 7.2 Design Fatigue Curves for Carbon, Low-Alloy, series 4XX, High-Alloy Steels and High Tensile Steels for Temperatures not exceeding 700°F

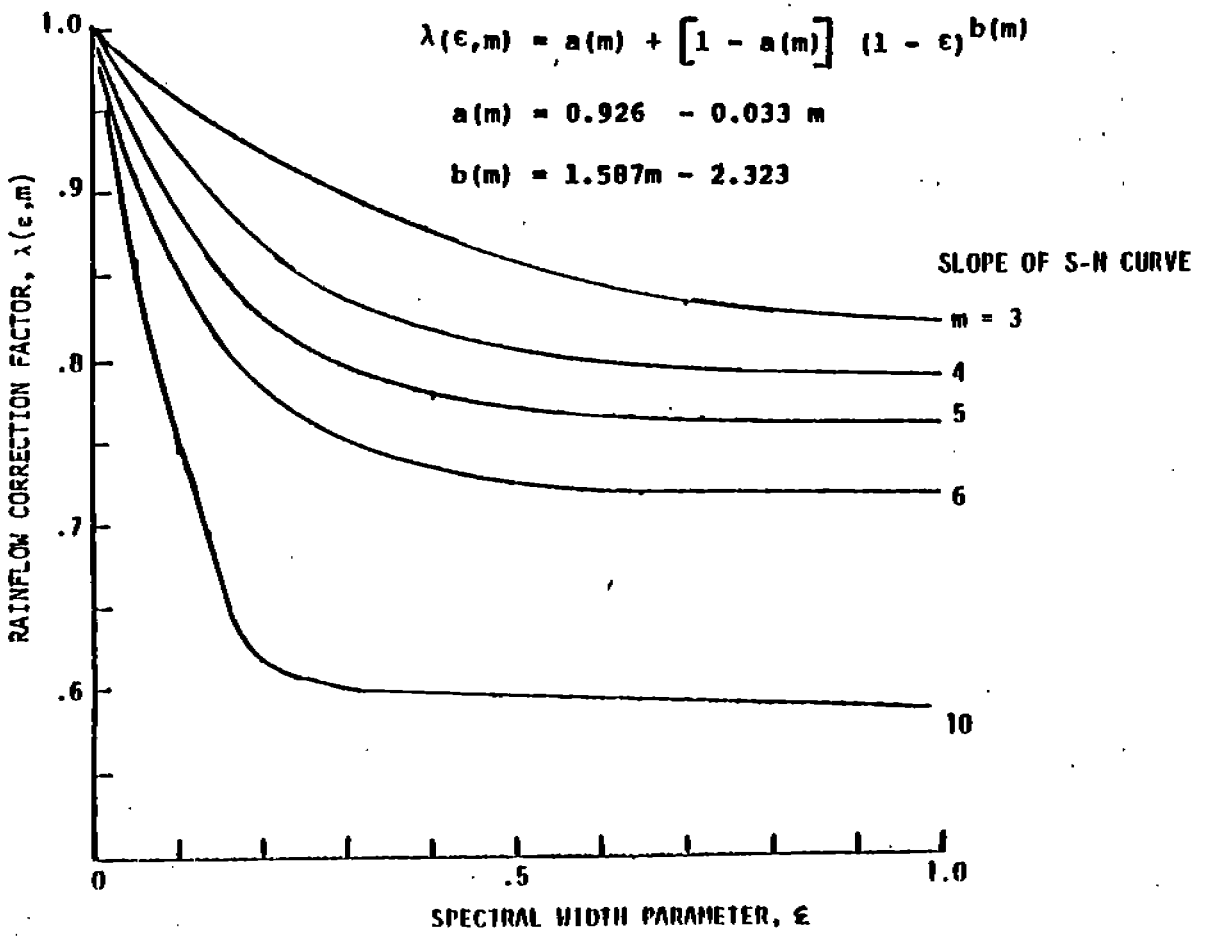

Figure 7.3 The Rainflow Correction Factor as a function of m and ε

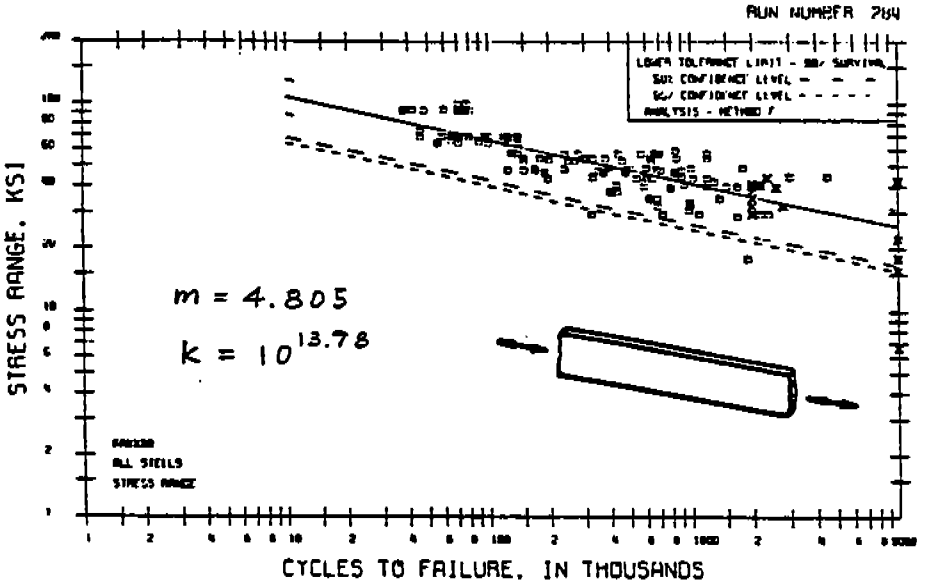

Detail No. 1(F)

Figure 7.4 S-N Curve for Structural Detail No. 1(F)

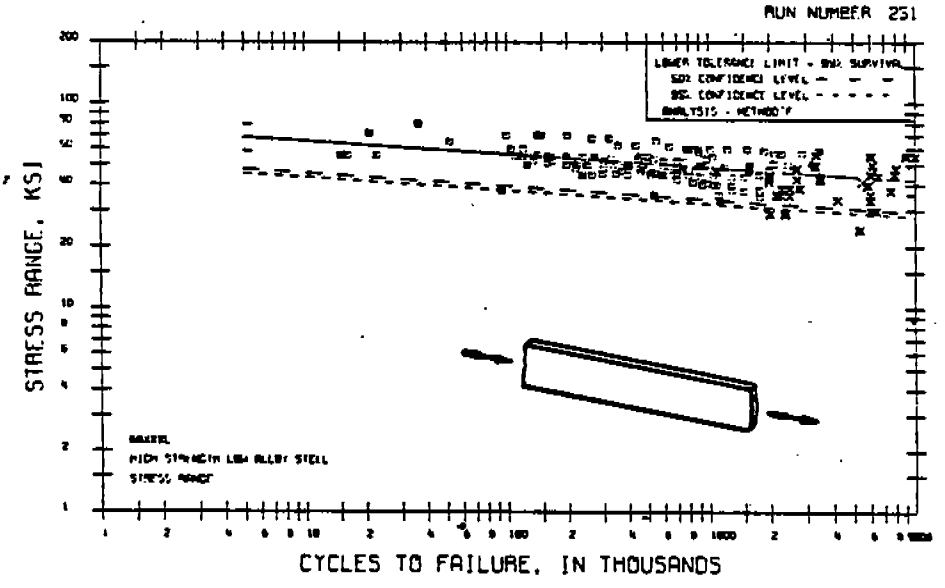

Detail No. 1H

Figure 7.5 S-N Curve for Structural Detail No. 1H

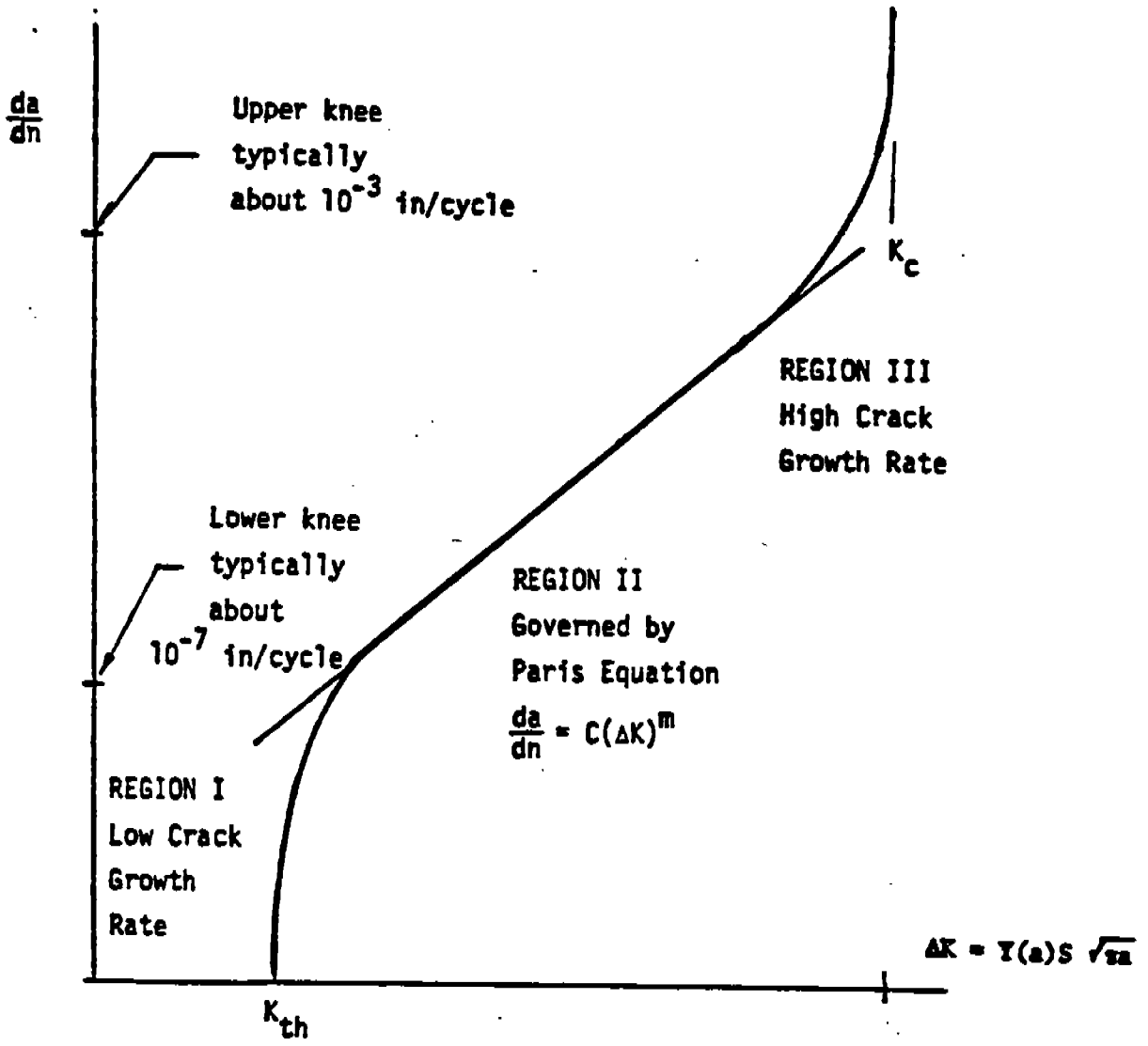

Fig. 7.6 A Model of Crack Propagation Rate Versus Stress Intensity Factor Range

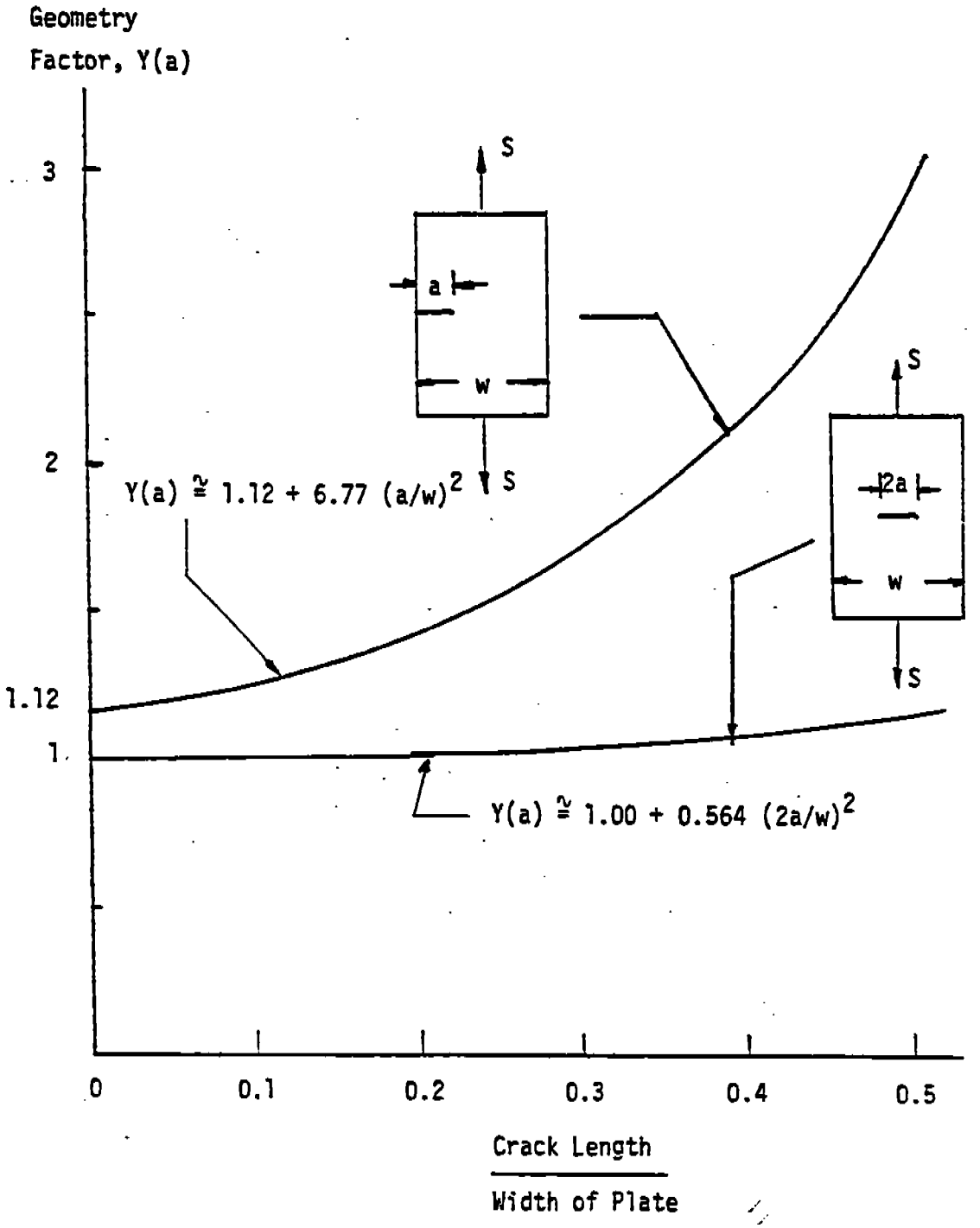

Fig. 7.7 Geometry Factor for Cracked Plates

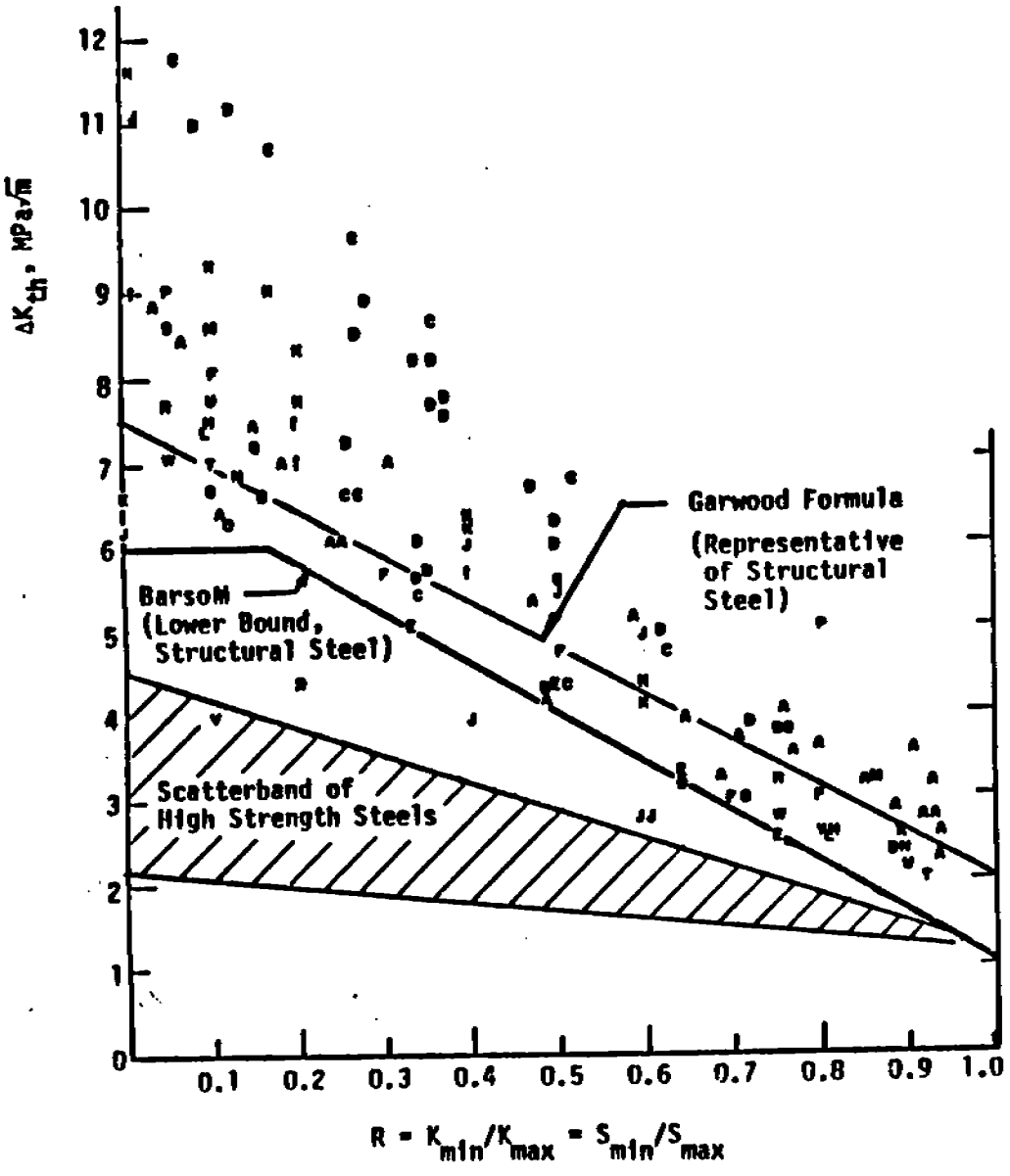

Symbol	Steel	Yield Strength, MPa
A	Low carbon	309
B	Low carbon	232
C	Medium carbon	337-434
D	Medium carbon	399-590
E	Low alloy	—
F	ASTM A533B	479
G	ASTM A508	479
H	2-1/2 NiCrMoV	618
I	Low carbon	168-192
J	High carbon	477-493
K	High carbon	532
L	2-1/2 NiCrMoV	618
M	3-1/2 NiCrMoV	742
N	3-1/2 NiCrMoV	607
O	ASTM A533B	445-463
P	ASTM SA387*	290
Q	ASTM SA516-70	327
R	ASTM SA592-3*	500
S	ASTM SA542-2*	575
T	2 NiCrMoV	575
U	3-1/2 NiCrMoV	602
V	NiMoV	661
W	ASTM SA542-2	769
X	API X65	460

*2-1/4 Cr^{-1}No Pressure Vessel Steels

Figure 7.8 Effect of Load Ratio on ΔK_{TH} for a Variety of Structural and Low Alloy Steels (After Burnside et al. (28))

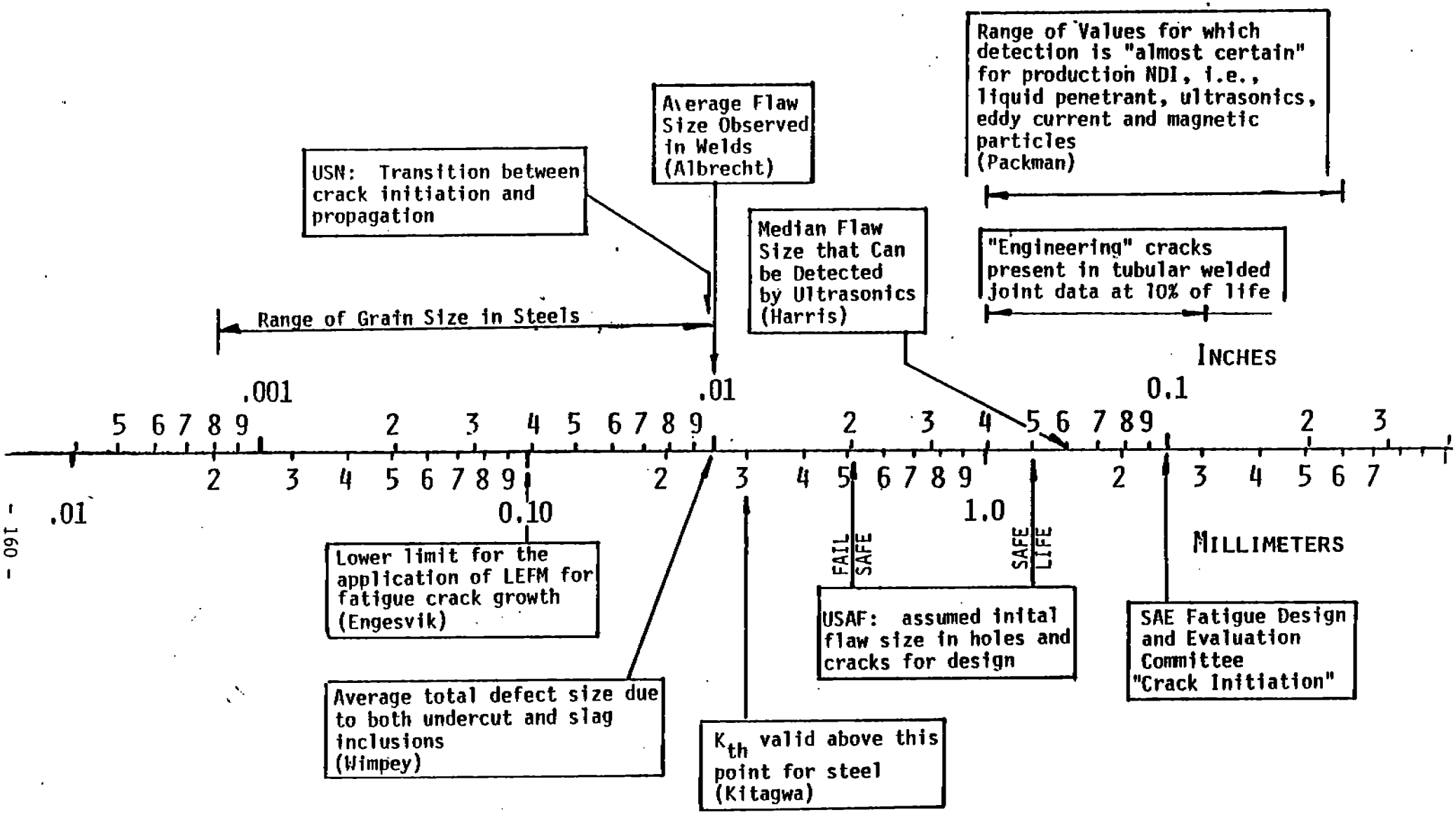

Figure 7.9 Crack Size in Perspective, From Wirsching

COMMITTEE ON MARINE STRUCTURES

Commission on Engineering and Technical Systems

National Academy of Sciences - National Research Council

The COMMITTEE ON MARINE STRUCTURES has technical cognizance over the interagency Ship Structure Committee's research program.

Stanley G. Stiansen (Chairman), Riverhead, NY
Mark Y. Berman, Amoco Production Company, Tulsa, OK
Peter A. Gale, Webb Institute of Naval Architecture, Glen Cove, NY
Rolf D. Glasfeld, General Dynamics Corporation, Groton, CT
William H. Hartt, Florida Atlantic University, Boca Raton, FL
Paul H. Wirsching, University of Arizona, Tucson, AZ
Alexander B. Stavovy, National Research Council, Washington, DC
Michael K. Parmelee, Secretary, Ship Structure Committee, Washington, DC

LOADS WORK GROUP

Paul H. Wirsching (Chairman), University of Arizona, Tucson, AZ
Subrata K. Chakrabarti, Chicago Bridge and Iron Company, Plainfield, IL
Keith D. Hjelmstad, University of Illinois, Urbana, IL
Hsien Yun Jan, Martech Incorporated, Neshanic Station, NJ
Jack Y. K. Lou, Texas A & M University, College Station, TX
Naresh Maniar, M. Rosenblatt & Son, Incorporated, New York, NY
Solomon C. S. Yim, Oregon State University, Corvallis, OR

MATERIALS WORK GROUP

William H. Hartt (Chairman), Florida Atlantic University, Boca Raton, FL
Fereshteh Ebrahimi, University of Florida, Gainesville, FL
Santiago Ibarra, Jr., Amoco Corporation, Naperville, IL
Paul A. Lagace, Massachusetts Institute of Technology, Cambridge, MA
John Landes, University of Tennessee, Knoxville, TN
Mamdouh M. Salama, Conoco Incorporated, Ponca City, OK
James M. Sawhill, Jr., Newport News Shipbuilding, Newport News, VA

SHIP STRUCTURE COMMITTEE PUBLICATIONS

SSC-327 Investigation of Steels for Improved Weldability in Ship Construction by L. J. Cuddy, J. S. Lally and L. F. Porter 1985

SSC-328 Fracture Control for Fixed Offshore Structures by P. M. Besuner, K. Ortiz, J. M. Thomas and S. D. Adams 1985

SSC-329 Ice Loads and Ship Response to Ice by J. W. St. John, C. Daley, and H. Blount 1985

SSC-330 Practical Guide for Shipboard Vibration Control by E. F. Noonan, G. P. Antonides and W. A. Woods 1985

SSC-331 Design Guide for Ship Structural Details by C. R. Jordan and R. P. Krumpen, Jr. 1985

SSC-332 Guide for Ship Structural Inspections by Nedret S. Basar & Victor W. Jovino 1985

SSC-333 Advance Methods for Ship Motion and Wave Load Prediction by William J. Walsh, Brian N. Leis, and J. Y. Yung 1989

SSC-334 Influence of Weld Porosity on the Integrity of Marine Structures by William J. Walsh , Brian N. Leis, and J. Y. Yung 1989

SSC-335 Performance of Underwater Weldments by R. J. Dexter, E. B. Norris, W. R. Schick, and P. D. Watson 1986

SSC-336 Liquid Slosh Loading in Slack Ship Tanks; Forces on Internal Structures & Pressures by N. A. Hamlin 1986

SSC-337 Part 1 - Ship Fracture Mechanisms Investigation by Karl A. Stambaugh and William A. Wood 1987

SSC-337 Part 2 - Ship Fracture Mechanisms - A Non-Expert's Guide for Inspecting and Determining the Causes of Significant Ship Fractures by Karl A. Stambaugh and William A. Wood 1987

SSC-360 Use of Fiber Reinforced Plastic in Marine Structures by Eric Greene 1990

SSC-361 Hull Strapping of Ships by Nedret S. Basar and Roderick B. Hulla 1990

None Ship Structure Committee Publications - A Special Bibliography 1983